

NTIS HC \$11.25

1 DECEMBER 1972

MSC 07384

CR-128688

# THE DEVELOPMENT OF A NON-CRYOGENIC NITROGEN/OXYGEN SUPPLY SYSTEM

Prepared Under Contract NAS9-10405

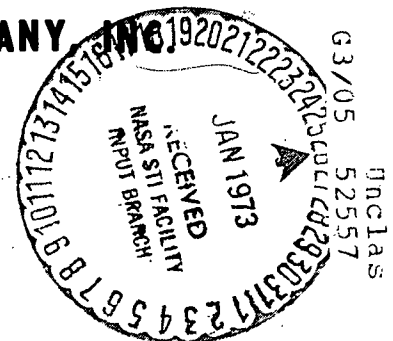
by

Biotechnology Organization  
LOCKHEED MISSILES & SPACE COMPANY  
Sunnyvale, California

for

NATIONAL AERONAUTICS AND SPACE ADMINISTRATION  
Manned Spacecraft Center  
Houston, Texas

(NASA-CR-128688) THE DEVELOPMENT OF A  
NON-CRYOGENIC NITROGEN/OXYGEN SUPPLY  
SYSTEM (Lockheed Missiles and Space Co.)  
183 p HC \$11.25  
CSCL 06K



1 December 1972

MSC 07384

THE DEVELOPMENT OF A  
NON-CRYOGENIC NITROGEN/OXYGEN  
SUPPLY SYSTEM

Prepared under Contract NAS9-10405

by

Biotechnology Organization  
LOCKHEED MISSILES & SPACE COMPANY, INC.  
Sunnyvale, California

B. M. Greenough

November 1972

NATIONAL AERONAUTICS AND SPACE ADMINISTRATION

Manned Spacecraft Center

Houston, Texas

LIST OF CONTRIBUTORS

<u>Name</u>	<u>Area of Contribution</u>
B. M. Greenough	Project Leader
R. A. Lamparter	System Test
R. B. Maine	Prototype Design
P. A. Wagner	Heat Exchanger Development

NASA TECHNICAL MONITOR

R. J. GILLEN

CREW SYSTEMS DIVISION

NASA, MANNED SPACECRAFT CENTER

## CONTENTS

<u>Section</u>	<u>Page</u>
LIST OF CONTRIBUTORS	11
ILLUSTRATIONS	v
TABLES	vi
SUMMARY	vii
1 INTRODUCTION	1
2 RESULTS AND TECHNICAL DISCUSSION	3
2.1 CATALYST ADDITIVES	3
2.1.1 Objectives	3
2.1.2 Test Facility and Procedure	3
2.1.3 Experimental Results and Discussion	4
2.2 CATHODE DEVELOPMENT	11
2.2.1 Objectives	11
2.2.2 Test Facility and Procedure	11
2.2.3 Experimental Results and Discussion	12
2.3 PROTOTYPE HEAT EXCHANGER	16
2.3.1 Requirements	16
2.3.2 Analysis and Design	18
2.3.3 Manufacture	29
2.3.4 Test Facility and Procedure	31
2.3.5 Experiment Results and Discussion	36
2.4 CABIN PO <sub>2</sub> CONTROL	41
2.4.1 Objectives	41
2.4.2 Control Technique Description	42
2.5 SYSTEM TESTING	42
2.5.1 Test Plan and Procedure	42
2.5.2 System Test Summary	46
2.5.3 Test Results and Discussion	52
2.6 PROTOTYPE DESIGN	92
2.6.1 Requirements	92
2.6.2 Analysis	92
2.6.3 Detailed Design	94
2.6.4 Specifications	106



## CONTENTS (Cont.)

<u>Section</u>	<u>Page</u>
2.7 RELIABILITY ANALYSIS	107
3 CONCLUSIONS	109
4 REFERENCES	111
5 LIBRARY CARD ABSTRACT	113
APPENDIX - TEST DATA LOGS	A-1

## ILLUSTRATIONS

<u>Figure</u>		<u>Page</u>
1	ANODE TEST RESULTS	10
2	CATHODE TEST DATA	13
3	CATHODE TEST RESULTS	14
4	SCALE-UP OF CATHODE TEST RESULTS	17
5	HEAT TRANSFER MODEL OF HEAT EXCHANGER	24
6	OVERALL HEAT EXCHANGER PERFORMANCE VS MECHANICAL PARAMETERS	26
7	HEAT EXCHANGER TEMPERATURE DISTRIBUTION	28
8	PHOTOGRAPH OF HEAT EXCHANGER AND COLD PLATE	32
9	CONTACT HEAT EXCHANGER TEST SCHEMATIC	33
10	PHOTOGRAPH OF TEST SETUP WITH INSULATION	34
11	PHOTOGRAPH OF TEST SETUP WITHOUT INSULATION	35
12	CABIN PO <sub>2</sub> CONTROL LOGIC DIAGRAM	43
13	UPDATED O <sub>2</sub> /N <sub>2</sub> BREADBOARD SYSTEM SCHEMATIC	45
14	TEST 1 SUMMARY RESULTS	49
15	TEST 2 SUMMARY RESULTS	50
16	TEST 3 SUMMARY RESULTS	51
17	TEST 1 PERFORMANCE PLOT	55
18	TEST 2 PERFORMANCE PLOT	60
19	TEST 3 PERFORMANCE PLOT	70
20	HYDRAZINE REACTION RATE, TEST 4	77
21	ANODIC GAS COMPOSITION, TEST 4	80
22	CROSS-PLOT OF HYDRAZINE AND ANODIC GAS DATA, TEST 4	81
23	DIFFUSION MODEL OF ELECTROLYSIS CELL	86
24	CABIN PO <sub>2</sub> AND P <sub>TOTAL</sub> CONTROL CHARACTERISTICS AS A FUNCTION OF GAS DEMAND	88
25	PROTOTYPE UNIT ASSEMBLY	96
26	PROTOTYPE UNIT SCHEMATIC	97

## TABLES

<u>TABLE</u>		<u>PAGE</u>
1	EXPERIMENTAL ELECTRODE FORMULATION	5
2	ELECTRODE PREPARATION PROCEDURE	6
3	HEAT EXCHANGER AND COLD PLATE THERMAL PERFORMANCE PARAMETERS	19
4	HEAT EXCHANGER AND COLD PLATE PARAMETERS	20
5	CANDIDATE HEAT EXCHANGER MATERIALS	21
6	COMPARISON OF TEST AND ANALYSIS VALUES OF THERMAL PERFORMANCE PARAMETERS	37
7	SUMMARY OF CALCULATED HEAT EXCHANGER DATA	39
8	SYSTEM TEST REQUIREMENTS	47
9	SYSTEM TEST SUMMARY	48
10	TEST 1 OPERATING CONDITIONS	53
11	TEST 1 TIME/EVENT LOG	54
12	TEST 2 TIME/EVENT LOG	66
13	TEST 3 OPERATING CONDITIONS	68
14	TEST 3 TIME/EVENT LOG	69
15	CHEMICAL ANALYSIS SUMMARY - TEST 4	83
16	GAS ANALYSIS SUMMARY RESULTS	89
17	PROTOTYPE UNIT DESIGN POINT SUMMARY	93
18	SYSTEM $\Delta P$ SUMMARY	95
19	SYSTEM VOLUME SUMMARY	95
20	PROTOTYPE UNIT DRAWING LIST	98
21	RESERVOIR VOLUME CONTROL FUNCTIONS SUMMARY	104

## SUMMARY

A development program was conducted concerned with the further development of the hydrazine/water electrolysis process with ultimate application in a manned spacecraft to provide metabolic oxygen and both oxygen and nitrogen for cabin leakage makeup. The development of this system capable of storing nitrogen in the chemical form of hydrazine offers potential advantages of weight savings and less difficult resupply for long-term missions compared to gaseous or cryogenic storage.

Phase I of this program was documented in a separate report, NASA CR 114912,<sup>1</sup> and was concerned with initial investigations in electrode development, fabrication and preliminary testing of a one-man breadboard  $N_2/O_2$  system, and preliminary design of a modular 12-man  $N_2/O_2$  system. The present program was an extension of this effort.

Electrode development efforts were continued and directed to specific improvements, namely, anode stability achieved with catalyst additives and improved processing techniques, and a higher hydrazine conversion efficiency, achieved by reducing the catalyst loading on the cathodes.

Extensive testing on the one-man breadboard  $N_2/O_2$  system was conducted, providing a more complete characterization of the cabin atmosphere control aspects and of certain system parametric effects. Cabin oxygen partial pressure control was improved by incorporating a new control technique.

A detailed design of a prototype modular  $N_2/O_2$  unit was conducted. This design produced engineering drawings and specifications sufficient to fabricate/procure the components necessary for an early prototype module assembly. The contact heat exchanger which is an integral component of this design was fabricated and successfully design-verification tested.

## Section 1

### INTRODUCTION

For extended space-base and space-station manned missions, a nitrogen/oxygen cabin atmosphere will be utilized. The inert diluent will reduce the fire hazard of the oxygen and will enhance the physiological habitability of the environment.

Oxygen consumed metabolically by the crew is recovered from metabolic wastes in a water/waste management and regenerative life support system and is recycled to the cabin. Water electrolysis is a process considered for use in this cycle to recover oxygen from water and provide hydrogen for carbon dioxide reduction.

Losses in cabin atmosphere due to cabin leakage necessitate storage of oxygen and nitrogen for leakage makeup on long-duration missions. For a mission of less than 30 days, it may be practical to carry nitrogen and oxygen onboard the spacecraft using either cryogenic or high-pressure gaseous storage. For an extended mission, however, the weight penalty associated with cryogenic or high-pressure gaseous tankage is excessive.

The development program described herein is concerned with the use of a hydrazine/water electrolysis technique to provide both the metabolic oxygen for crew needs and the oxygen and nitrogen for cabin leakage makeup. With this system, oxygen and nitrogen are stored chemically as water and hydrazine in low-pressure (and therefore low-weight) tankage. This system also has the feature of providing automatic control of both the space cabin total pressure and oxygen partial pressure.

Phase I of the program consisted of preliminary electrode evaluation, fabrication, and checkout testing of a one-man breadboard  $N_2/O_2$  system, and preliminary design of a modular 12-man spacecraft  $N_2/O_2$  system. This effort is documented in a separate report, NASA CR 114912.

The primary objectives of the present phase of the program were to improve the performance of the electrochemical cells and the laboratory breadboard  $N_2/O_2$  system and to provide a detailed design of components for an electrochemical module suitable for use in a flight-prototype, full-scale system.

The specific tasks that were completed in meeting the program objectives were as follows:

- o Experimental anodes with various loadings of different catalyst additives were evaluated as a means of improving long-term performance stability.
- o Experimental cathodes with various reduced catalyst loadings were evaluated as an approach to improving the hydrazine reaction efficiency.
- o A prototype heat exchanger was designed, fabricated, and tested to verify the design concept generated in a previous phase of this work.<sup>2</sup>
- o A new approach to controlling hydrazine feed to the breadboard  $N_2/O_2$  system was experimentally evaluated as a means of improving the responsiveness of the control of cabin oxygen partial pressure.
- o Tests were conducted using the one-man breadboard  $N_2/O_2$  system to determine parametric effects, allowable rates and ranges of changes in control conditions, and performance of zero gravity compatible components.
- o Design drawings and specifications were prepared of flight-prototype components of a full-scale module in sufficient detail to permit fabrication/procurement of these components.

The sections that follow in this report are concerned primarily with the areas of electrode development, heat exchanger fabrication and testing, and system testing. The engineering drawings of the heat exchanger and the prototype module detail drawings and specifications have been documented separately.

## Section 2

### RESULTS AND TECHNICAL DISCUSSION

#### 2.1 CATALYST ADDITIVES

##### 2.1.1 Objectives

A large number of contributions to the literature have advanced theories to explain the complex reaction mechanisms of the oxygen electrode, both anodically and cathodically. No one explanation has gained universal acceptance; the oxygen electrode remains an enigma. It has been well documented in previous programs<sup>3,4</sup> that commercial black platinum oxygen electrodes operated anodically in basic electrolyte show a tendency toward performance degradation when operated for long periods of time.

For ultimate application in a spacecraft, electrical performance degradation imposes an undesirable power penalty on the electrochemical system. In previous work at LMSC, over 250,000 cell hours of testing has been conducted using a commercial electrode material containing a proprietary mixture including Teflon and black platinum catalyst. In these tests, performance degradation of the anode (oxygen electrode) could be observed as voltage increase with time at constant applied current. It was found, with the best electrodes tested, to characteristically consist of an approximate 10 percent voltage increase in the first few hundred hours with stabilization to a ramp leading to a total of approximately 15 percent over a 5,000 hour period.

The purpose of this program task was to investigate the effects of electrode preparation and processing techniques and certain catalyst additives on the electrical performance characteristics of experimental anodes with the objective of reducing long-term performance degradation.

##### 2.1.2 Test Facility and Procedure

The test facility used for the conduct of the experimental anode tests consists of independently powered and controlled cell test stations in the Bioengineering Laboratory. A detailed description of this facility can be found in Section 2.1 of NASA CR 114912.

A series of electrodes with an active area of  $18 \text{ cm}^2$  were prepared using several different catalyst additives as shown in Table 1.

The catalyst additives which were used were rhodium black, ruthenium black and iridium black. The two extenders were methyl cellulose (M.C.) and a water soluble polymer, brand name Jaguar (JF3).

The procedures used to prepare these electrodes are presented in Table 2. Finished electrodes were visually inspected for mechanical integrity. Those which passed this inspection were subjected to thermogravimetric analysis to determine organic residue. Test cells were operated at  $2.7\text{A}$  ( $150 \text{ mA/cm}^2$ ) ambient temperature and pressure, with 30% KOH electrolyte. The test duration varied from a few hours for those electrodes which failed early to several hundred hours where they showed promise.

### 2.1.3 Experimental Results and Discussion

#### Formulations Processing

The electrode processing procedures shown in Table 2 were partially developed under Contract NAS 9-11848.<sup>5</sup> Key elements of the formulation are described below.

Extender.--A water-soluble polymer extender is added to the catalyst formulation to occupy space when the catalyst mixture is applied to the substrate. It is subsequently removed in the post-treatment leaching process, leaving the desired porosity in the active material.

Teflon.-- An aqueous dispersion of Teflon is added to the formulation to act as a binder to permit high loadings of catalyst on the substrate.

Catalyst.-- Noble metal blacks are used as the catalyst to provide high surface area.

Mineral Oil.-- The catalyzed substrate is sprayed with a light film of mineral oil to lubricate the surfaces during calendaring and to prevent catalyst from adhering to the Mylar backing.

Post-treatment of the electrode material is necessary to remove the extender, the mineral oil, and organic residue from the Teflon dispersion. It has been found that residual extender has a serious detrimental effect on



Table 1

## EXPERIMENTAL ANODE FORMULATION

Anode Number	Cell Number	Formulation			
		Pt	Teflon	Extender	Catalyst Additives
1		0.765	0.85	M.C. 1.70 <sup>(1)</sup>	Rh 0.085
2		0.765	0.85	M.C. 1.70	Ru 0.085
3		0.765	0.85	M.C. 1.70	Ir 0.085
4		0.637	0.85	M.C. 1.70	Rh 0.213
5		0.637	0.85	M.C. 1.70	Ru 0.213
6		0.637	0.85	M.C. 1.70	Ir 0.213
7	71-1	0.85	0.85	JF3 1.70 <sup>(2)</sup>	None
8		0.85	0.85	M.C. 1.70	None
9	71-7	0.68	0.85	JF3 1.70	Rh 0.17
10	71-8	0.68	0.85	JF3 1.70	Ru 0.17
11	71-9	0.68	0.85	JF3 1.75	Ir 0.17
12		0.51	0.85	JF3 1.70	Rh 0.34
13		0.51	0.85	JF3 1.70	Ru 0.34
14		0.51	0.85	JF3 1.70	Ir 0.34
15	71-10	0.81	0.85	JF3 1.70	Rh 0.0425
16	71-11	0.81	0.85	JF3 1.70	Ir 0.0425

(1) M.C. Methyl Cellulose

(2) JF3 Jaguar JF3 - A water soluble polymer used as a commercial extender.

Table 2  
ELECTRODE PREPARATION PROCEDURE

Catalyst Mixture

1. Additively weigh ingredients with a chainomatic balance to the nearest mg.
2. Manually mix ingredients with addition of up to 5 cm<sup>3</sup> distilled water to achieve a spreadable consistency.

Electrode Active Material

1. Cut expanded nickel substrate to size.
2. Ultrasonically degrease with acetone.
3. Apply Mylar film backing and mask perimeter of substrate.
4. Apply catalyst mixture to substrate.
5. Dry in oven at 50°C for one hour.
6. Spray coat with mineral oil and hand roll. Apply Mylar film to front surface.
7. Machine roll two passes at 200 kN/m<sup>2</sup> (29 psi) and remove Mylar film and masking tape.

Post Treatment

1. Leach the prepared electrode active material as follows:

<u>Solution</u>	<u>Time in Ultrasonic (Min.)</u>	<u>Time in Solution (Min.) Soak</u>
Hexane/Heptane	2	0
Isopropanol	2	0
Distilled water	2	0
KOH (30%)	2	0
Distilled water	0	30
H <sub>2</sub> SO <sub>4</sub> (10%)	2	0
Distilled water	2	0
Distilled water	0	30
110°C KOH (30%)	0	120
Distilled water	0	120

2. Allow material to dry completely before proceeding.

Table 2

ELECTRODE PREPARATION PROCEDURE  
(Continued)

Electrode Assembly

1. Form depression in electrode rim to accept catalyzed substrate.  
Adjust depression fixture to same thickness as electrode material substrate.
2. Insert electrode material and rim in spotwelding fixture and overlap spotweld around periphery. Scribe outside weld line, remove from fixture and break off excess substrate.
3. Cut and spotweld together spacer and support screens.
4. Spotweld screen assembly to electrode rim.
5. Apply vinyl tape to rim.

electrical performance if the residue is present at levels greater than one percent.<sup>5</sup> Mineral oil which is left in electrode will slowly oxidize when the electrode is operated producing carbon monoxide at levels as high as 20 ppm. The Teflon dispersion is a proprietary DuPont product and its exact composition is not known. It is reasonable to assume, however, that any organic residue in the mixture would be detrimental to the electrode performance.

The leaching procedure to remove these undesirable constituents is as follows:

Mineral Oil - Hexane/Heptane

Isopropanol

Water

- o Mineral oil is a long straight chain hydrocarbon and is, therefore, soluble in shorter straight chain hydrocarbons such as hexane or heptane.
- o Hexane/Heptane are not soluble in water. Isopropanol is used to remove the hexane/heptane.
- o Isopropanol is water soluble and is, therefore, removed with distilled water.

Extender - KOH (30%)

Water

- o The extender is saponified with 30% KOH.
- o Water is used to remove the KOH and saponified residue.

Other Residuals -  $H_2SO_4$  (10%)

$H_2O$

- o Sulfuric acid is used to remove any other residuals not affected by the strong base treatment
- o Water is used to remove the sulfuric acid.

A final 2-hour soak in hot KOH is used to vaporize and/or react residual solutions used in prior steps.

The first series of experimental anodes which were prepared in this program (Table 1, Anode Nos. 1-6) used methyl cellulose as the extender. It was found that these electrodes did not maintain mechanical integrity during the post-treatment leaching process.

To investigate the problem, two platinum-only electrodes were prepared (Anode Nos. 7 and 8, Table 1), one with methyl cellulose and one with Jaguar F3, a commercial extender. Both were subjected to post-treatment and only the Jaguar-extended electrode survived the leaching process. All subsequent anodes in the series were successfully prepared with JF3 extender.

Electrodes which passed the mechanical integrity inspection after post-treatment were subjected to TGA analysis. All showed one percent or less residue.

#### Cell Tests

The results of the cell testing of rhodium and iridium-containing electrodes are plotted in Figure 1 and complete test data are presented in the Appendix. For the purpose of comparison, the performance of the best experimental electrode tested in Phase I (NASA CR 114912), electrode T-124; the best of the commercial materials, AB-4X; and an experimental platinum-only electrode, 71-1, are co-plotted in this figure.

Both the 5 and 20% iridium electrodes had slightly better performance than the rhodium-additive electrodes. The "flatness" of these curves is indicative of time-stability and is the most significant result of the series of tests. Note that even the platinum-only electrode (71-1) has evidenced time stability which is probably due in large part to the effectiveness of the post-treatment procedure.

A ruthenium electrode was tested in Cell 71-8. After a few hours of operation of this cell, the electrolyte began to turn yellow. An atomic absorption analysis of a sample of the electrolyte indicates the presence of ruthenium ion. A small amount of bulk ruthenium black was then placed in a beaker of electrolyte; this solution also turned yellow, but in a matter of a few days rather than a few hours. From these tests, it appears that the ruthenium black is already partially oxidized as evidenced by the beaker test, and that in the

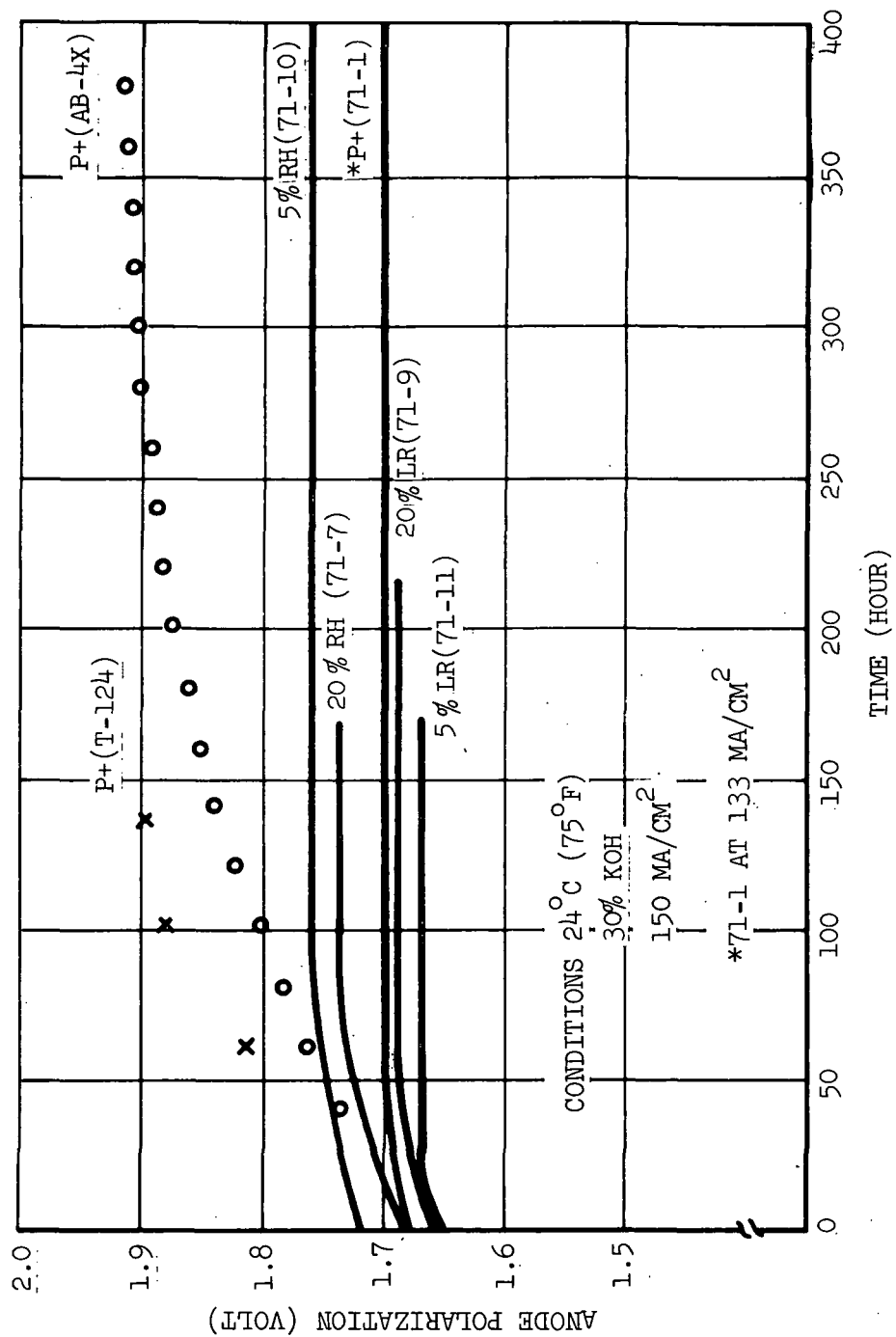


Figure 1 Anode Test Results

strong oxidizing environment of the operating anode, oxidation proceeds to the soluble tetroxide state. This material was, therefore, deemed unsatisfactory as a catalyst additive; no further cell tests were conducted with this type of anode.

## 2.2 CATHODE DEVELOPMENT

### 2.2.1 Objective

It is known that hydrazine undergoes auto-oxidation in the presence of a suitable catalyst. In the hydrazine/water electrolysis system, hydrazine is injected in the circulating electrolyte for the purpose of generating nitrogen admixed with the anodic oxygen produced by water electrolysis. Any hydrazine which reacts at the catalyzed cathodes within the electrolysis cell stack represents an inefficiency in the process of generating nitrogen at the anodes.

The objective of this task, then, was to determine experimentally the optimum catalyst loading of the cathode considering the conflicting parameters of anodic conversion efficiency and of cell voltage penalty for reduced catalyst loading of the cathode.

### 2.2.2 Test Facility and Procedure

The test facility used for the conduct of the experimental cathode tests consists of independently powered and controlled cell test stations located in the Bioengineering Laboratory. A detailed description of this facility can be found in Section 2.1 of NASA CR 114912.

A series of four electrolysis cells were assembled, each cell containing a 90 cm<sup>2</sup> cathode with different catalyst loading as follows:

<u>Cell No.</u>	<u>Cathode No.</u>	<u>Formulation</u>		
		<u>Pt.</u>	<u>Teflon</u>	<u>Extender</u>
71-2	C-1	2.5	2.5	5.0
71-3	C-2	1.0	1.0	3.0
71-5	C-3	0.5	0.5	-0-
71-4	C-4	-0-	-0-	-0-

The catalyst formulations were applied to 0.25 mm thick expanded nickel screen substrates. The extender, Jaguar Polymer F-3 was then leached out in a sequence of ultrasonically agitated baths containing hexane, isopropyl alcohol, water, 110°C (230°F) KOH, water, 10% H<sub>2</sub>SO<sub>4</sub>, and water.

Each cell was operated for approximately 48 hours at 150 mA/cm<sup>2</sup> current density and 27°C (80°F) without hydrazine to determine the cathode polarization. Then each cell was operated for approximately 48 hours under the same conditions with an initial charge of approximately 2 gram moles of hydrazine.

Voltage and current data were recorded every two hours during the day shift. Gas flow rates, anodic and cathodic, were measured with soap bubble flowmeters every two hours during the day shift, and electrolyte samples were titrated three times each day during the hydrazine portion of the tests. Care was taken to keep liquid samples small (less than one percent of total system volume) to keep sample effects negligible. Gas samples were analyzed for N<sub>2</sub> periodically.

### 2.2.3 Experimental Results and Discussion

A summary of the experimental data from the cathode evaluation tests is presented in Figure 2. In this figure, the hydrazine concentration in the electrolyte and the increase in cathodic gas flow rate due to hydrazine decomposition are plotted as a function of time. The plots of  $\Delta H_c$  show the increase in hydrogen flow of the cathodes with hydrazine over the cathode with no hydrazine. The increasing voltage performance of the cathodes was the following:

C-1	2.5 Pt	0.179 volts
C-2	1.0 Pt	0.200 volts
C-3	0.5 Pt	0.520 volts
C-4	bare nickel	0.700 volts

With the above data and the data shown in Figure 2, a cross-plot of cathode flow versus cathode polarization was made with hydrazine concentration as a parameter. This plot is shown in Figure 3.

Referring back to Figure 2, the anodic hydrazine conversion efficiency (defined as the mole-percent of the total hydrazine added that reacts at the anode) was determined for each cell using the following procedure. The reaction rate constant,  $m$ , is defined by:

$$m = \frac{\ln C - \ln C_0}{t}$$

At any time,  $t$ , the hydrazine reaction rate is  $\frac{dc}{dt} = C_t m = X_T$ .



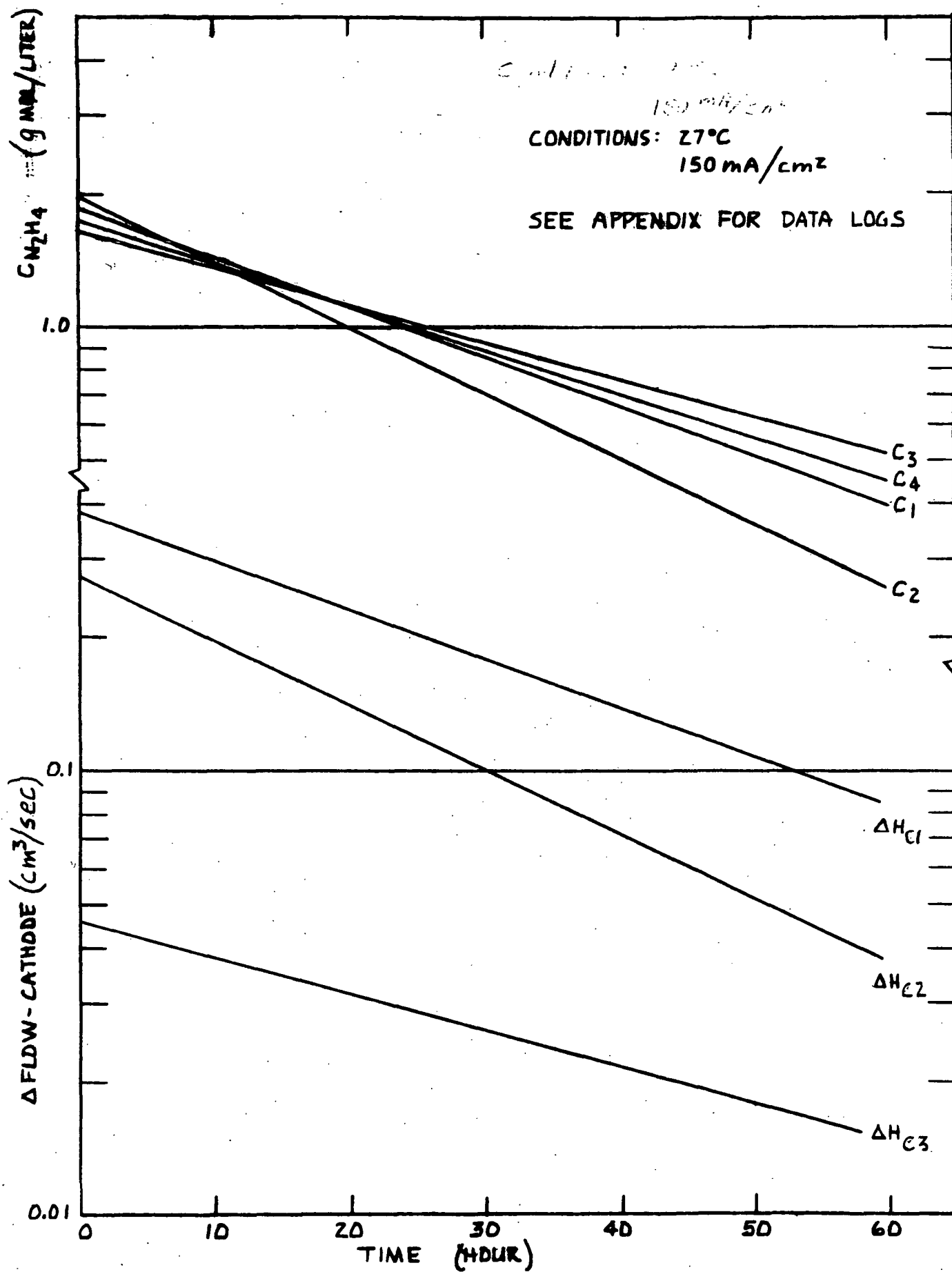


Figure 2 Cathode Test Data

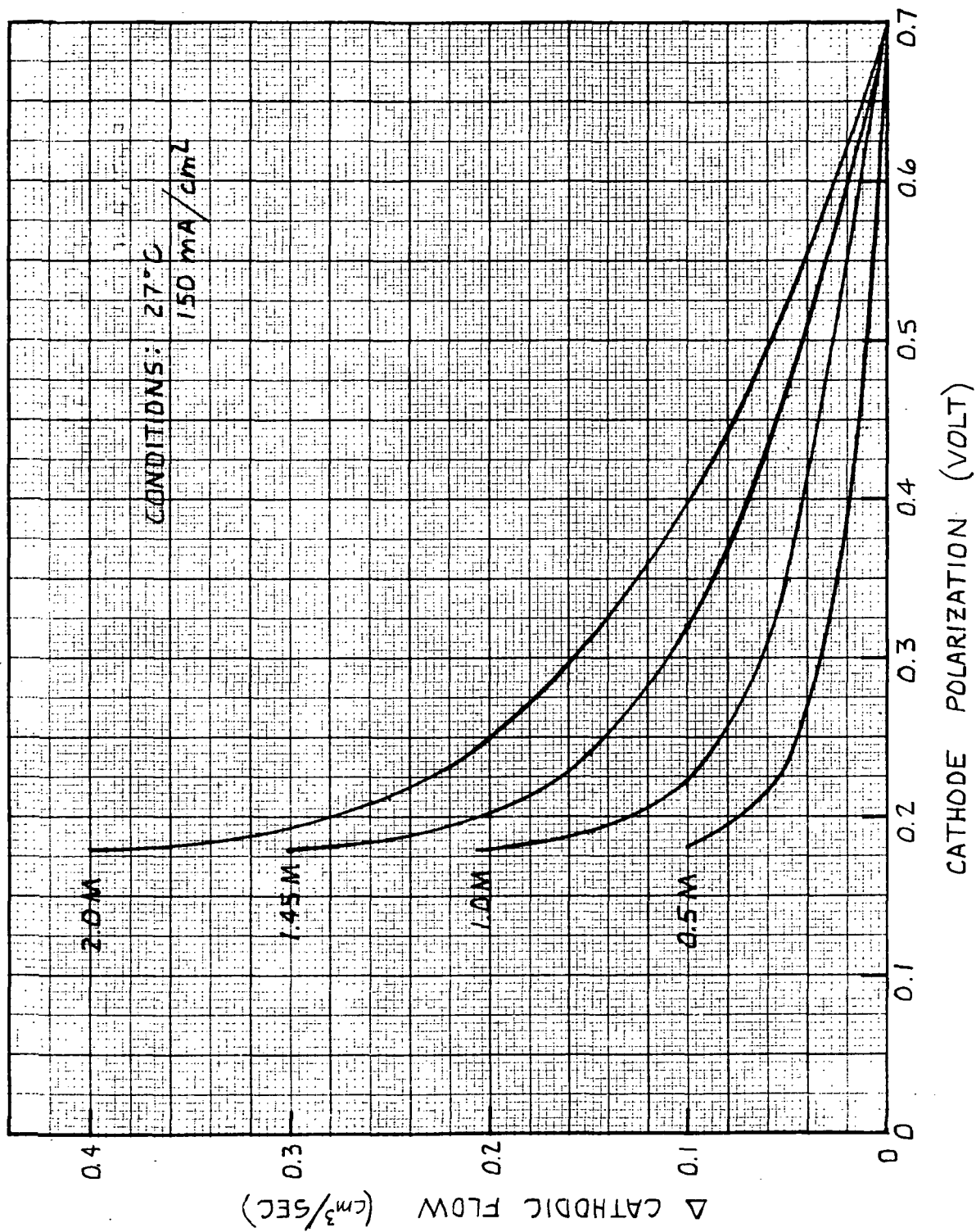


Figure 3 Cathode Test Results

Hydrogen gas is generated electrochemically at a rate defined by:

$$(H_2)_e = 2(0.0096)I \text{ g-mols/hr}$$

Where I = electrolysis current (amperes)

The amount of hydrazine reacting at the cathode at this time, t, is computed with the equation:

$$X_c = \frac{\dot{m}_{TC} - (H_2)_e}{3} \text{ g-mols/hr}$$

Where  $\dot{m}_{TC}$  = measured cathodic gas flow rate. The quantity,  $\dot{m}_{TC} - (H_2)_e$  can also be determined by measuring the cathodic gas flow rate, with and without hydrazine. This quantity then is equivalent to the measured  $\Delta H$  shown in Figure 2. The factor, 3, in the equation arises from the fact that one mole of hydrazine reacting produces three moles of gas.

The amount of hydrazine reacting at the anode is obtained by difference:

$$X_a = X_T - X_c.$$

The reaction efficiency is defined as

$$\eta = \frac{X_a}{X_T} \times 100$$

For the four cells which were tested, efficiency was computed using the above procedure with the following results:

<u>Cathode</u>	<u><math>\eta</math> %</u>
C-1	60.9
C-2	79.6
C-3	93
C-4	100

There is some uncertainty in the absolute values of the efficiencies computed by the above technique, principally due to the possibility of errors in measurement of very small differences in cathodic flow rate. As a check on the technique, efficiency was computed for two cases using two different methods. In the first case, the efficiency for C-1 was computed using the empirical equation

$$X_a = \left[ 4.77C + 0.0134C(150) \right] \quad (60) \quad (4.06 \times 10^{-5})$$

which was determined experimentally with the breadboard  $N_2/O_2$  system (Ref. NASA CR 114912).  $X_t$  was computed in the same manner as in the previous technique. This computation yielded a value of  $\eta$  of 64.1% compared to the previously determined value of 60.9%.

In the second case, efficiency was calculated for C-3 based on gas chromatographic analysis and total gas flow rate measurement. This method yielded an efficiency of 92% compared to the previously determined value of 93%.

Having established that the efficiency values determined by the different techniques are in reasonable agreement, the original values were used to trade off hydrazine tankage and power and cooling penalty versus cathode polarization for a full scale 12-man system. Penalty factors for power and cooling and tankage for hydrazine storage were taken from LMSC/A977498, "Preliminary Design of a Space Station Electrolytic Oxygen-Nitrogen Generator". The results are shown in Figure 4. It is evident from this figure that system total equivalent weight (TEW) can be optimized by controlling the composition of the cathode. While the four data points which were obtained were not sufficient to determine the exact catalyst loading, it is apparent that the normal loading should be reduced by 40 to 50 percent to achieve maximum TEW. These results substantiate the prediction of Curve C, Figure C4 in LMSC/A977498.<sup>2</sup>

## 2.3 PROTOTYPE HEAT EXCHANGER

### 2.3.1 Requirements

The heat exchanger design conceived for the 12-man unit preliminary design effort (LMSC/A977498) was to be subjected to analysis, detailed design, fabrication, and design verification testing in this program task. The heat exchanger and cold plate assembly were required to simulate, as closely as possible, the final  $N_2/O_2$  flight prototype configuration. Thermal performance was the most important consideration, although physical configuration had to be as close as possible to a flight prototype design, especially in the heat exchanger, which was to be internally coated to prevent gas formation in the electrolyte loop. The cold plate had only to simulate the flight item in performance characteristics.

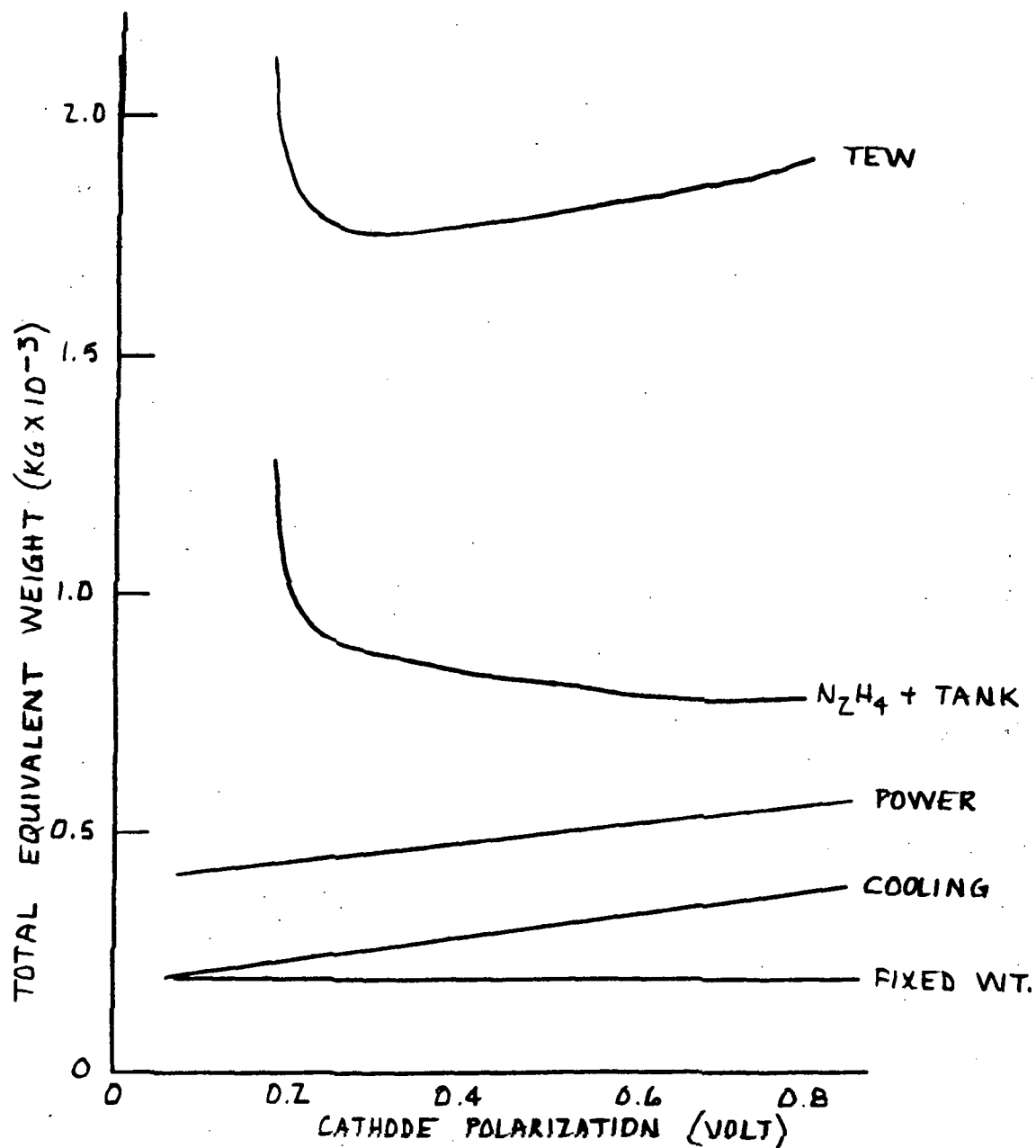


Figure 4 Scaleup of Cathode Test Results

Thermal performance parameters, as listed in Table 3, are those associated with the  $N_2/O_2$  preliminary design. These values are for a 1.5-man module, and were the best available at the time the analysis was performed. All analysis and design were based on these values.

### 2.3.2 Analysis and Design

During the analysis and design phase, the optimum configurations for both heat exchanger and cold plate were determined. The analysis and design tasks were integrated because the design detail, necessary to assure producibility and meet the required cost target, significantly impacted the thermal design. This was especially true for the heat exchanger, where internal coating was necessary, and in the contact interface between the heat exchanger and cold plate. During the analysis and design phase, attention was focused on material considerations, optimization of the heat exchanger and cold plate assemblies, interface analysis, overall performance, and detail design.

A summary of the mechanical and predicted thermal parameters for the chosen heat exchanger and cold plate configuration is presented in Table 4.

#### Material Considerations

Desirable material properties included high thermal conductivity, chemical resistance to the coolant fluids, good machinability and brazability, and availability. For this reason, materials commonly used in heat exchangers, and other alloys specifically attractive to this particular design, were considered.

Candidate materials and their properties are summarized in Table 5. Nickel 200 was selected for both the heat exchanger and cold plate, as it has the highest thermal conductivity of the materials which were completely compatible with all fluids involved. Also, it is readily obtainable and fairly inexpensive. It has the drawback that it is very soft, and therefore is difficult to machine, but this was not considered serious enough to preclude its use. Other materials considered were aluminum, stainless steel, and molybdenum.

Table 3

HEAT EXCHANGER AND COLD PLATE THERMAL  
PERFORMANCE REQUIREMENTS

OVERALL HEAT TRANSFER:

Heat Load (max) = 266 watts (306 BTU/hr)  
Max Envelope = 22.8 x 29.8 cm (9 x 11.75 inches)  
LMTD Available = 7.8°C (14°F)

HEAT EXCHANGER:

Fluid = 30% KOH  
 $T_{in}$  = 32.7°C (at max load) (90.8°F)  
 $T_{out}$  = 26.6°C (at max load) (79.9°F)  
 $\dot{W}$  = 12 g/s (94 lb/hr)  
 $P$  = 3.44 kN/m<sup>2</sup> (max) (10.5 psi)

COLD PLATE:

Fluid = Water  
 $T_{in}$  = 18.3°C (65°F)  
 $\dot{W}$  = 9.5 g/s (75 lb/hr)

Table 4  
HX AND CP PARAMETERS

PREDICTED THERMAL PERFORMANCE PARAMETERS

OVERALL

$Q = 266 \text{ watt (max)}$	(906 BTU/hr)
$U_{\text{overall}} = 5.9 \text{ J/s} \cdot ^\circ\text{C} \cdot \text{m}^2$	(915 BTU/hr $^\circ\text{F ft}^2$ )
Flow arrangement - Counterflow	
LMTD required = $7.9^\circ\text{C}$	(14.2 $^\circ\text{F}$ )

Heat Exchanger

$U_{\text{HX}} = 1420 \text{ J/s } ^\circ\text{C m}^2$	(250 BTU/hr)
Fluid = 30% KOH	
$\dot{W} = 12 \text{ mkg/s}$	(94 lb/hr)
$\Delta P = 0.689 \text{ kN/m}^2$	(0.1 psi)

Cold Plate

$U_{\text{CP}} = 1760 \text{ J/s } ^\circ\text{C m}^2$	(310 BTU/hr)
Fluid = Water	
$\dot{W} = 9.5 \text{ mkg/s}$	(75 lb/hr)

Interface

$U_{\text{I}} = 1530 \text{ J/s } ^\circ\text{C m}^2$	(270 BTU/hr $^\circ\text{F ft}^2$ )
Area = $0.068 \text{ m}^2$	(0.735 $\text{ft}^2$ )

MECHANICAL VARIABLES (Heat Exchanger and Cold Plate)

Material	Nickel 200	
Horiz. Plate Thickness	0.75 mm	(0.030 in.)
Passage Height	1.5 mm	(0.060 in.)
No. of Layers of Passages	2	
No. Vertical Bars/Inch	4	
Vertical Bar Thickness	1.88 mm	(0.075 in.)
Baseplate Thickness	3.12 mm	(0.125 in.)
Baseplate Dimensions	22.8 x 29.8 cm	(9 x 11.75 in.)
Braze Alloy	85% gold, 15% nickel	



Table 5  
CANDIDATE MATERIALS

	Compati- bility with KOH	Compati- bility with H <sub>2</sub> O	Thermal Cond. J/s m OC (BTU/hr OF ft <sup>2</sup> )	Avail- ability & Rel. Cost	Machina- bility	Brazena- bility	Yield Strength Mn/m <sup>2</sup> (KSI)	Density kg/m <sup>3</sup> (lb/in <sup>3</sup> )
Aluminum	Low	Good	0.173-0.207 (100 - 120)	Good Low	Good	Excellent	276 (40)	2.77 x 10 <sup>3</sup> (0.1)
300 Series Cres	Good	Excellent	0.0156 (9)	Good Low	Good	Good	241-310 (35-45)	8.03 x 10 <sup>3</sup> (0.29)
Molybdenum	Fair	Excellent	0.146 (84.5)	Poor High	Good	Good	565 (82)	10.2 x 10 <sup>3</sup> (0.37)
Nickel 200	Excellent	Excellent	0.0306 (36.3)	Fair	Fair	Good	103-206 (15-30)	8.85 x 10 <sup>3</sup> (0.32)

Aluminum has the highest thermal conductivity of common materials, is readily available and workable, and is often used in conventional heat exchangers. It is compatible with the cold plate coolant fluids and although it is not compatible with KOH, it could possibly be used in the heat exchanger due to the coating required to prevent electrolytic action. It was felt, however, that a pinhole in the coating could cause rapid deterioration of the aluminum due to chemical attack. Also, although it appears compatible with fluids which would be used in the cold plate, Hamilton Standard has stated that it is not acceptable for SSP. Aluminum was thus considered inappropriate for both heat exchanger and cold plate use.

Stainless steel is also commonly used in heat exchangers and is completely compatible with all fluids involved. In addition, it is readily obtainable and workable. It, however, has the drawback of low thermal conductivity.

Molybdenum has excellent thermal conductivity but is not completely compatible with KOH, is difficult to obtain, and is expensive.

Composite or laminated materials and special alloys were not considered practical at this time, but have some merit and should be considered in advanced program phases.

Kynar was selected for the internal coating because it is resistant to chemical attack, is non-porous, and can be poured through internal passages. Teflon coatings were not feasible, as they are porous and also cannot be poured through internal passages. The application of the coating was controlled by the vendor in accordance with his experience.

#### Heat Exchanger and Cold Plate Optimization

Optimization consisted of determining the best possible dimensions for all elements of the heat exchanger and cold plate, taking into account thermal, mechanical, and manufacturing criteria. Due to budget limitations, and to allow an opportunity to evaluate the effect of the Kynar coating on thermal performance, the cold plate is identical to the heat exchanger except that it is not internally coated.

For purposes of analysis, the heat exchanger was assumed to consist of horizontal plates, vertical bars, and a base plate. Heat passes from the fluid through the coating, into the metal and through the various component parts, finally exiting through the interface surfaces.

Heat transfer from the fluid to the vertical bars was determined by considering the horizontal plates as fins. As shown in Fig. 5, the heat transfer from fluid into a surface through a fin is given by the equation

$$Q_f = hA \Delta T_{f-b} \eta_f$$

where:

$h$  is the liquid to fin surface film coefficient,

$A$  is the surface area of the fin or  $\left(\frac{W}{2} \times L\right)$ ,

and  $T_{f-b}$  is the temperature difference between the fluid and fin base.

$\eta_f$  is the film efficiency term and is defined as

$$\eta = \frac{\tanh \frac{W}{2} \sqrt{\frac{2h}{kt}}}{\frac{W}{2} \sqrt{\frac{2h}{kt}}}$$

where  $k$  is the thermal conductivity of the material and the other terms are as previously defined.

Where there is no fin, the heat transfer into the vertical bar is simply  $Q = h A \Delta T_{f-b}$ , where  $A = (h \times L)$ .

The total heat transfer into the vertical bar, is therefore, the sum of those individual terms of  $(Q + Q_f)$ . Heat transfer through the vertical bars to the base plate was calculated by a similar approach, with all the heat applied at the passage center, and the fin height representative of the actual geometry. Heat transfer within the base plate was calculated by direct conduction. In this case, between any two points,  $Q = K A_m \frac{\Delta T}{\Delta X}$ , where  $A_m$  is the area normal to the direction of heat transfer, and  $\Delta X$  is the distance the heat travels.

Variables determined from the analysis were the horizontal plate thickness, the passage height, the number of layers of fluid passages, the number of vertical bars per inch, the vertical bar thickness, and the base plate thickness.

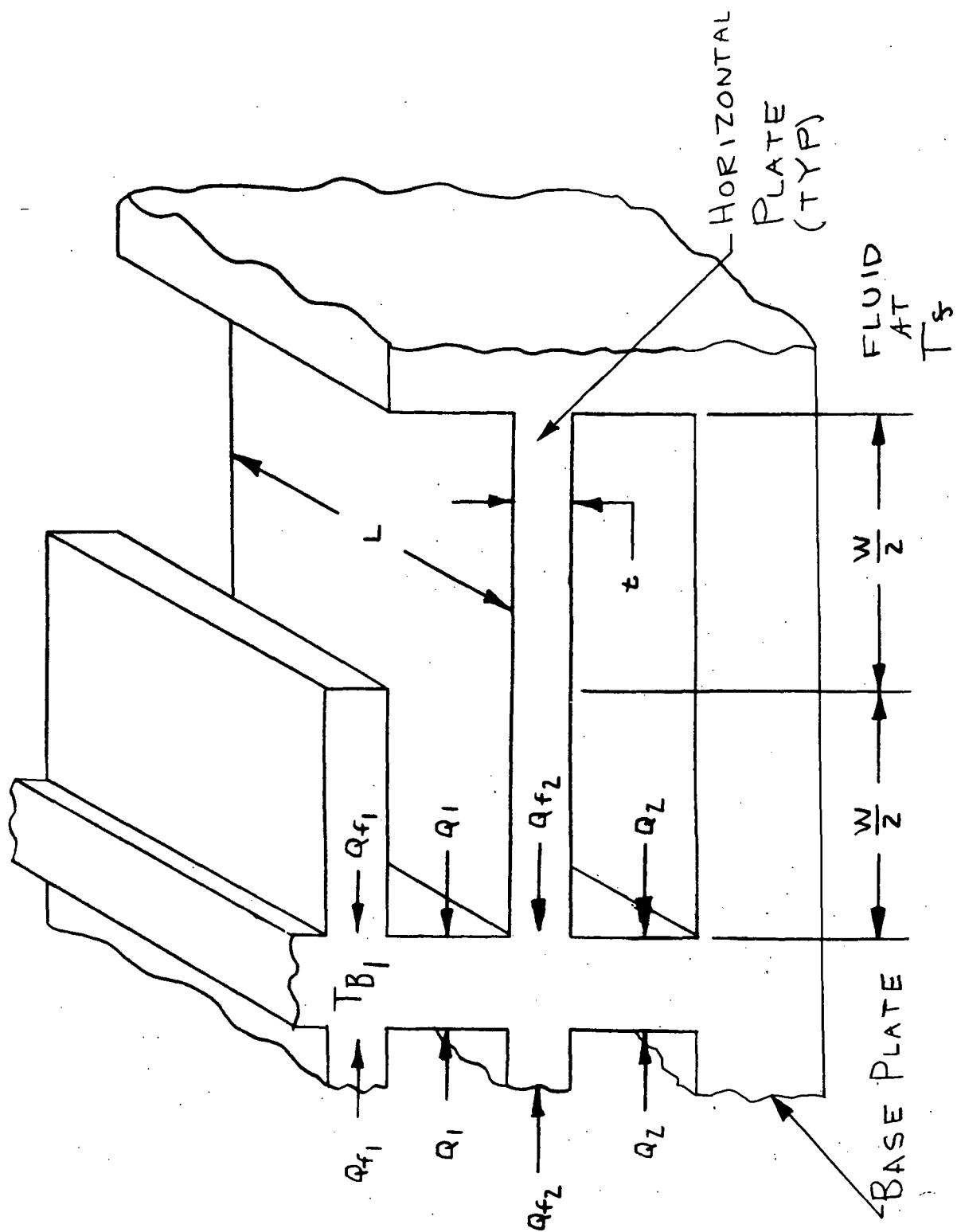


Figure 5 Heat Transfer Model of Heat Exchanger

Horizontal plates were limited to a minimum thickness of 0.75 cm (0.3 in) by manufacturing considerations. Ideal thickness would be much thinner than this, as the fin efficiency for a 0.75 cm (0.3 in) fin in the selected configuration is 97%. This would drop to only 93% if the thickness were cut in half and would affect a significant reduction in unit weight.

The passage height effects the hydraulic diameter and therefore the film coefficient. It is desirable to have the height as small as possible, within the constraints of manufacturing considerations and pressure drop. The 1.5 mm (0.060 in) height chosen is based on providing sufficient height for the Kynar coating.

The number of layers of passages is a function of the required heat transfer and the available base plate area. As can be seen from Fig. 6, the minimum number of layers necessary is desirable as additional layers become less and less efficient. The heat load present in this case required 2 layers of passages.

The number of vertical bars per cm should be the maximum possible. Due to the requirement for coating, however, and since the horizontal plates were limited to 0.75 mm (0.030 in) thickness, 1.57 fins/cm (4 fins/in) was selected as a reasonable compromise.

The vertical bar thickness is a function of the number of fins/cm and the number of layers of passages. Fig. 6 also shows this relationship for the selected package size. It should be noted that this figure is based on average fluid temperatures, but that it neglects the non-linear  $T$  gradient created by the reduced heat transfer per layer and constant mass flow per layer. This effect is significant for large numbers of layers. A 1.9 mm (0.075 in) vertical bar was selected, as it gave good heat transfer and eliminated any possibility of the non-linear temperature gradient affecting the exchanger performance.

A base plate thickness of 0.318 (0.125 in) was selected as providing reasonable axial heat distribution with a minimum of vertical resistance. Also, it provides sufficient mechanical strength to prevent warping of the interface surface. Slight variations in the base plate thickness significantly affect the weight of the heat exchanger but do not have too much effect on thermal performance.

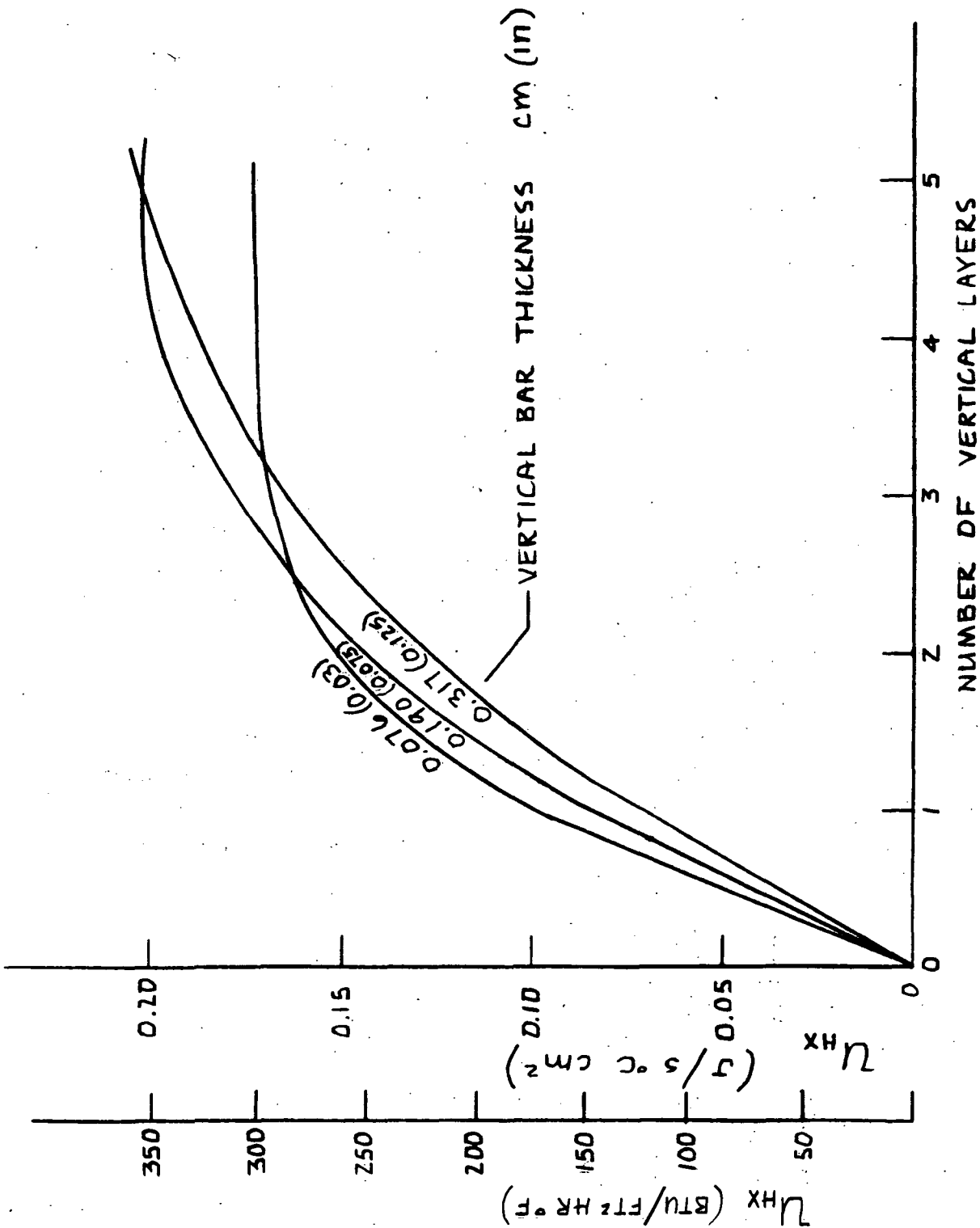


Figure 6 Overall Performance versus Mechanical Parameters

Due to the low fluid flow rate inside the passages, flow is laminar with a Reynolds number of about 15, and the film coefficient is based on the minimum Nusselt number of 3.65. Therefore,

$$h = \frac{NuK}{D} = 3.65 \frac{K}{D}$$

where K is the thermal conductivity of the fluid and D is the hydraulic diameter of the passage. h, for this case, is about 990 J/s m<sup>2</sup> °C (175 BTU/hr ft<sup>2</sup> °F). For a 2-layer 0.2 mm (0.008 in) thick Kynar coated heat exchanger of the chosen configuration, the overall heat transfer coefficient, U<sub>hx</sub> equals 1420 J/s °C m<sup>2</sup> (250 BTU/hr ft<sup>2</sup> °F) of base area.

Due to the low flow rate, pressure drop is less than 0.69 kN/m<sup>2</sup> (0.1 psi).

#### Cold Plate Optimization

The cold plate is identical to the heat exchanger, with the exception that it is not internally Kynar coated.

Optimization was conducted in a method identical to that of the heat exchanger, and the overall heat transfer coefficient U<sub>cp</sub>, is 1760 J/s °C m<sup>2</sup> (310 BTU/hr ft<sup>2</sup> °F) of base area. The surface flatness of the material is much more important than the finish, as surface deviations obtained by grinding can be kept small, on the order of 76 μm (0.000030 in.).

#### Overall Performance Analysis

The overall heat transfer coefficient for the combined heat exchanger and cold plate is determined from the formula:

$$U_{total} = \frac{1}{\frac{1}{U_{HX}} + \frac{1}{U_I} + \frac{1}{U_{CP}}}$$

This calculation resulted in a value of U<sub>total</sub> = 519 J/s °C m<sup>2</sup> (91.5 BTU/hr ft<sup>2</sup> °F).

To evaluate this in terms of the SSP requirements, it is necessary to introduce the concept of log mean temperature difference (LMTD). For a counter-flow heat exchanger, the temperature distribution with distance along the heat exchanger is shown by Fig. 7.

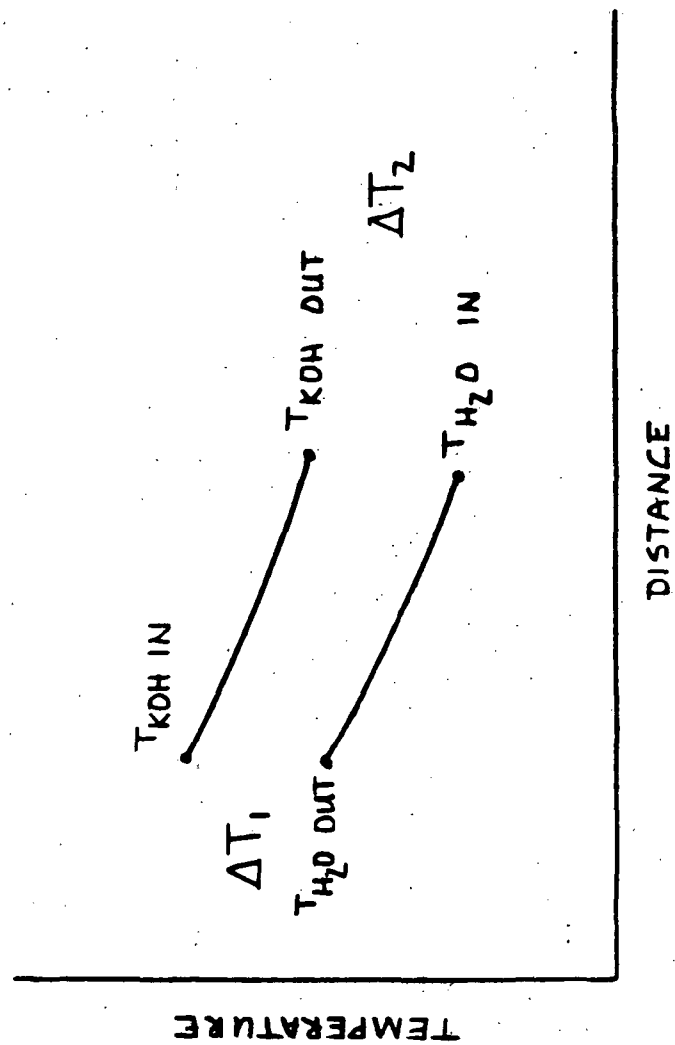


Figure 7 Heat Exchanger Temperature Distribution



LMTD is defined as

$$LMTD = \frac{\Delta T_1 - \Delta T_2}{\ln \frac{\Delta T_1}{\Delta T_2}}$$

Since  $Q = U_{\text{total}} A_{\text{base}} LMTD$ , the LMTD required to transfer 266 watts of heat is  $7.9^{\circ}\text{C}$  ( $14.2^{\circ}\text{F}$ ). The SSP requirements show that a  $7.8^{\circ}\text{C}$  ( $14.0^{\circ}\text{F}$ ) LMTD is available under the worst conditions, and thus the heat exchanger should work properly.

#### Detail Design

The passage plates are machined from one piece each, and then brazed to the base plate to reduce costs and facilitate fabrication. The base plate is initially thicker than required to keep the part from warping during brazing, and to provide sufficient material for machining operations which are conducted after brazing.

The large slots at each end of the plate allow fluid inlet and outlet with simple headers, while still affording access for the Kynar coating which must be applied after the assembly is brazed. The tapped holes allow attachment of the fluid headers without requiring bolting of the interface, thus allowing evaluation of thermal performance as a function of interface pressure. Also, two blind holes are provided in the center of the plate to accept thermocouples and thus give an indication of the temperature close to the interface surface. Nine through bolt holes are provided to allow uniform clamping over the entire interface surface.

Headers are plastic for complete compatibility with the fluid and to eliminate electrolyte problems. A face "O" ring seal assures a leak tight connection. Design of the headers places the fluid inlet and outlet on opposite corners of the plate, thus assuring a uniform distribution of flow within the passages inside the plates.

#### 2.3.3 Manufacture

During manufacture, the passage plates and base plate detail parts for both the heat exchangers and cold plate were machined, and then brazed together. The heat exchanger was internally coated with Kynar and then finish machined. This last operation consisted of drilling the required holes and the finishing of the interface surfaces.

Machining of the slots in the passage plates was accomplished by using a thin, large diameter milling cutter. Some difficulty was experienced as the material did not machine cleanly but tended to be "gummy". This required high tool pressure and caused warpage of the plates. Also, some projection of material was experienced on the side opposite the side being machined. This projection was removed from the passage plate which was to be placed next to the base plate on each assembly, and this was accomplished by grinding the entire surface plate.

Brazing was accomplished by using an 85% gold, 15% nickel alloy and furnace brazing the parts together in an evacuated atmosphere, while clamping pressure was continuously applied.

X-rays taken after brazing showed 100% braze integrity in the center of the assembly. Some small localized voids were noted near the edges, however, These probably were caused by stresses induced in the shearing of the raw stock.

Kynar coating of the interior of the heat exchanger was accomplished by thinning the Kynar and pouring it through the interior passages. Exterior areas were masked and the Kynar was sprayed on. Three coats of Kynar were applied, and each coat was individually cured by heating to about 300°C (550°F). Total Kynar thickness was about 0.5 to 0.8  $\mu\text{m}$  (0.002 to 0.003 in.).

The final machining operation consisted of drilling all the required holes, and the finishing of the interface surface. This latter task was accomplished by grinding. Lapping was tried, but pre-stresses induced during grinding were released, making the surface flatness worse rather than better. On both the heat exchanger and cold plate, the final surface finish was about 0.6  $\mu\text{m}$  (0.6 microinches) and the flatness was within 200  $\mu\text{m}$  (0.008 TIR). This flatness was not sinusoidal in nature, but varied gradually from one end of the plate to the other.

Recommendations for achieving better assemblies in the future include developing an alternate milling procedure which would not warp the passage plates, and the use of larger raw stock so that the portions affected by shearing stresses could be removed.

#### 2.3.4 Test Facility and Procedures

After manufacture, the completed heat exchanger and cold plate assemblies, as shown in Fig. 8, were subjected to a comprehensive test program, with the objective of determination of the actual performance parameters. The program included development of a test schematic and selection of test equipment; development of a test procedure and the actual running of the test including data taking; and a study of the results and conclusions evident upon reduction of the test data.

Important information to be determined from the test included both thermal performance parameters and mechanical parameters. Thermal performance parameters are  $U$  overall,  $U_{HX}$ ,  $U_{CP}$ ,  $U_L$ , flow distribution, and effect of flow velocity. Mechanical parameters are effect of bolting torque, finish and flatness of both heat exchanger and cold plate surfaces, and the coating integrity.

##### Test Schematic & Equipment

A schematic of the test setup is shown by Fig. 9. Also, Figs. 10 and 11 show the actual test setup, both with and without the thermal insulation. The setup consisted of a test station and support rack, and the equipment necessary to separately supply fluid to both the heat exchanger and cold plate.

The heat exchanger fluid loop consisted of a reservoir, a pump, a heater, thermometers to indicate temperature at both inlet and outlet of the heat exchanger, a flowmeter, and various lines and flow control valves. All components of this loop were compatible with KOH.

The centrifugal pump was of the magnetically driven variety, while the heater consisted of an 750 watt, 2.22 cm (0.875 in.) diameter Incoloy sheathed calrod element inside a 3.8 cm (1-1/2 inch) diameter stainless steel tube. Heater power input was controlled by a variac and read on a Weston Model 432 Wattmeter. This unit had both 0-250 and 0-500 watt scales. Heat exchanger inlet and outlet temperatures were measured by 7.6 cm (3 inch) immersion thermometers with  $0.11^{\circ}\text{C}$  ( $0.2^{\circ}\text{F}$ ) divisions. The flow meter was

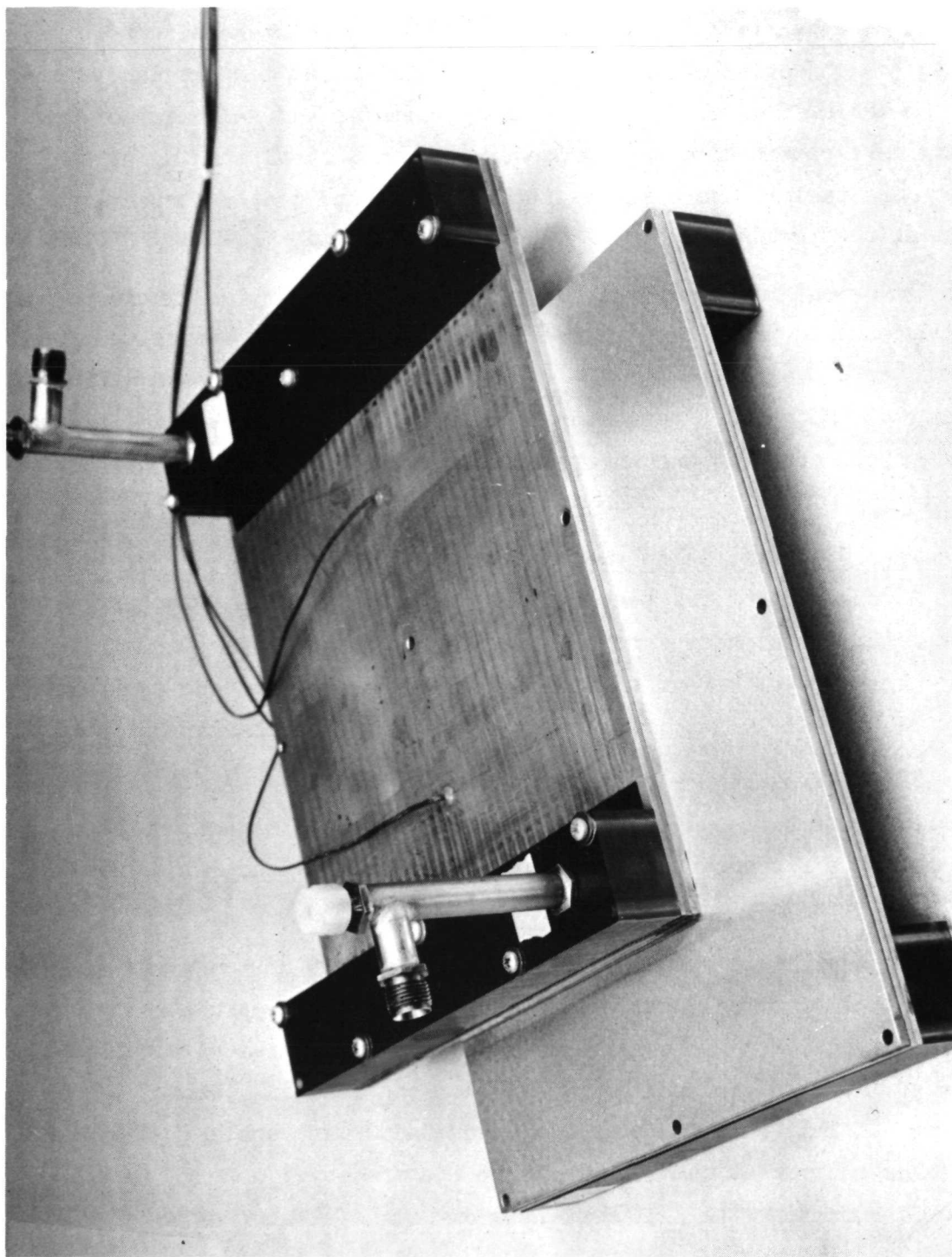


Fig. 8 Prototype Heat Exchanger and Cold Plate Assemblies

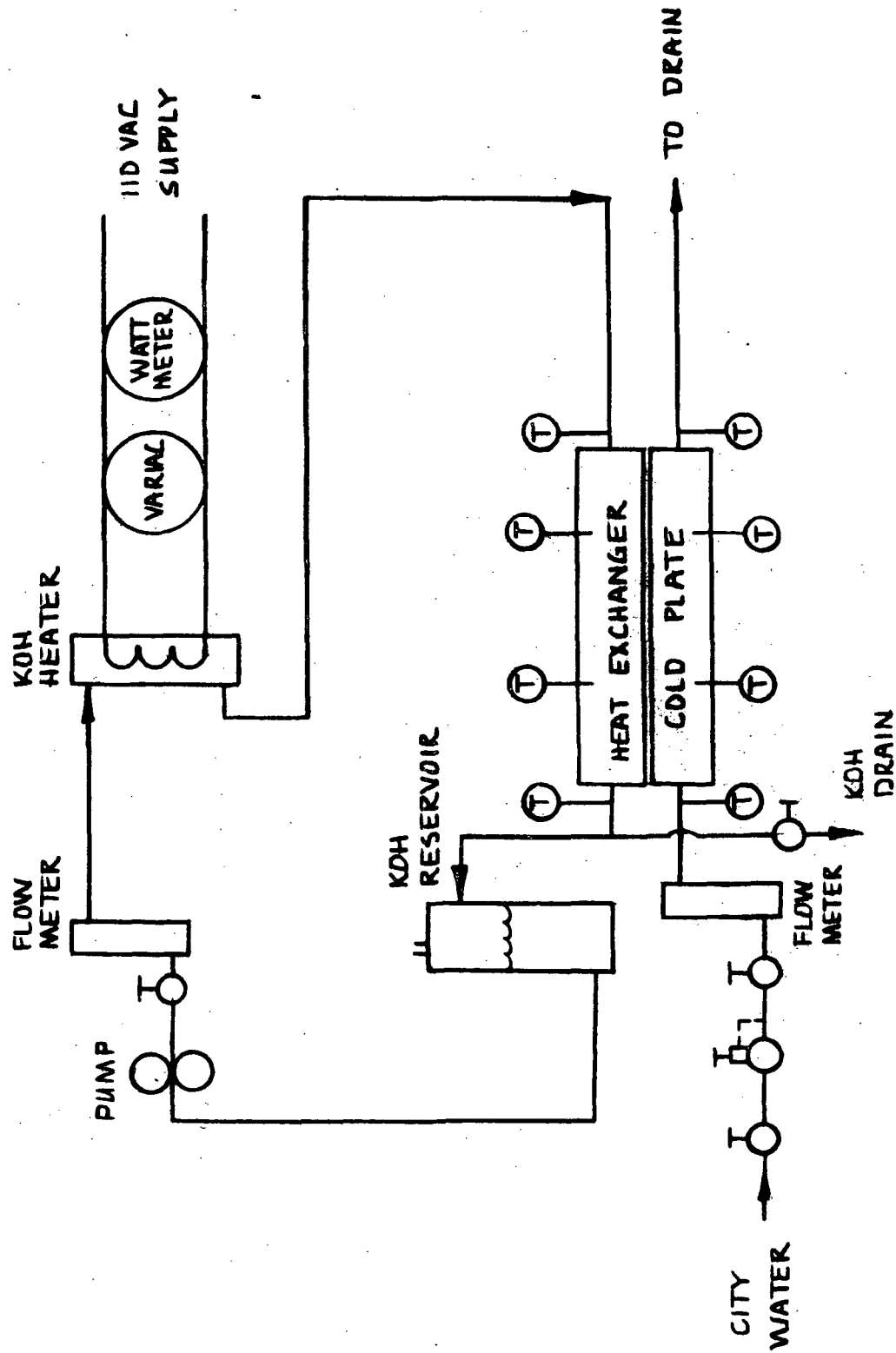


Figure 9 Contact Heat Exchanger Test Schematic

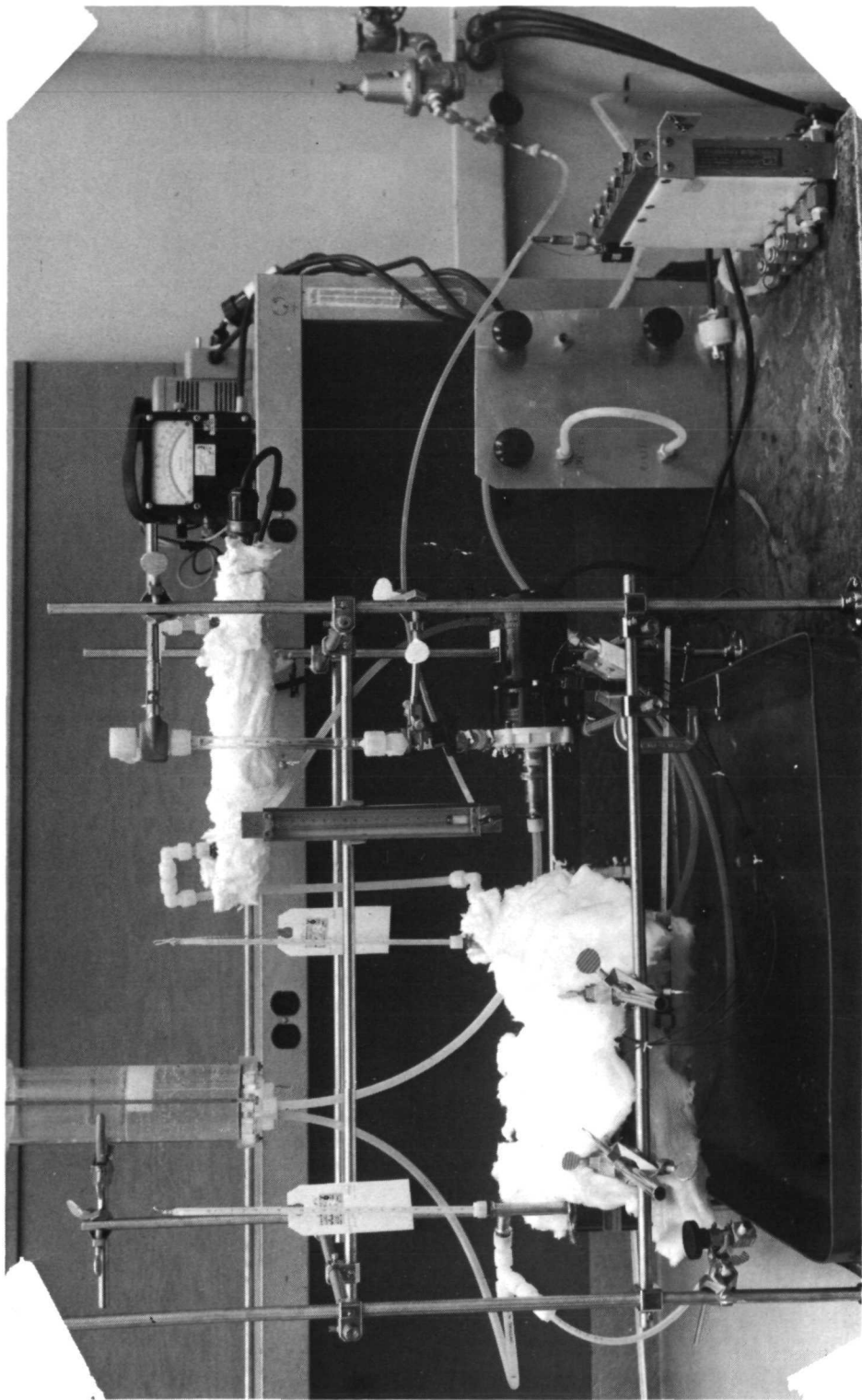


Figure 10 Photograph of Test Setup with Insulation

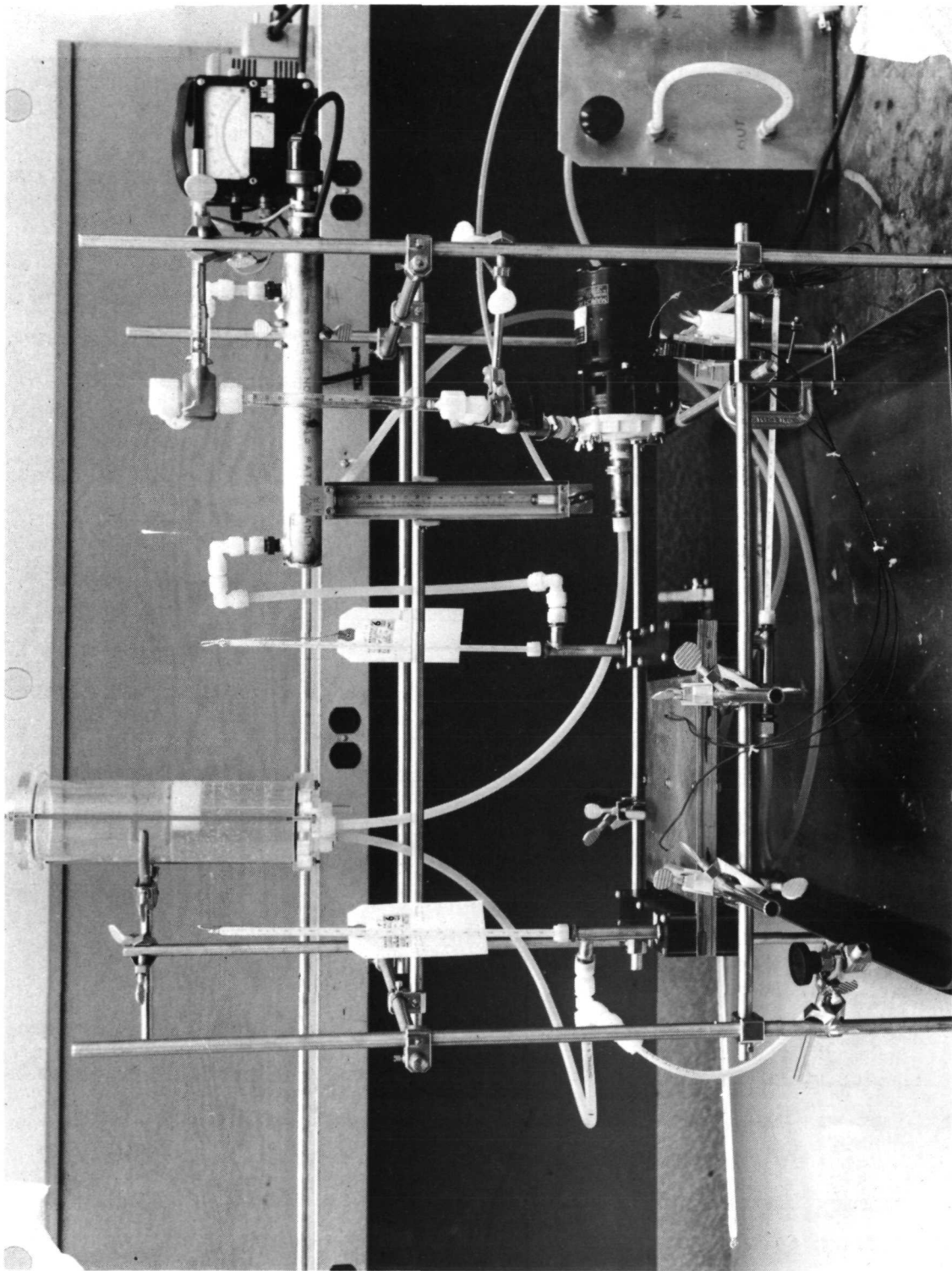


Figure 11 Photograph of Test Setup Without Insulation

a Brooks with a 6-15-2 glass tube and a stainless steel ball. Maximum flow capacity of this meter is  $2 \text{ cm}^3/\text{s}$  (19 GPH) of KOH and  $2.3 \text{ cm}^3/\text{s}$  (22 GPH) of water. Iron constantan thermocouples were imbedded in the heat exchanger and were used in conjunction with a Leeds & Northrop bridge to give temperature close to the interface.

The cold plate fluid loop consisted of a pressure regulator and flow control valve attached to the city water supply, a flowmeter, thermometers, and plumbing. The Watts model U5B pressure regulator was set at about  $240 \text{ kN/m}^2$  (35 psi) and was used to prevent city water line pressure fluctuations from affecting the flow rate in the cold plate. The flow meter, thermometers, and thermocouples were identical to those used in the heat exchanger loop.

#### Test Procedure

Procedures for each run consisted of adjusting the fluid flow rates and power input, allowing the system to thermally stabilize, and taking temperature readings. Recorded data are shown in the Appendix.

Runs 1 and 2 were preliminary checkout runs using water on both sides of the system. Runs 3 to 8 were conducted at the nominal design point with KOH in the heat exchanger, and were intended to establish the effect of interface bolting, and the overall system performance parameters. Run 9 was intended to establish the amount of power added to the system by the circulation pump. Runs 10 to 14 were to establish statistical data for performance calculations. Runs 14 to 20 were to investigate the effect of flow rate on performance parameters. Runs 21 and 22 were to establish the effect of the Kynar coating, and had equal water flow rates in both the heat exchanger and cold plate.

#### 2.3.5 Experimental Results and Conclusions

A summary of actual performance parameters compared to values predicted by the analysis is presented in Table 6. After the completion of testing, an attempt was made to determine all of the significant thermal and mechanical parameters which had not previously been determined. These included the primary thermal performance parameters, the mechanical variables such as the effect of the interface bolting, and the coating integrity and the effect of flow rate on thermal performance.



Table 6

COMPARISON OF TEST & ANALYSIS VALUES  
OF THERMAL PERFORMANCE PARAMETERS

PARAMETER	ANALYSIS	TEST
	PREDICTED VALUE $\text{J/s m}^2 \text{ } ^\circ\text{C}$ ( $\text{BTU/hr ft}^2 \text{ } ^\circ\text{F}$ )	AVERAGE VALUES $\text{J/s m}^2 \text{ } ^\circ\text{C}$ ( $\text{BTU/hr ft}^2 \text{ } ^\circ\text{F}$ )
$U_{\text{overall}}$	520 (91.5)	658 (116)
$U_{\text{interface}}$	1530 (270)	1815 (320)
$U_{\text{HX}}$	1420 (250)	2060 (364)
$U_{\text{CP}}$	1760 (310)	2070 (365)

### Thermal Performance Parameters

Performance parameters determined from the test consisted of the overall, interface, heat exchanger, and cold plate heat transfer coefficients. The first two, the overall and interface coefficients, can be calculated directly from the test data, by the following procedure.

First, the heat input to the system is calculated from the relationship  $Q_{\text{calc}} = \dot{m} C_p \Delta T$  where  $\dot{m}$ ,  $C_p$  and  $\Delta T$  are respectively the cold plate flow rate, fluid specific heat, and inlet to outlet temperature difference. This method is used because the cold plate fluid always was water with a known specific heat, whereas KOH was usually used in the heat exchanger and its specific heat is not known exactly.

Then, the log mean temperature difference (LMTD) is calculated and then overall heat transfer coefficient,  $U_{\text{overall}}$ , is calculated from

$$U_{\text{overall}} = \frac{Q_{\text{calc}}}{(\text{LMTD}) (A)}$$

where

A is the interface area. Also, the interface heat transfer coefficient,  $U_I$ , is calculated from

$$U_I = \frac{Q_{\text{calc}}}{(T_{\text{interface}}) (A)}$$

These were calculated for all runs and are summarized in Table 7. Also, included is the calculated heat input and LMTD. For design point conditions, as in runs 5 to 8 and 10 to 14, the average  $U_{\text{overall}}$  and  $U_{\text{interface}}$  were respectively 670 (118) and 1825 J/s °C m<sup>2</sup> (320 BTU/hr ft<sup>2</sup> °F). The value for  $U_{\text{overall}}$  was fairly consistent, as the thermometers used to measure the fluid temperatures could be read to within 0.056°C (.1°F). The value of  $U_{\text{interface}}$  varied more, however, as thermocouples were used to measure temperatures and it was possible to read these only within 0.27 to 0.56°C (0.5 to 1°F). Also, since the thermocouples were imbedded in the base plate, the recorded value could include some of its resistance in addition to the interface resistance, and, in addition, local hot spots due to surface irregularities could contribute to the inaccuracy of the readings which were taken only at two points.

Table 7

## SUMMARY OF CALCULATED HEAT EXCHANGER DATA

Run Number	P <sub>interface</sub> kN/m <sup>2</sup> (psi)	Q <sub>calculated</sub> watts	LMTD °C (°F)	U <sub>overall</sub> J/s m <sup>2</sup> °C (BTU/hr ft <sup>2</sup> °F)	U <sub>interface</sub> J/s m <sup>2</sup> °C (BTU/hr ft <sup>2</sup> °F)	U <sub>overall</sub> - Corrected J/s m <sup>2</sup> °C (BTU/hr ft <sup>2</sup> °F)
1	0	957	6.23 (11.21)	670 (118.0)	--	
2	0	950	6.48 (11.65)	629 (110.7)	--	
3	0	957	7.09 (12.76)	578 (101.8)	1640 (289.2)	
4	0	957	7.27 (13.08)	564 (99.4)	1640 (289.2)	
5	104 (15)	965	6.12 (11.01)	673 (118.9)	1860 (328.1)	
6	104 (15)	965	6.21 (11.17)	665 (117.2)	1990 (349.5)	
7	208 (30)	980	6.21 (11.17)	675 (119.0)	1680 (295.9)	
8	208 (30)	972	6.18 (11.11)	673 (118.8)	1770 (310.6)	
9	208 (30)	185	1.19 (2.14)	671 (118.1)	1910 (336.0)	
10	208 (30)	994	6.21 (11.17)	686 (120.8)	1700 (300.4)	
11	208 (30)	972	6.30 (11.32)	661 (116.5)	1880 (330.6)	
12	208 (30)	987	6.53 (11.76)	646 (113.9)	1610 (282.0)	
13	208 (30)	994	6.18 (11.10)	690 (121.5)	2020 (360.3)	
14	208 (30)	965	6.11 (11.00)	676 (119.1)	1860 (328.1)	
15	208 (30)	1068	6.18 (11.11)	742 (130.6)	1880 (341.3)	
16	208 (30)	1009	6.30 (11.32)	686 (120.9)	2080 (365.6)	
17	208 (30)	1276	5.40 (9.73)	1010 (177.9)	2180 (385.4)	794 (140.0)
18	208 (30)	1201	5.46 (9.83)	940 (165.7)	1950 (342.8)	782 (138.0)
19	208 (30)	1314	5.56 (10.00)	1012 (178.2)	2380 (419.6)	770 (135.8)
20	208 (30)	1238	5.61 (10.10)	945 (166.4)	2120 (374.1)	765 (135.2)
21	208 (30)	1026	6.10 (10.98)	720 (126.8)	2260 (399.1)	
22	208 (30)	1017	5.70 (10.25)	765 (134.7)	2240 (395.8)	

It was not possible to directly determine  $U_{HX}$  and  $U_{CP}$  from the test data. However, Runs 21 and 22 which used the same fluid and flow rate on both sides, showed that the thin Kynar coating had little effect on the heat transfer, and therefore, the  $U_{HX}$  and  $U_{CP}$  were approximately the same. Using this assumption, the  $U_{HX}$  and  $U_{CP}$  were computed to be  $2060 \text{ J/s m}^2 \text{ }^\circ\text{C}$  ( $364 \text{ BTU/hr ft}^2 \text{ }^\circ\text{F}$ ).

The test values presented in Table 6 are higher than the predicted values in all cases. This is due to the conservative analytical approach taken to assure a high probability of achieving the required performance. The predicted value of interface conductance is higher than anticipated because final machined surfaces were flatter than anticipated. Both the heat exchanger and cold plate had higher film coefficients than assumed, as the design was based on the most conservative laminar flow correlations. Further, the heat exchanger and cold plate overall heat transfer coefficients were closer together than anticipated due primarily to a thinner Kynar coating of  $0.5 - 0.8 \mu\text{m}$  ( $0.002 - 0.003 \text{ in.}$ ) rather than the worst case  $2 \mu\text{m}$  ( $0.008 \text{ in.}$ ) used in the analysis. The flow rate for runs 17 - 20 was evidently inaccurate, as the calculated input power did not correspond to the actual value. Correction of the  $U_{\text{overall}}$  by the ratio of calculated to actual input power is shown in Fig. 13.

#### Effect of Interface Bolting

As can be seen from runs 3 through 8, bolting of the interface tends to increase the overall heat transfer coefficient due to the increased contact pressure. This value is considered more reliable than the calculated interface coefficient as the data used in the analysis is more accurate. With the plate unbolted (runs 3 and 4), the warpage of the plate was such that fairly intimate contact was initially achieved. However, increasing the surface pressure (runs 5 and 6) by tightening all bolts to  $5.75 \text{ cm kg}$  (5 inch pounds), thus producing an average interface contact force of  $104 \text{ kN/m}^2$  (15 psi) improved the overall conductivity from about  $567$  to  $670 \text{ J/s m}^2 \text{ }^\circ\text{C}$  ( $100$  to  $118 \text{ BTU/hr ft}^2 \text{ }^\circ\text{F}$ ). A further increase in bolt torque to  $11.5 \text{ cm kg}$  (10 inch pounds) had no apparent effect on the interface conductivity.

### Coating Integrity

An attempt was made to establish the integrity of the Kynar coating. First, a visual examination of all external and part of the internal surfaces was conducted. No breaks in the coating were observed, although it was impossible to see much in the internal passages. Then a resistance check was made between the heat exchanger shell and the KOH loop, using a resistance bridge. This showed a resistance of about 5 ohms, which is lower than desired. It was not determined however, whether this low resistance was due to many pin holes, or one or more larger gaps in the coating. Subsequent testing of the heat exchanger was successful. However, no conclusive integrity tests are defined as yet.

### Effect of Flow Rate on Thermal Performance

An attempt was made in runs 15 to 20 to establish the effect of flow velocity on thermal performance. Higher flow rates should give higher overall heat transfer coefficients, and indeed, those of runs 15-20 were 56 to 112 J/s m<sup>2</sup> °C (10 to 20 BTU/hr ft<sup>2</sup> °F) higher than those of runs 2 to 14. This variation may be due to measurement accuracy, however, so an exact correlation between flow rate and heat transfer coefficient was not made.

## 2.4 CABIN PO<sub>2</sub> CONTROL

### 2.4.1 Objectives

The cabin pO<sub>2</sub> control technique which was tested in Phase I employed a fixed hydrazine input rate during the portion of the control cycle where nitrogen addition to the cabin was called for; when the cabin pO<sub>2</sub> reached a minimum set point, the hydrazine feed was shut off. The hydrazine feed rate was set so that the pO<sub>2</sub> in the effluent N<sub>2</sub>/O<sub>2</sub> mixture from the electrolysis module would not be driven below a set minimum. Because of this limitation, on hydrazine input rate, the cabin pO<sub>2</sub> was observed to overshoot the control band during the long period of time (usually several hours) required to increase the hydrazine concentration in the electrolyte sufficiently to effect decrease in pO<sub>2</sub>.

Under steady-state conditions, the control of cabin pO<sub>2</sub> achieved in the model system with this technique would be acceptable. A typical cycle of cabin pO<sub>2</sub> at a set control band of 19.3 to 20.0 kN/m<sup>2</sup> (2.8 to 2.9 psia) takes approximately 16 hours with an overshoot to approximately 21.4 kN/m<sup>2</sup> (3.1 psia). However, the control is sluggish and may be a limiting factor in the ability of the system to respond to sudden changes in demand.

The objective of this program task was to modify the control technique so that the hydrazine feed rate is increased to allow a fast ramp of the nitrogen output with two additional set points which cycle the hydrazine feed off at minimum effluent  $pO_2$  levels corresponding to the high and low current modes. This type of control was expected to affect a faster decrease of cabin  $pO_2$  when required and substantially reduce the overshoot.

#### 2.4.2 Control Technique Description

The control logic flow diagram is shown in Figure 12. In operation, the control proceeds as follows: An oxygen partial pressure sensor in the cabin simulator loop has an adjustable control band. When the cabin  $pO_2$  reaches the low limit of the band, hydrazine feed is commanded off and remains off until cabin  $pO_2$  returns to the high limit of the band. At this point, a signal is sent to the sensor monitoring the  $pO_2$  in the anodic gas being supplied to the cabin from the electrolysis cell stack. This block in the logic receives a signal from the current mode status, either high or low current. For each state, this  $pO_2$  sensor has an adjustable low limit. Hydrazine feed is then commanded on or off, depending on the current mode,  $pO_2$  and the limit settings. The selection of the limit settings is dependent upon the current density settings selected for the system. As an example, in test 2 of the system testing, the  $N_2H_4$  was shut off at an oxygen partial pressure of  $23.9 \text{ kN/m}^2$  (3.47 psia) for the low current density setting of  $50 \text{ mA/cm}^2$ , and at  $62.5 \text{ kN/m}^2$  (9.06 psia) for the high current density setting of  $150 \text{ mA/cm}^2$ . In Figures 17 and 18, the high and low cycle switch over can be seen directly on the cabin  $pO_2$  curve. The point at which the slope increases is one from low to high current. The change to a lower slope is from high to low current. The results of the testing of this  $pO_2$  control technique are presented and discussed in Section 2.5.

### 2.5 SYSTEM TESTING

#### 2.5.1 Test Plan and Procedure

The system test plan was established to meet the following objectives:

- o Checkout testing of the new  $pO_2$  control circuit logic
- o Determination of the maximum hydrazine feed rate compatible with the controls
- o Evaluation of the effect of cabin  $pO_2$  control band on  $pO_2$  cycle time

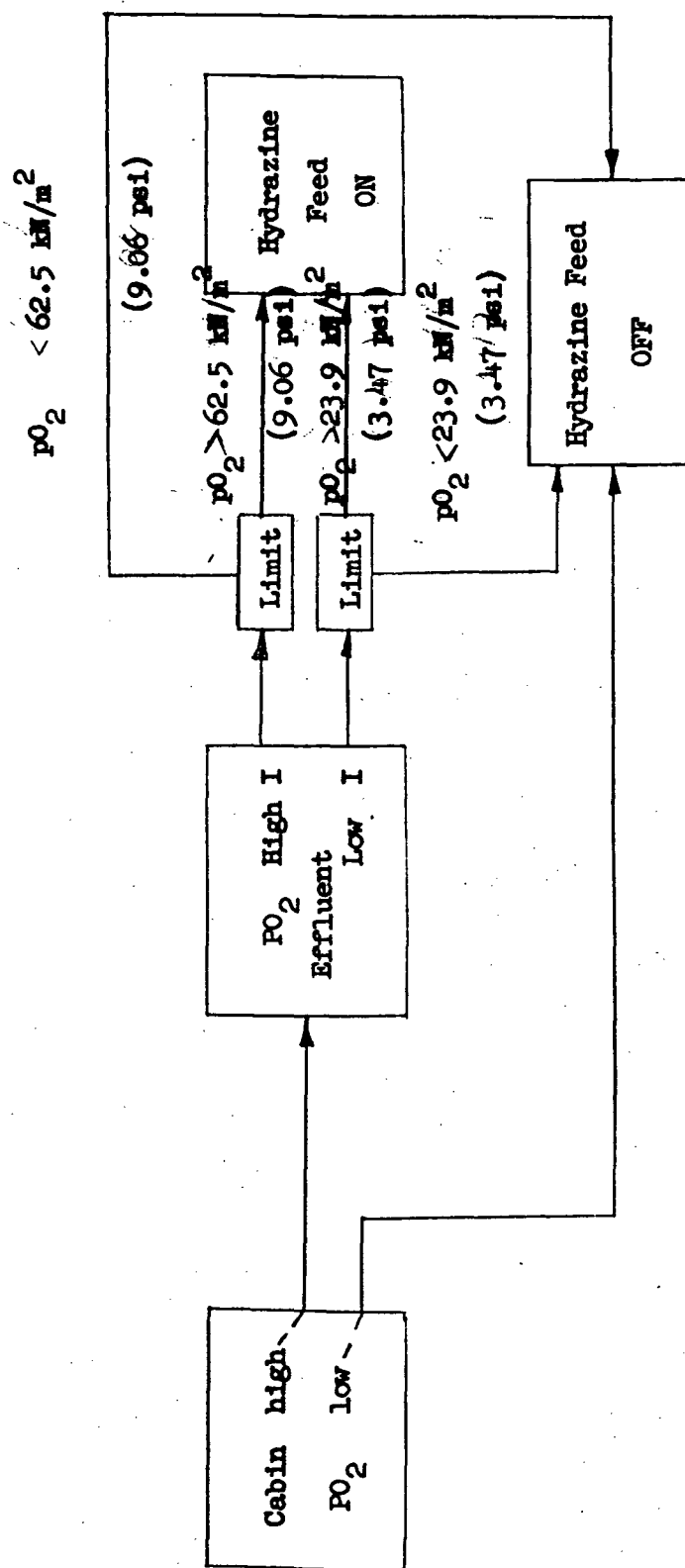


Figure 12 Cabin  $pO_2$  Control Logic Diagram

- o Optimization of current levels to achieve a more responsive  $pO_2$  cycle
- o Evaluation of system response to step changes in  $N_2/O_2$  demand
- o Parametric temperature and current evaluation
- o Identification of the chemical constituents of the generated gases
- o Demonstration of zero-gravity operational components

A complete description of the breadboard system and the operating procedures is given in the Phase I report, NASA CR 114912. Modifications in the system which were implemented to effect the new  $pO_2$  control technique, and to incorporate the zero-gravity bubble separator, are reflected in the updated schematic shown in Figure 13. Incorporation of the new cabin  $pO_2$  control technique, in which the hydrazine feed is set high to rapidly ramp the concentration, necessitated the addition of a second reservoir (as a test expediency) in the electrolyte loop to absorb the volume change due to hydrazine addition. In a full-scale system, the reservoir would be properly sized to handle this volume excursion.

To allow incorporation of the prototype dynamic vortex bubble separator device in the system, the reservoir was moved from the inlet to the discharge side of the electrolysis cell stack. A vacuum pump and regulator were installed on the vortex bubble separator gas discharge line to maintain the necessary gas/electrolyte differential pressure. In a full scale system, the reservoir pressure would be high enough to allow the bubble separator gas to vent directly at cabin ambient pressure. The vortex separator was installed in the system prior to the start of Test 4.

The plastic sheel-and-tube heat exchanger which was used in the system in Phase I was replaced with the prototype contact heat exchanger before the start of testing.

Changes in the system requirements for Phase II of the program were made at the direction of the NASA technical monitor. These changes required a re-analysis of the breadboard  $N_2/O_2$  system operating conditions and operating ranges. Because of the addition of a maximum metabolic oxygen requirement and the change from a 12-man to a 6-man full-scale system (leakage allocation for



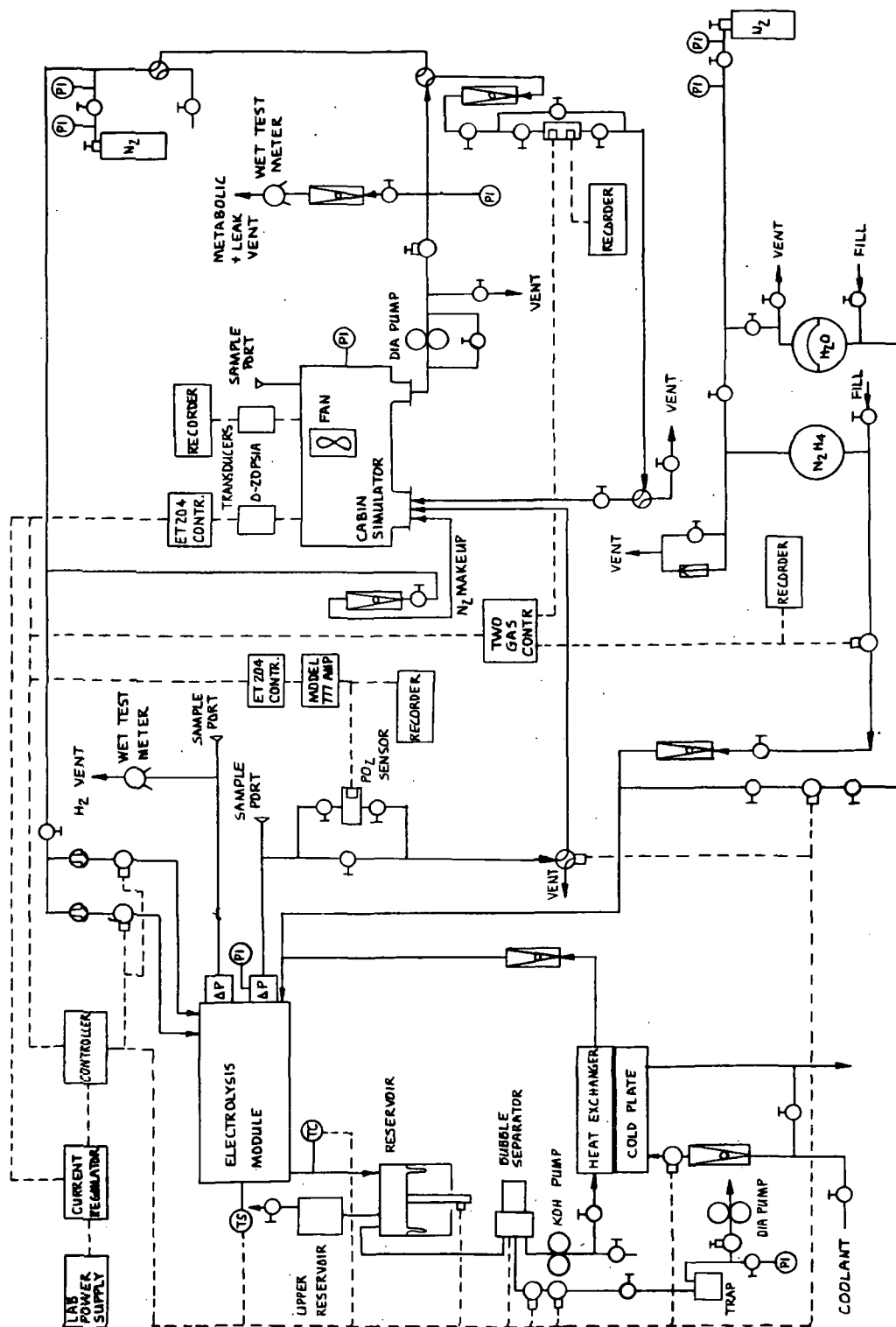


Figure 13 Updated  $O_2/N_2$  Breadboard System Schematic

the breadboard is now 1/6 rather than 1/12 of the total cabin leakage), the existing 17-cell electrolysis stack has, at its optimum current density of 150 mA/cm<sup>2</sup>, an output capacity of 78 percent of the maximum one-man metabolic and leakage load. A summary of the new requirements is given in Table 8.

#### 2.5.2 System Test Summary

A summary of the system testing results is presented in Table 9. Prior to the start of these tests, a preliminary checkout period was devoted to calibration of sensors and flowmeters, setting of sensor control and limit points, and a 2.5-hour operational test of the electrolysis cell stack.

The objectives of the first system test were to determine the maximum hydrazine feed rate possible with the new cabin pO<sub>2</sub> control technique and the new cabin pO<sub>2</sub> control characteristics. Summary results showing cabin total pressure and pO<sub>2</sub> control are given in Figure 14.

In Test 2, the conditions of Test 1 were repeated except that the cabin pO<sub>2</sub> control band was reduced in half in an effort to reduce pO<sub>2</sub> cycle time. Summary results of this test are shown in Figure 15.

There were two objectives in Test 3; namely, to determine the effect of increasing the low mode current and to determine the cabin atmosphere control characteristics under varying metabolic and leakage loads. Results of this test are shown in Figure 16.

Test 4 was conducted without the cabin simulator, with generated gases being vented to ambient. The objectives of the test were to obtain steady-state parametric data regarding operating temperature and current density, and to make a comprehensive analysis of the chemical composition of the generated gases. Detailed test results are discussed in Section 2.5.3.

The last test period, Test 5, was devoted to a long-term test of zero-gravity closed loop operation. Of primary interest was the performance of the vortex bubble separator, its ability to operate automatically for long periods of time, and its effectiveness in preventing electrolyte carryover during start-stop operation.

Table 8  
SYSTEM OPERATING REQUIREMENTS

Condition	1	2	3	4	5
Metabolic Oxygen	kg/day (lb/day)	5.01 (11.04)	5.01 (11.04)	6.97 (15.36)	6.97 (15.36)
Cabin Leakage	kg/day (lb/day)	2.27 ( 5.00)	.907 ( 2.00)	2.27 ( 5.00)	4.54 (10.00)
Oxygen Leakage	kg/day (lb/day)	.56 ( 1.23)	.20 ( .45)	.56 ( 1.23)	1.16 ( 2.46)
Nitrogen Leakage	kg/day (lb/day)	1.71 ( 3.77)	.68 ( 1.51)	1.71 ( 3.77)	3.42 ( 7.54)
O <sub>2</sub> eq N <sub>2</sub> Leakage	kg/day (lb/day)	1.95 ( 4.31)	.78 ( 1.73)	1.95 ( 4.31)	3.91 ( 8.62)
Total Eq O <sub>2</sub>	kg/day (lb/day)	7.52 (16.58)	6.01 (13.26)	9.48 (20.90)	11.99(26.44)
Scale Factor	0.1305				
Total Eq O <sub>2</sub>	kg/day (lb/day)	0.98 ( 2.16)	0.78 ( 1.73)	1.24 ( 2.73)	1.56 ( 3.45)
Current	Amps	8.45	6.75	10.6	13.5
Current Density	mA/cm <sup>2</sup>	126	75	118	150
Total Oxygen Generated	kg/day (lb/day)	0.73 (1.60)	0.68 (1.51)	0.98 (2.16)	1.05 (2.32)
Total Nitrogen Gen.	kg/day (lb/day)	.223 (.492)	.103 (.226)	.223 (.492)	.447 (.985)
Conditions:	1 Normal metabolic - normal leakage	Maximum Metabolic O <sub>2</sub> Rate	6.97 kg/day (15.36 lb/day)		
	2 Normal metabolic - maximum leakage	Maximum Leakage	4.54 kg/day (10.00 lb/day)		
	3 Normal metabolic - minimum leakage	Leakage O <sub>2</sub>	1.12 kg/day ( 2.46 lb/day)		
	4 Maximum metabolic - normal leakage	Leakage N <sub>2</sub>	3.42 kg/day ( 7.54 lb/day)		
	5 Maximum metabolic - maximum leakage	Leakage N <sub>2</sub> (N <sub>2</sub> $\frac{28}{32}$ ) =			
		O <sub>2</sub> Equivalent	3.91 kg/day ( 8.62 lb/day)		
Maximum Current Density	150 mA/cm <sup>2</sup>				
Cell Area	90 cm <sup>2</sup>				
Stack	17 unit cells				
Stack Oxygen Rate @ 150 mA/cm <sup>2</sup>	1.56 kg/day (3.45 lb/day)				
Scale Factor	1.56 kg/day / 12 kg/day				
Man Rating (6)	(.1305)				
		Total O <sub>2</sub> Equivalent	12.00 kg/day (26.44 lb/day)		

Table 9

## SYSTEM TEST RESULTS SUMMARY

Test No.	Duration (Hours)	Objective	Summary Results
1	68	Determine maximum hydrazine feed rate.  Determine $\text{pO}_2$ control characteristics.	Maximum $2.3 \text{ cm}^3/\text{min}$ . Higher rates drive effluent $\text{pO}_2$ below low mode limit. Average cycle time: 10.7 hours. Amplitude: $2.34 \text{ kN/m}^2$ (3.4 psi).
2	96	Decrease $\text{pO}_2$ cycle time by tightening cabin $\text{pO}_2$ control band.	Decreased $\text{pO}_2$ control band from $1.38$ to $0.69 \text{ kN/m}^2$ (.1 psi). $\text{pO}_2$ cycle time decreased from 10.7 to 8.8 hours.
3	92	Determine effect of increasing low mode current.  Evaluate effects of step changes in $\text{N}_2/\text{O}_2$ demand.	Increased low mode from 50 to $70 \text{ mA/cm}^2$ . $\text{pO}_2$ cycle time decreased from 8.8 to 6 hours.  $\text{pO}_2$ control maintained under all conditions tested.
4	92	Parametric temperature and current tests.  Chemical composition of generated gases.	Increasing current increases hydrazine reaction rate. Temperature effects not well defined. Trace amounts of nitrogen compounds.
5	811	Demonstrated closed loop zero-g type operation.	Excellent performance of zero-g bubble separator.

$P_{Total}$  (psia)  
 Max/Min.  
 15.0  
 14.0

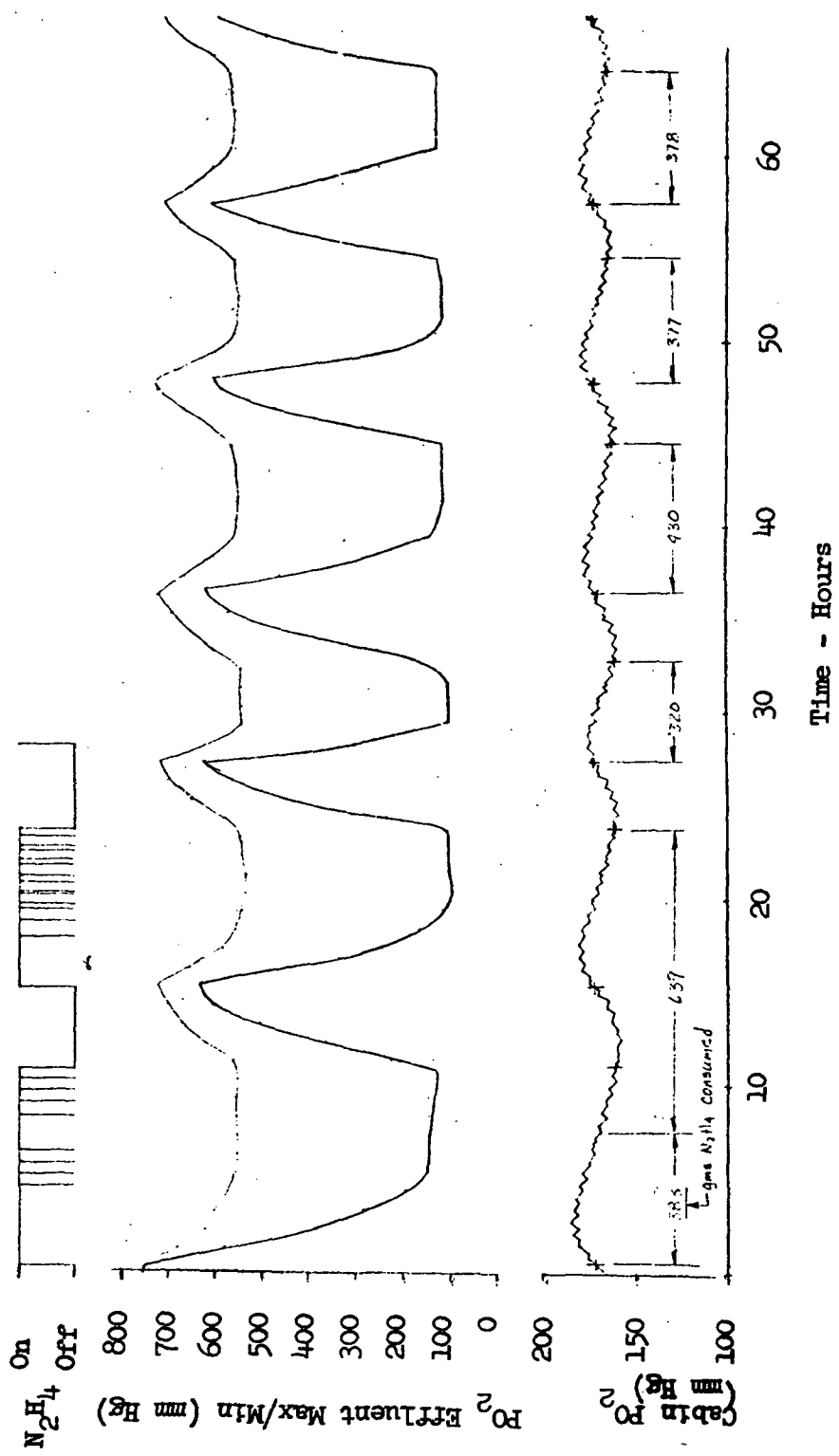


Fig. 14 Test 1 Summary Results

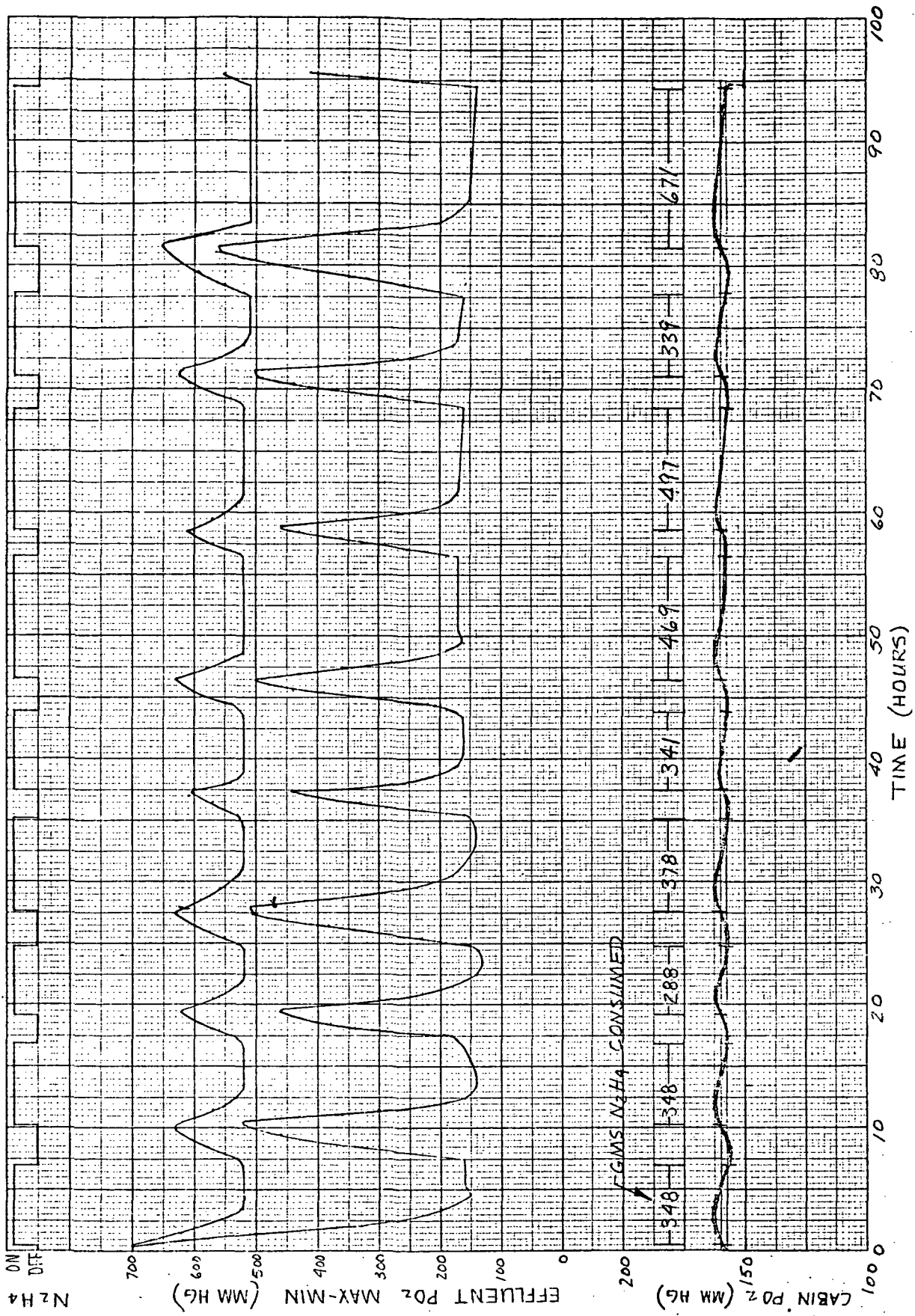


Fig. 15 Test 2 Results

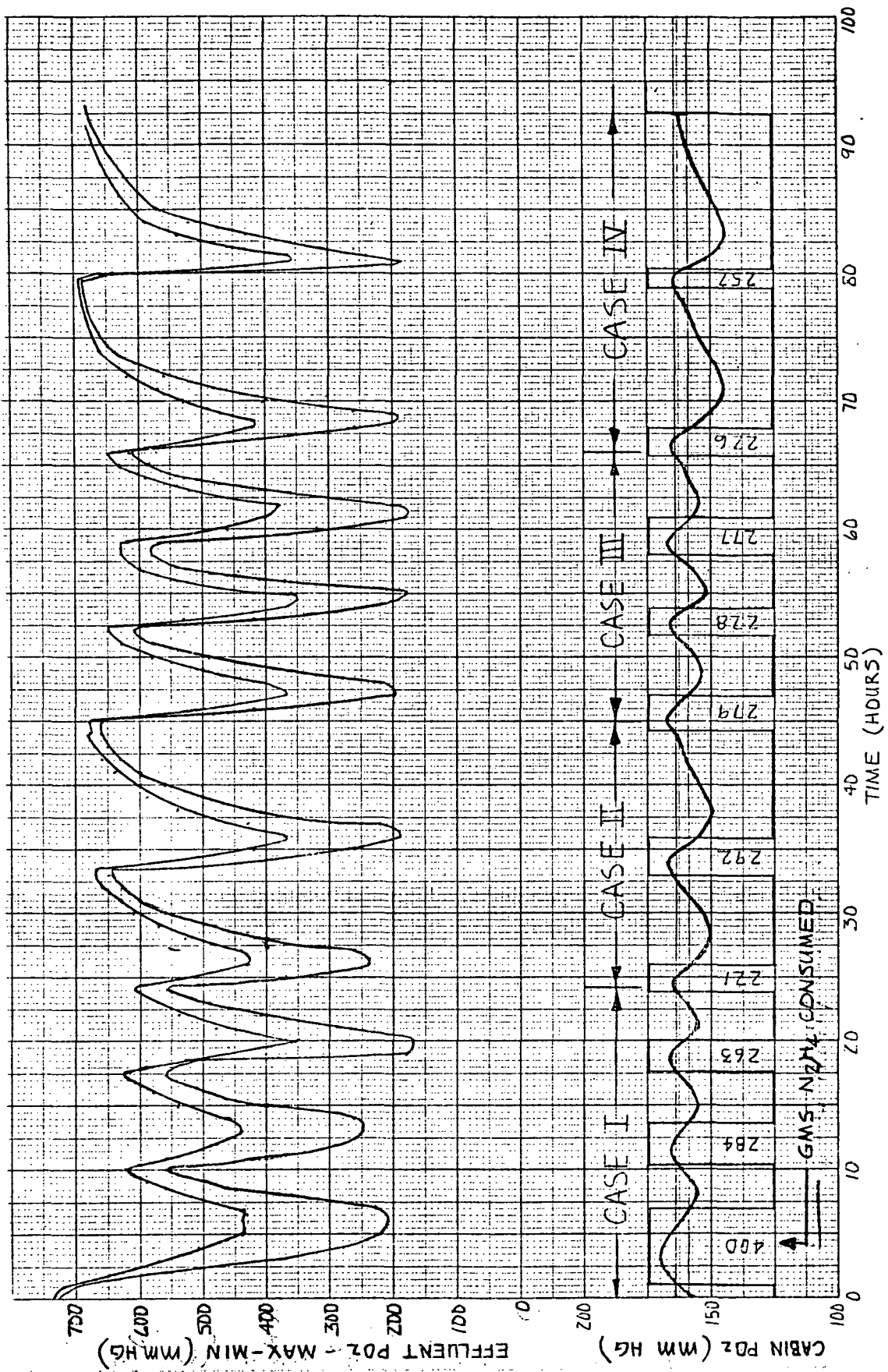


Fig. 16 Test 3 Results

### 2.5.3 Test Results and Discussion

The test results are presented in this section in the form of summary test logs and performance plots. Analyses of the test results are presented in the last part of the section. Detailed test logs are included in the Appendix.

#### 2.5.3.1 Test Logs and Performance Data

Test 1.- The first test was run at the design point conditions, i.e., normal metabolic and leakage loads. The test conditions are presented in Table 10. The duration of the test was 68 hours. A summary test log is given in Table 11.

The hydrazine feed rate was varied during the first 24 hours of the test to determine the maximum allowable without driving the effluent  $pO_2$  below  $13.3 \text{ kN/m}^2$  (1.93 psi). This limit was arbitrarily set as the safe operating minimum. From the performance data shown in Figure 17, it can be seen that the effluent  $pO_2$  was substantially undershooting the low mode limit of  $23.9 \text{ kN/m}^2$  (3.5 psi). This large an effect had not been anticipated, and it resulted in limiting of the hydrazine feed rate to  $2.33 \text{ cm}^3/\text{min}$ . This effect is discussed in more detail in Section 2.5.3.2.

For the conditions selected for Test 1, the cabin  $pO_2$  control characteristics were an average cycle time of 10.7 hours and an amplitude of approximately  $2.35 \text{ kN/m}^2$  (0.34 psi). This represents an improvement over the control characteristics achieved in Phase I with the original control technique, however, a direct comparison cannot be made because the leakage loads are different.

Test 2.- The next test was conducted at the same conditions as Test 1, except that the cabin  $pO_2$  control band was reduced by a factor of two in an effort to reduce the cabin  $pO_2$  cycle time. The test was run for a total of 96 hours. As shown in the performance plot, Figure 18, the average  $pO_2$  cycle time during the first five cycles was approximately 8.8 hours, as compared to 10.7 hours in Test 1. An anomalous shift in  $pO_2$  cycle time after the first five cycles was observed. As this was the last cycle of the test, there is no indication that it represented a permanent shift in performance. A possible explanation would be an increase in the bleed rate from the tank. However, this was not confirmed. A summary test log is given in Table 12.



Table 10

## TEST 1 OPERATING CONDITIONS

## Normal Metabolic and Leakage Loads

Low Current	50 mA/cm <sup>2</sup>	
High Current	150 mA/cm <sup>2</sup>	
N <sub>2</sub> Makeup	1050 cm <sup>3</sup> /min	(.386 lb/day)
Meta/Leak (Cabin gas)	1566 cm <sup>3</sup> /min	(.597 lb/day)
KOH flow	500 cm <sup>3</sup> /min	
N <sub>2</sub> H <sub>4</sub> flow	1.81 to 2.90 cm <sup>3</sup> /min	
pO <sub>2</sub> Effluent Limits:		
High	62.5 - 65.0 kN/m <sup>2</sup>	(9.06-9.42 psi)
Low	23.9 kN/m <sup>2</sup>	(3.47 psi)
Cabin pO <sub>2</sub> Control Band	21.7-23.0 kN/m <sup>2</sup>	(3.14-3.34 psi)
Cabin P <sub>Total</sub> Control Band	99.3-99.9 kN/m <sup>2</sup>	(14.4-14.5 psi)

Table 11  
TEST 1 TIME/EVENT LOG

Elapsed Time (Hr.)	Events/Action	Comments
6.0	Adjusted high mode currents.	Currents had been drifting upward. Test equipment characteristic.
7.5	Recharged $N_2H_4$ tank; consumption 383 g.	Procedure.
20.0	Changed $N_2H_4$ flowmeter reading from 8.0 to 10.0 (scale units).	To determine effect of high flow rate.
21.0	Changed $N_2H_4$ flowmeter reading from 10.0 to 8.0.	Flow reading of 10 too high; effluent $pO_2$ undershooting in low mode.
23.5	Changed $N_2H_4$ flowmeter reading from 8.0 to 9.0.	Continuing flow rate investigation.
24.0	Recharged $N_2H_4$ tank; consumption 639 g.	Procedure.
29.0	Changed high mode $pO_2$ effluent limit from 65.2 to 62.5 kN/m <sup>2</sup> (9.45 to 9.05 psi).	For test evaluation.
33.5	Recharged $N_2H_4$ tank; consumption 320 g.	Procedure.
38.5	Low $P_{total}$ set point adjusted to normal.	Drift in set point had been observed.
43.7	Analyzed electrolyte sample; $N_2H_4$ at 2.51M.	Procedure.
44.5	Recharged $N_2H_4$ tank; consumption 430 g.	Procedure.
47.3	Analyzed electrolyte sample; $N_2H_4$ at 0.94M.	Procedure.
55.0	Recharged $N_2H_4$ tank; consumption 377 g.	Procedure.
59.0	Adjusted high mode currents.	Currents had been drifting upwards.
64.0	Analyzed electrolyte sample; $N_2H_4$ at 2.7M.	Procedure.
64.5	Drained $N_2H_4$ tank; consumption 378 g.	Procedure.
67.6	Deactivated $N_2H_4$ feed.	Insufficient time remaining in test to complete another cycle.
67.7	Analyzed electrolyte sample; $N_2H_4$ at 0.78M.	Procedure.

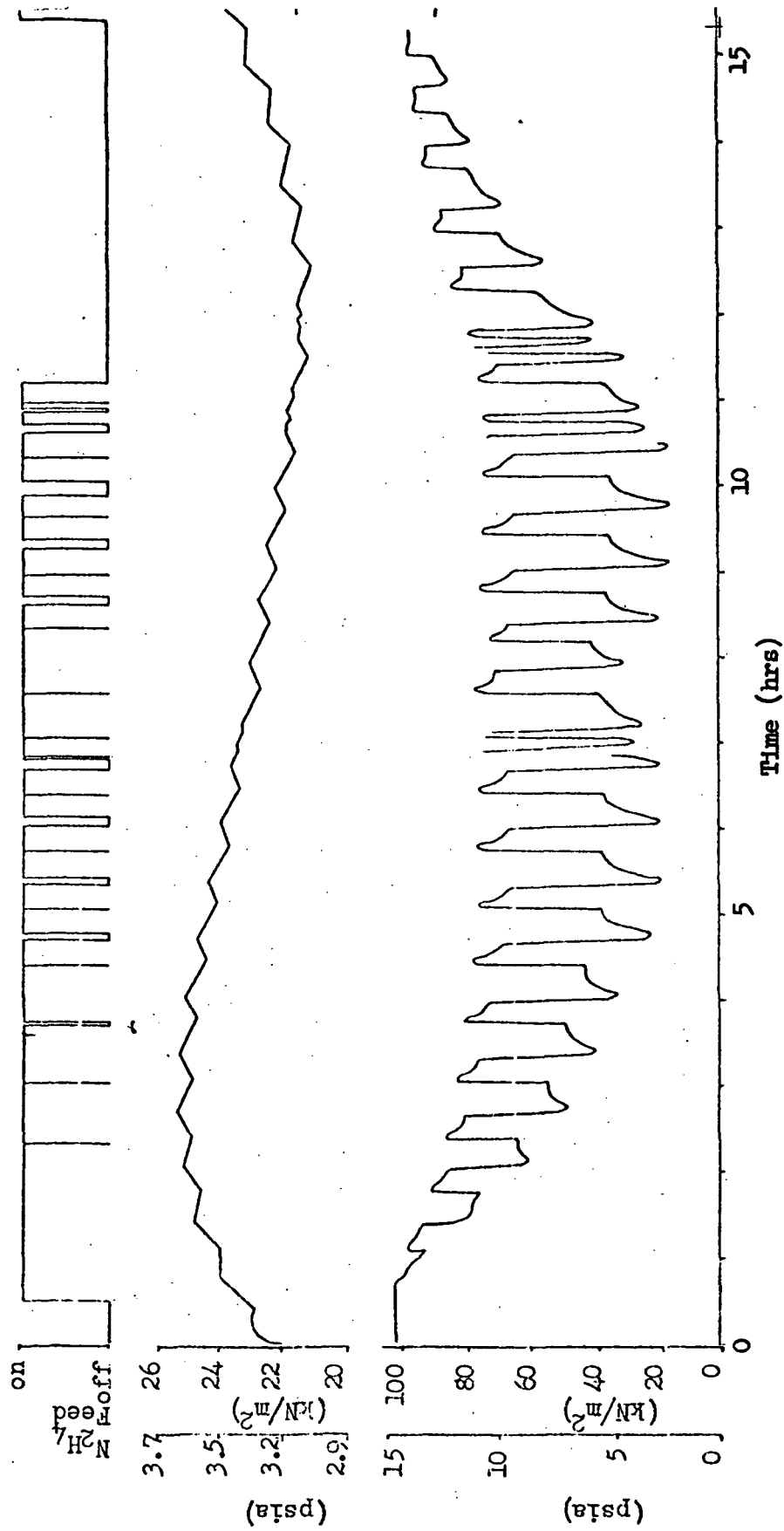


Fig. 17a Test 1 Performance Plot

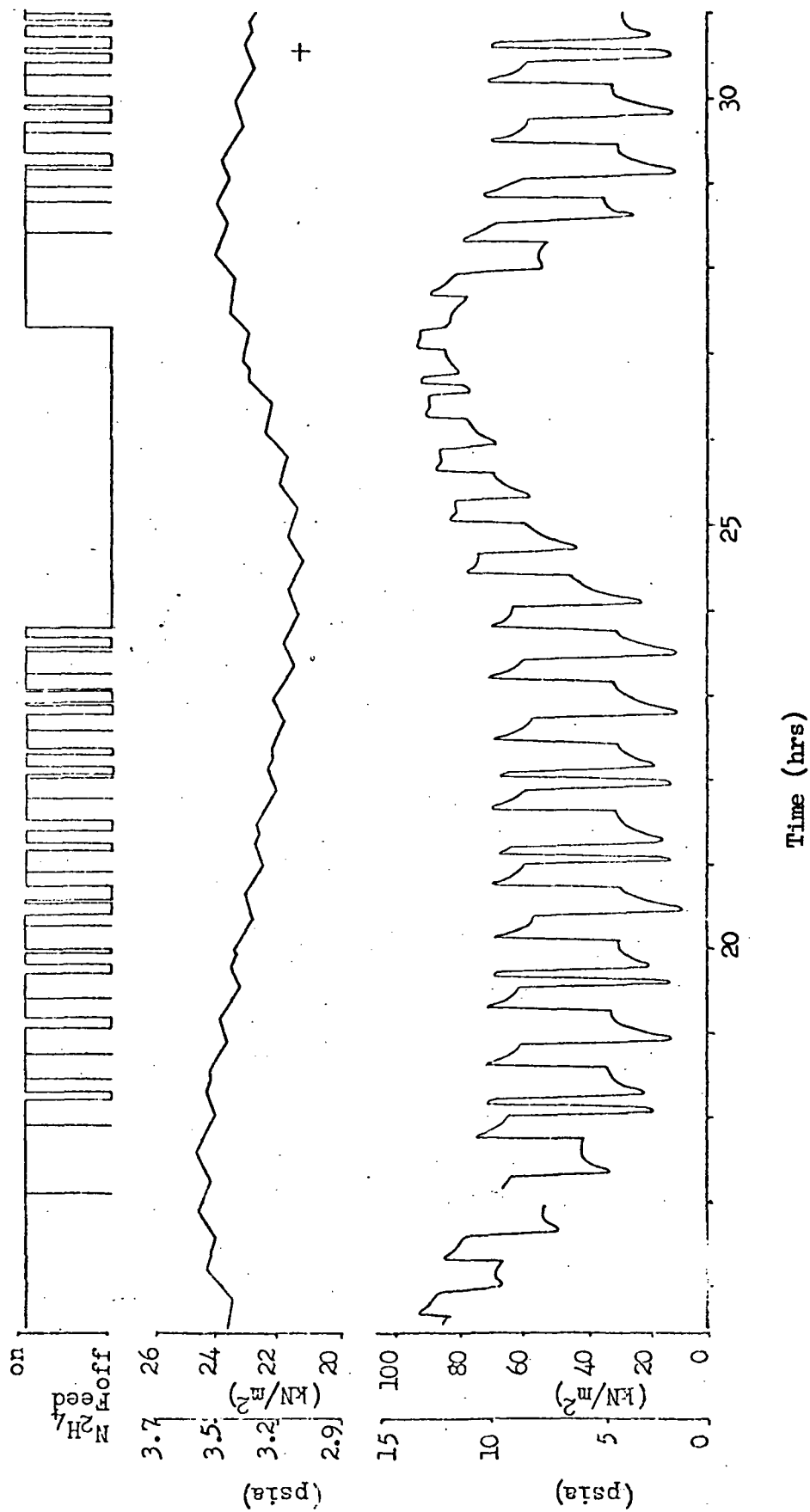


Fig. 17b Test 1 Performance Plot

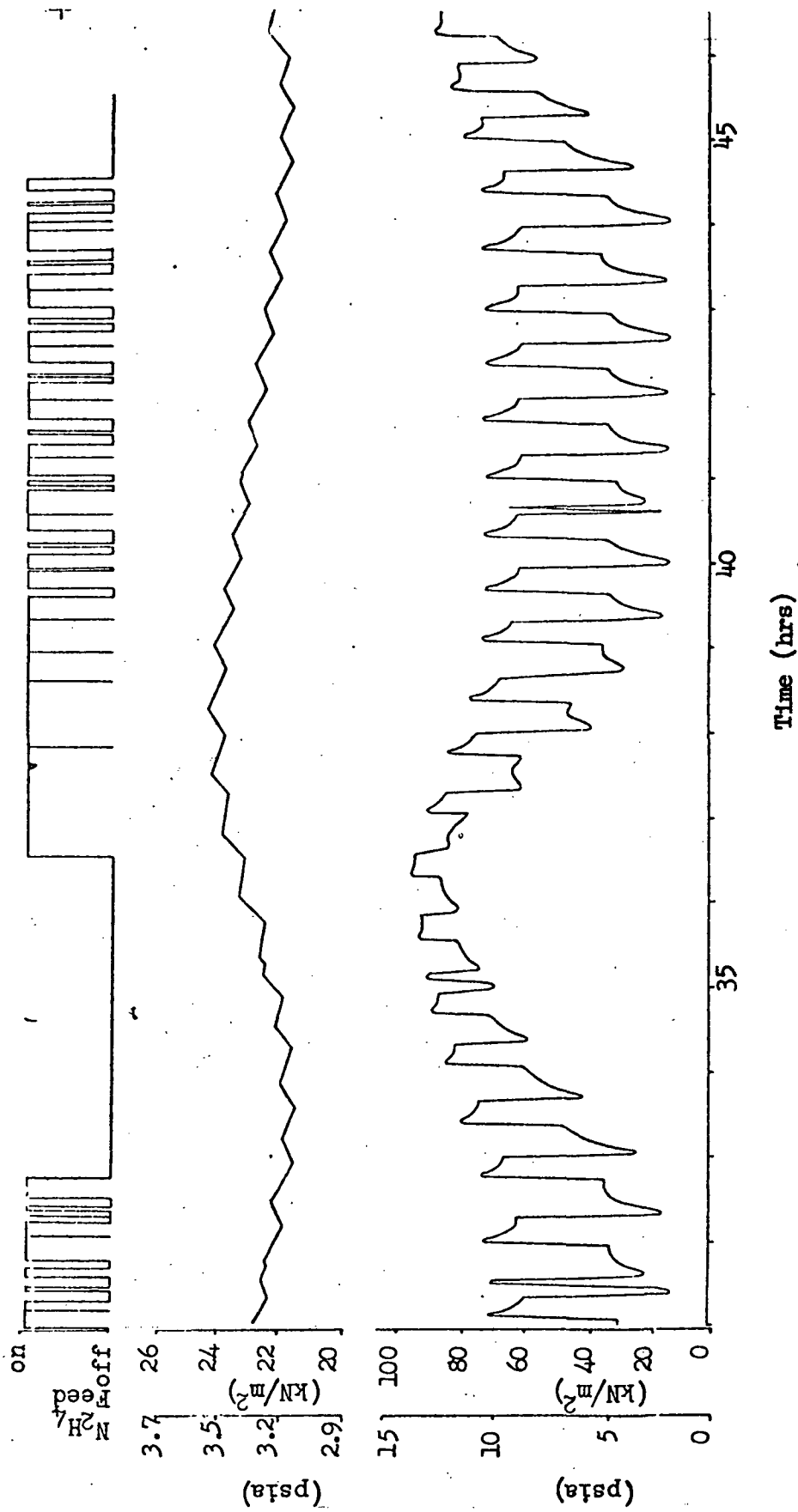


Fig. 17c Test 1 Performance Plot

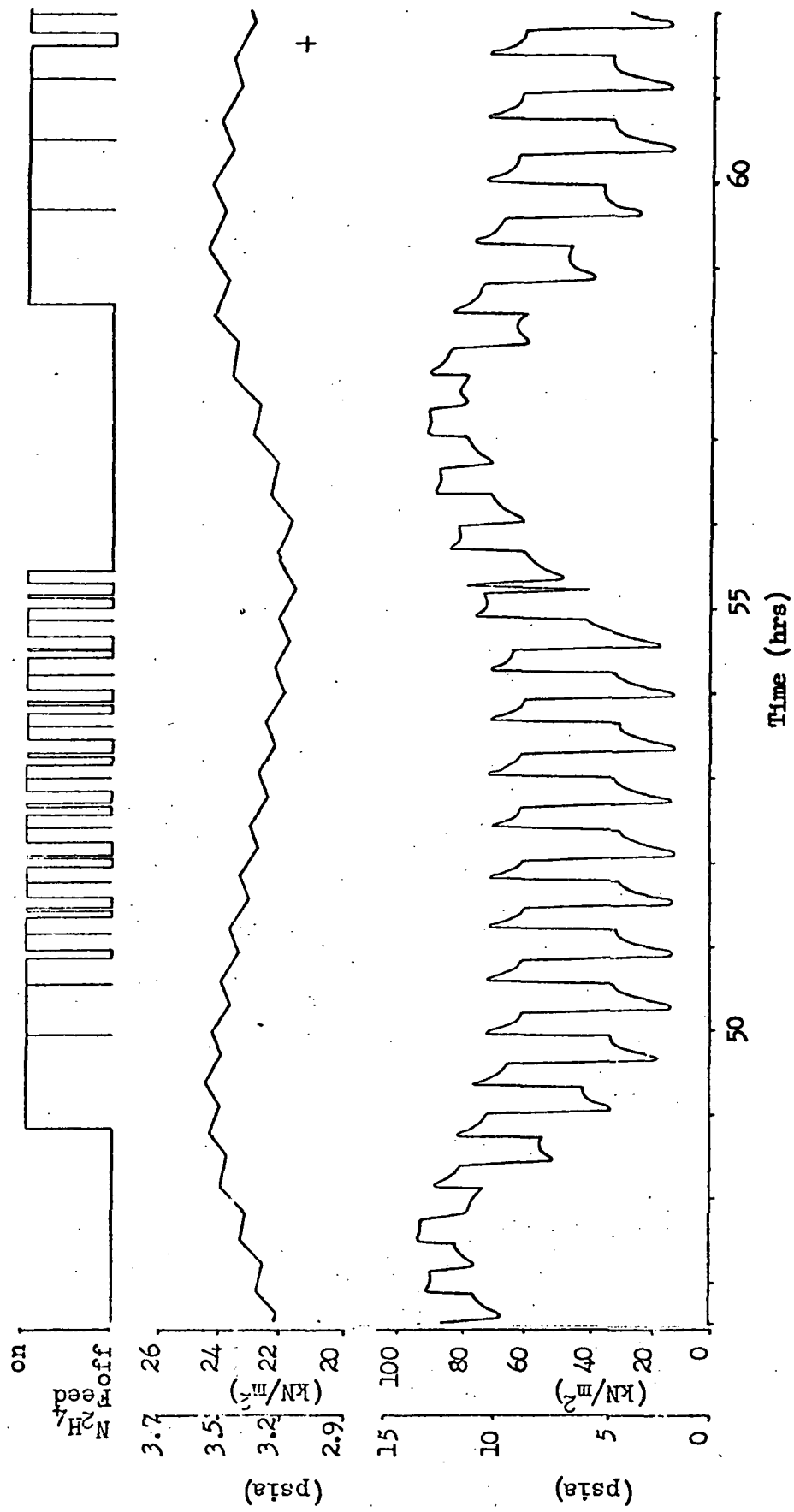


Fig. 17d Test 1 Performance Plot

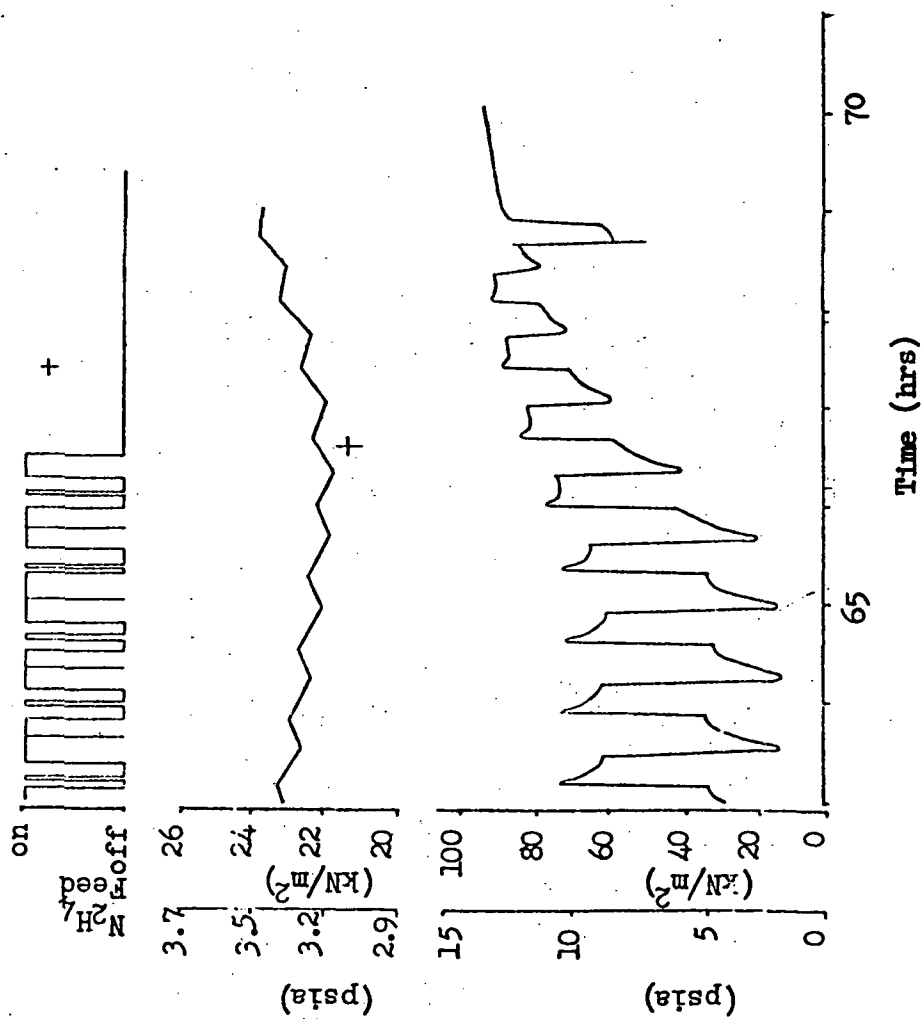


Fig. 17e Test 1 Performance Plot

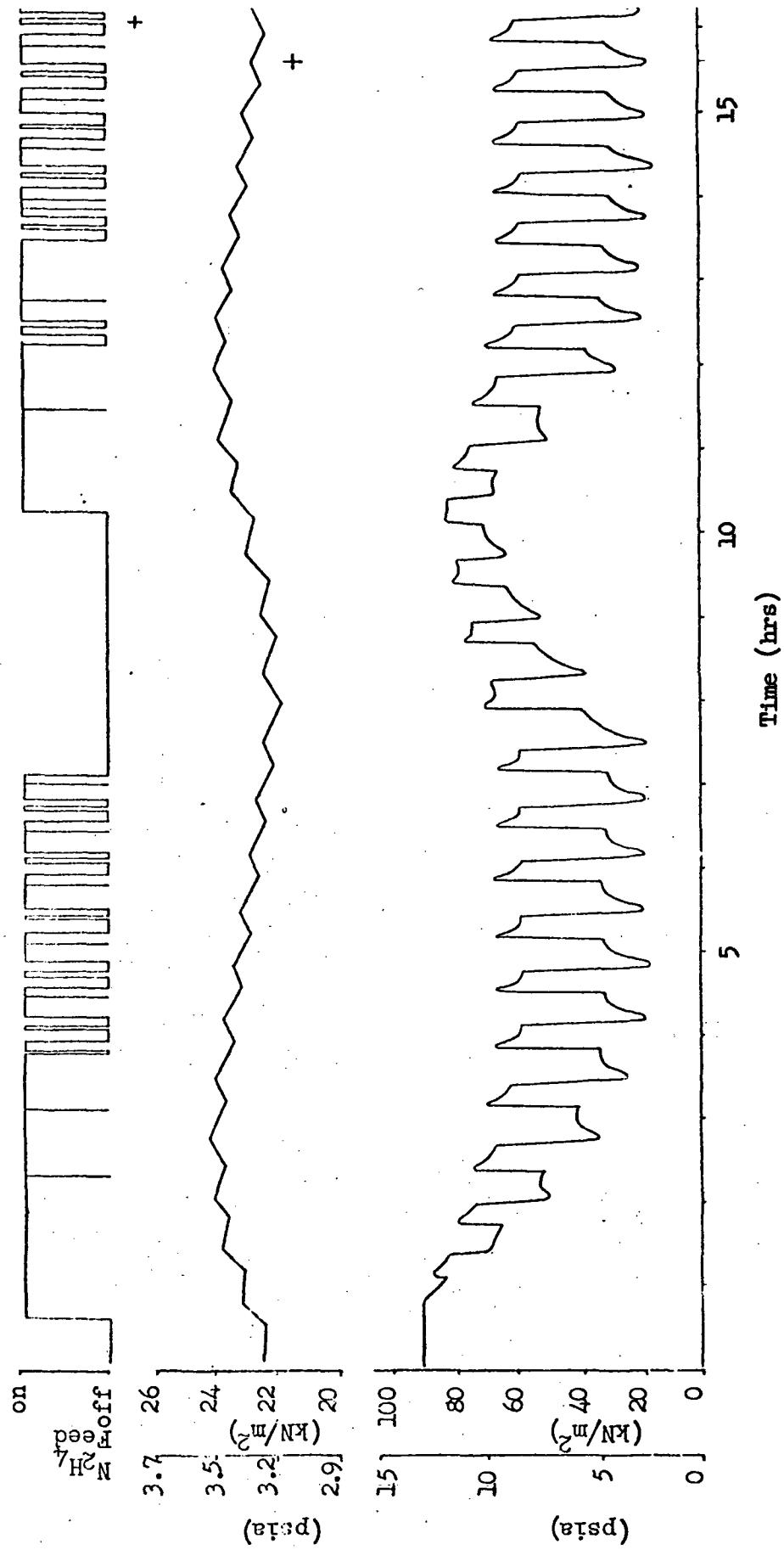


Fig. 18a Test 2 Performance Plot



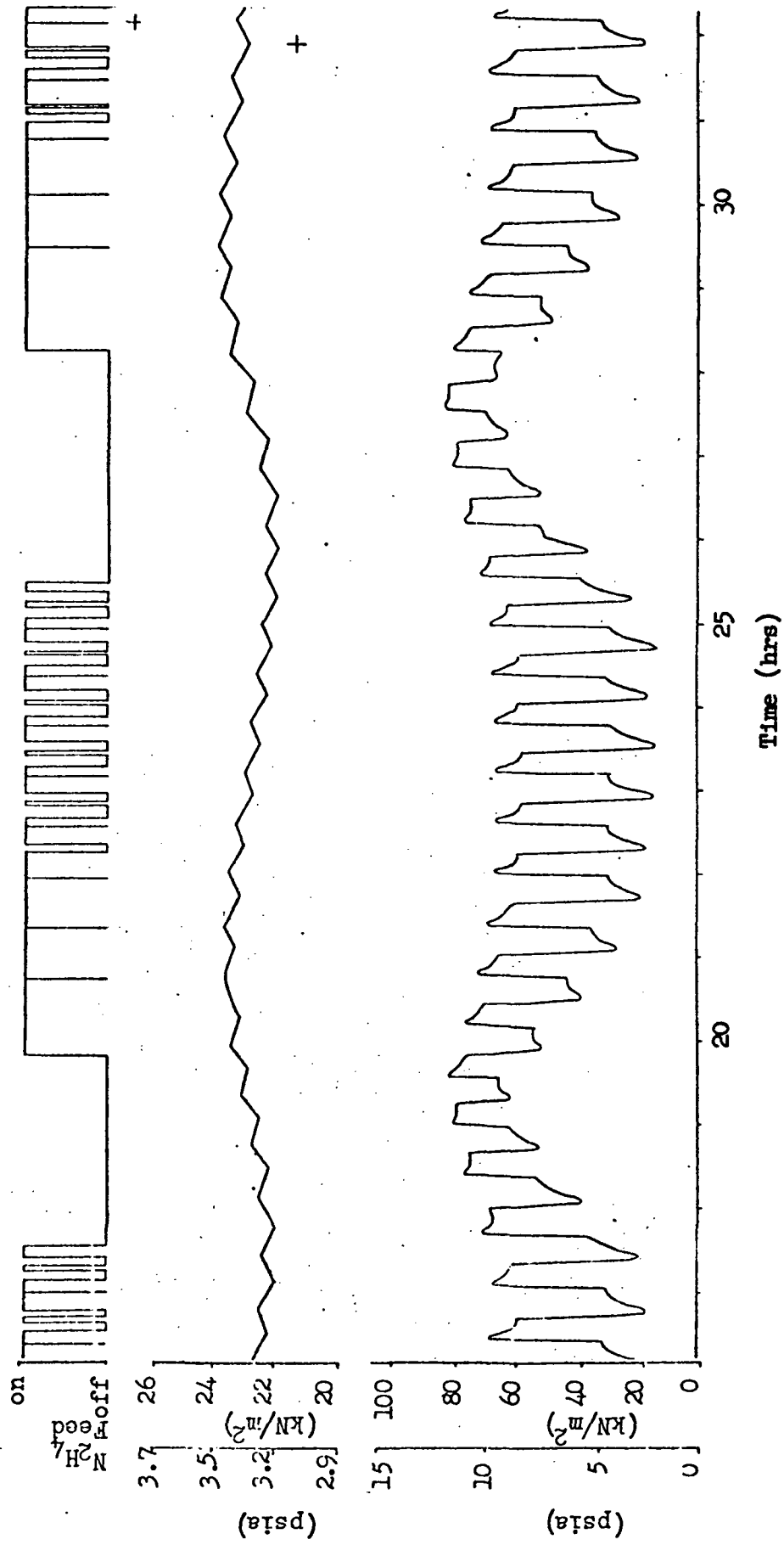


Fig. 18b Test 2 Performance Plot

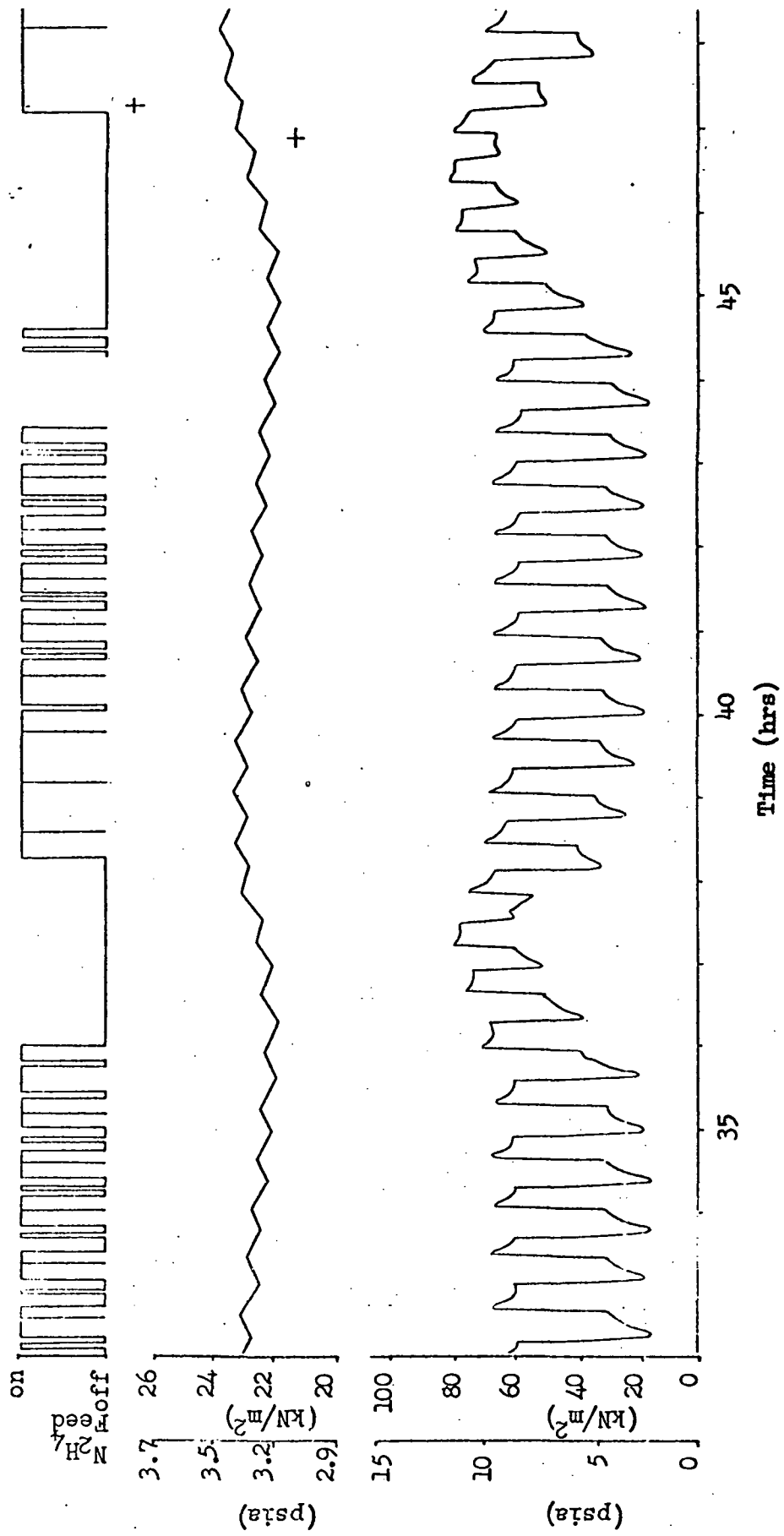


Fig. 18c Test 2 Performance Plot

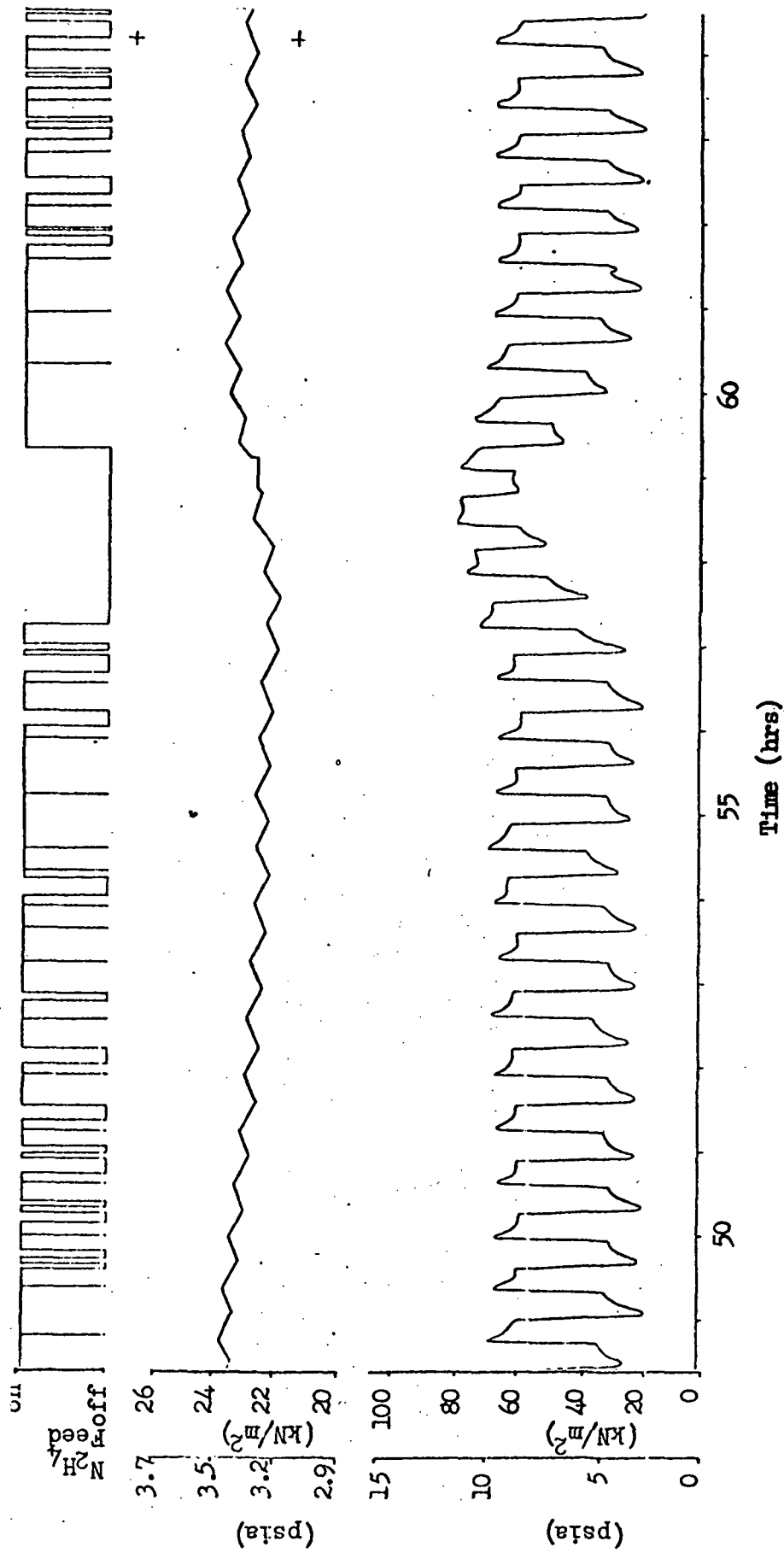


Fig. 18d Test 2 Performance Plot

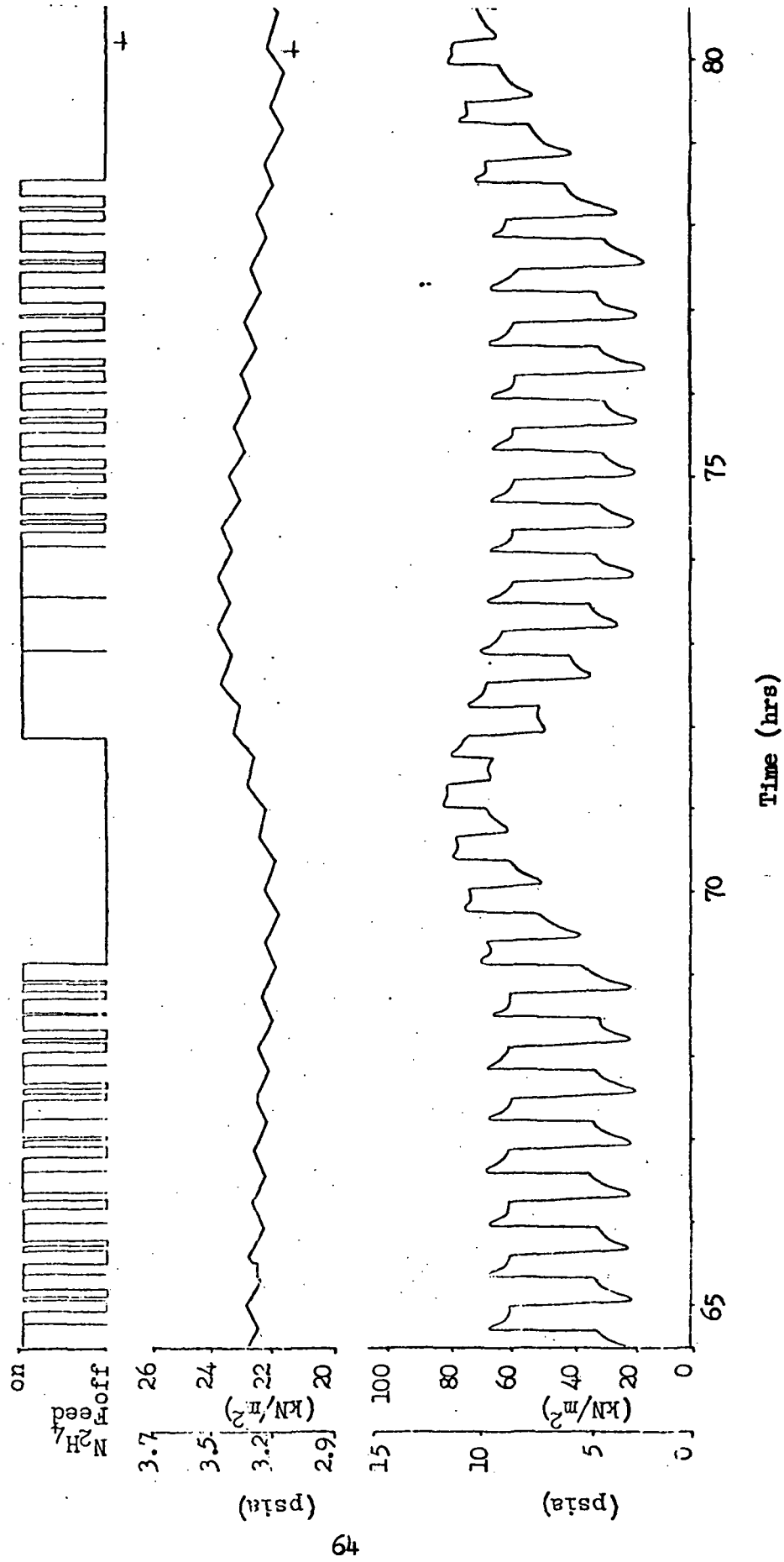


Fig. 18e Test 2 Performance Plot

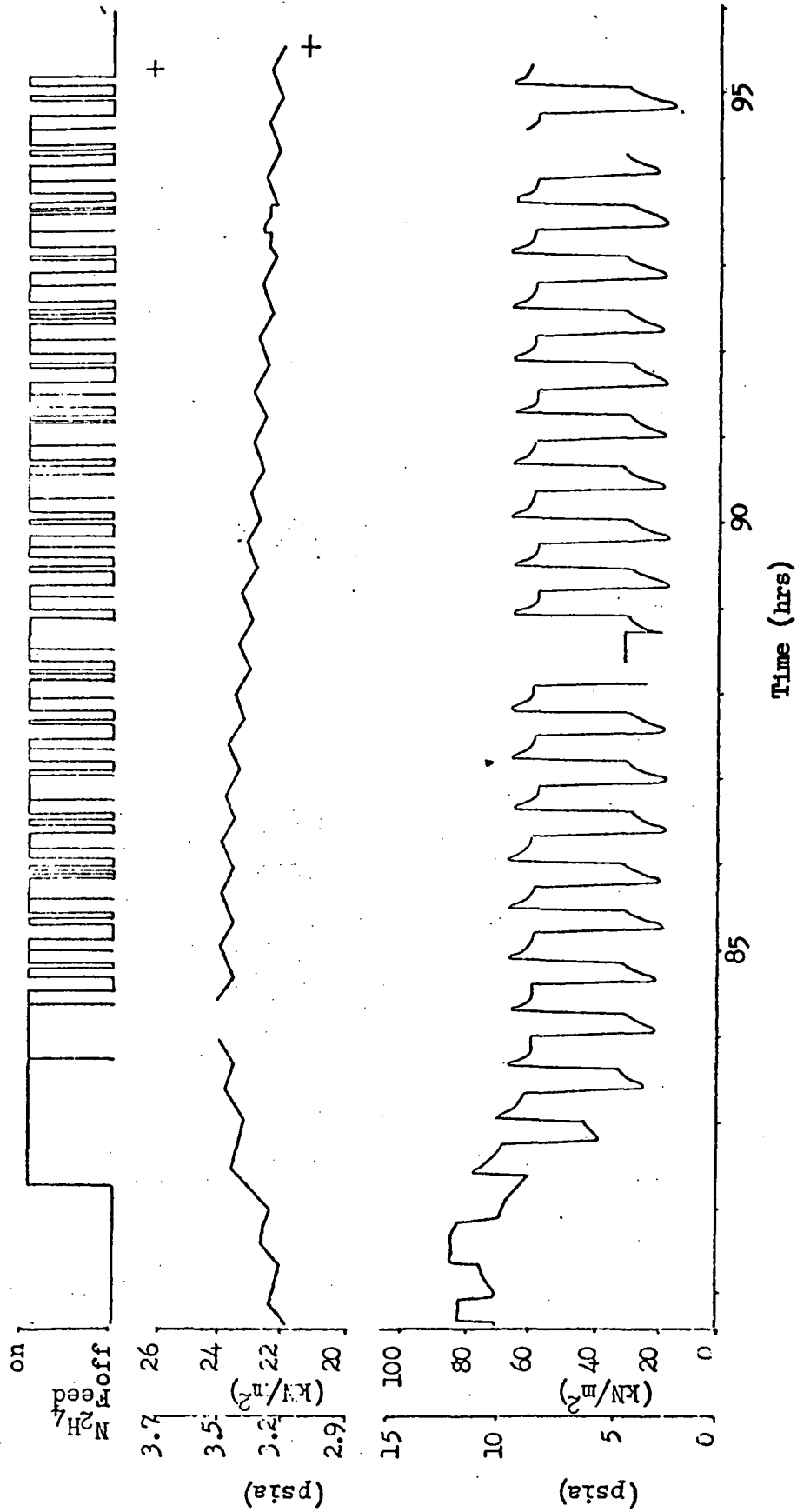


Fig. 18f Test 2 Performance Plot

Table 12  
TEST 2 TIME/EVENT LOG

Elapsed Time (Hr.)	Events/Action	Comments
7.5	Recharged $N_2H_4$ tank; consumption 348 g.	Procedure.
13.7	Adjusted low currents.	Slight drift upward had been noted.
17.0	Recharged $N_2H_4$ tank; consumption 348 g.	Procedure.
26.0	Recharged $N_2H_4$ tank; consumption 288 g.	Procedure.
35.2	Recharged $N_2H_4$ tank; consumption 378 g.	Procedure.
29.5	$N_2H_4$ floats freed by increasing setting to 10.0 for a short period.	Flowmeter floats had become stuck together making reading impossible.
44.0	Recharged $N_2H_4$ tank; consumption 341 g.	Procedure.
57.0	Recharged $N_2H_4$ tank; consumption 469 g.	Procedure.
57.7	Noted much higher gassing rate in electrolyte.	Observation -- no explanation.
57.8	Adjusted high currents.	Slight decrease had been noted.
58.8	Analyzed electrolyte sample; $N_2H_4$ at 1.1M.	Procedure.
64.2	Analyzed electrolyte sample; $N_2H_4$ at 2.21M.	Procedure.
69.0	Recharged $N_2H_4$ tank; consumption 479 g.	Procedure.
71.2	Slight adjustment of cabin $pO_2$ high limit and effluent $pO_2$ high limit.	Some drift in settings had been noted.
78.2	Recharged $N_2H_4$ tank; consumption 339 g.	Procedure.
81.7	Analyzed electrolyte sample; $N_2H_4$ at 0.77M.	Procedure.
86.4	Analyzed electrolyte sample; $N_2H_4$ at 2.44M.	Procedure.
91.3	Increased $N_2H_4$ flow to 9.4 reading.	$pO_2$ decrease noted to be very sluggish.
96.0	Drained $N_2H_4$ tank; consumption 671 g.	Procedure.

Test 3.- This test was conducted for a period of 92 hours. Changes in the test conditions from the previous tests are reflected in Table 13. The low mode current was increased from 50 to 70 mA/cm<sup>2</sup>. A corresponding change in the pO<sub>2</sub> effluent limit was also made. The test log is given in Table 14, and the performance plot in Figure 19.

For the first three cabin pO<sub>2</sub> cycles, the normal metabolic and leakage loads were used so that the pO<sub>2</sub> control characteristics at a low mode of 70 mA/cm<sup>2</sup> could be compared with Test 2 at 50 mA/cm<sup>2</sup>. As shown in Figure 19, this increase in low mode resulted in a decrease in pO<sub>2</sub> cycle time from 8.8 hours in Test 2 to 6.0 hours in Test 3.

Three other cases of metabolic and leakage loads were run in the remainder of the test with each change in conditions made as a step function. Two cabin pO<sub>2</sub> cycles were completed for each case. The performance plot, Figure 19, shows that both cabin P<sub>total</sub> and pO<sub>2</sub> were in control throughout the test. Cabin P<sub>total</sub> was completely unaffected by changes in load except for the expected variation in time in high current mode. Both the amplitude and cycle time of cabin pO<sub>2</sub> varied with load, with the best response being achieved as expected at the design point normal conditions.

During the normal metabolic and minimum leakage condition, the low leakage rate results in a slow recovery in pO<sub>2</sub>. These two cycles show long recovery times from the turnaround in pO<sub>2</sub> at 28.5 hours and 38 hours. The second cycle is somewhat longer than the first. A review of the data showed no apparent explanation. Possibly, small variations outside the normal control band have a large effect on this condition.

Test 4.- This test was conducted for 92 hours in the manual mode without the cabin and metabolic/leakage simulator for the purpose of obtaining steady-state parametric data regarding operating temperature and current density, and to make a comprehensive analysis of the chemical composition of the generated gases. The vortex bubble separator was installed for this test, and the gas removed from the electrolyte by this device from the electrolyte by this device was also analyzed.

Table 13  
TEST 3 OPERATING CONDITIONS

Variable Metabolic and Leakage Loads

Low Current	70 mA/cm <sup>2</sup>	
High Current	150 mA/cm <sup>2</sup>	
N <sub>2</sub> Makeup	1050 to 1690 cm <sup>3</sup> /min.	(.386 - .62 lb/day)
Meta/leak (Cabin gas)	1566 to 2350 cm <sup>3</sup> /min.	(.597 - .9 lb/day)
KOH Flow	500 cm <sup>3</sup> /min.	
N <sub>2</sub> H <sub>4</sub> Flow	2.33 to 3.52 cm <sup>3</sup> /min.	
pO <sub>2</sub> Effluent Limits		
High	53.2 kN/m <sup>2</sup>	(7.72 psia)
Low	26.6 kN/m <sup>2</sup>	(3.84 psia)
Cabin pO <sub>2</sub> Control Band	21.0 to 22.0 kN/m <sup>2</sup>	(3.04 - 3.19 psia)
Cabin P <sub>Total</sub> Control Band	99.3 to 99.9 kN/m <sup>2</sup>	(14.4 - 14.5 psia)



Table 14  
Test 3 Time/Events Log

Elapsed Time (hr.)	Events/Action	Comments
0.2	Closed manual N <sub>2</sub> purge valve.	Noted N <sub>2</sub> solenoids leaking.
0.6	Water feed not working.	
1.0	Shut down and replaced I.C. chip in water feed circuit.	Failure caused by problem with power supply prior to test start.
5.9	Increased N <sub>2</sub> H <sub>4</sub> flowmeter reading from 9.0 to 10.0 scale units.	Low pO <sub>2</sub> limit not being reached. Further increase in N <sub>2</sub> H <sub>4</sub> flow possible.
7.0	Recharged N <sub>2</sub> H <sub>4</sub> tank; consumption 400 g.	Procedure.
15.0	Recharged N <sub>2</sub> H <sub>4</sub> tank; consumption 284 g.	Procedure.
17.6	Increased N <sub>2</sub> H <sub>4</sub> flowmeter reading to 11.0.	Low pO <sub>2</sub> limit not being reached.
20.5	Recharged N <sub>2</sub> H <sub>4</sub> tank; consumption 263 g.	Procedure.
24.2	Changed Meta flowmeter to 13.0; N <sub>2</sub> makeup to 10.0.	Procedure; step change from normal metabolic and leakage to normal metabolic; min. leakage.
26.1	Recharged N <sub>2</sub> H <sub>4</sub> tank; consumption 221 g.	Procedure.
36.5	Recharged N <sub>2</sub> H <sub>4</sub> tank; consumption 299 g.	Procedure.
42.7	System stayed in low mode 70 min.; Normal is 45 minutes.	Cause not determined.
45.0	Changed Meta flowmeter to 17.0; N <sub>2</sub> makeup to 12.8.	Procedure; step change from normal metabolic, min. leakage to max. metabolic, normal leakage.
47.1	Recharged N <sub>2</sub> H <sub>4</sub> tank; consumption 279 g.	Procedure.
54.7	Recharged N <sub>2</sub> H <sub>4</sub> tank; consumption 228 g.	Procedure.
61.1	Recharged N <sub>2</sub> H <sub>4</sub> tank; consumption 277 g.	Procedure.
64.0	N <sub>2</sub> makeup flowmeter reading too high; 13.5; adjusted to 12.8.	N <sub>2</sub> supply cylinder pressure had changed.
66.2	Changed Meta flowmeter to 16.0; N <sub>2</sub> makeup unchanged.	Procedure; step change from max metabolic, normal leakage to max metabolic, minimum leakage.
69.0	Recharged N <sub>2</sub> H <sub>4</sub> tank; consumption 226 g.	Procedure.
90.0	Drained N <sub>2</sub> H <sub>4</sub> tank; consumption 252 g.	Procedure.

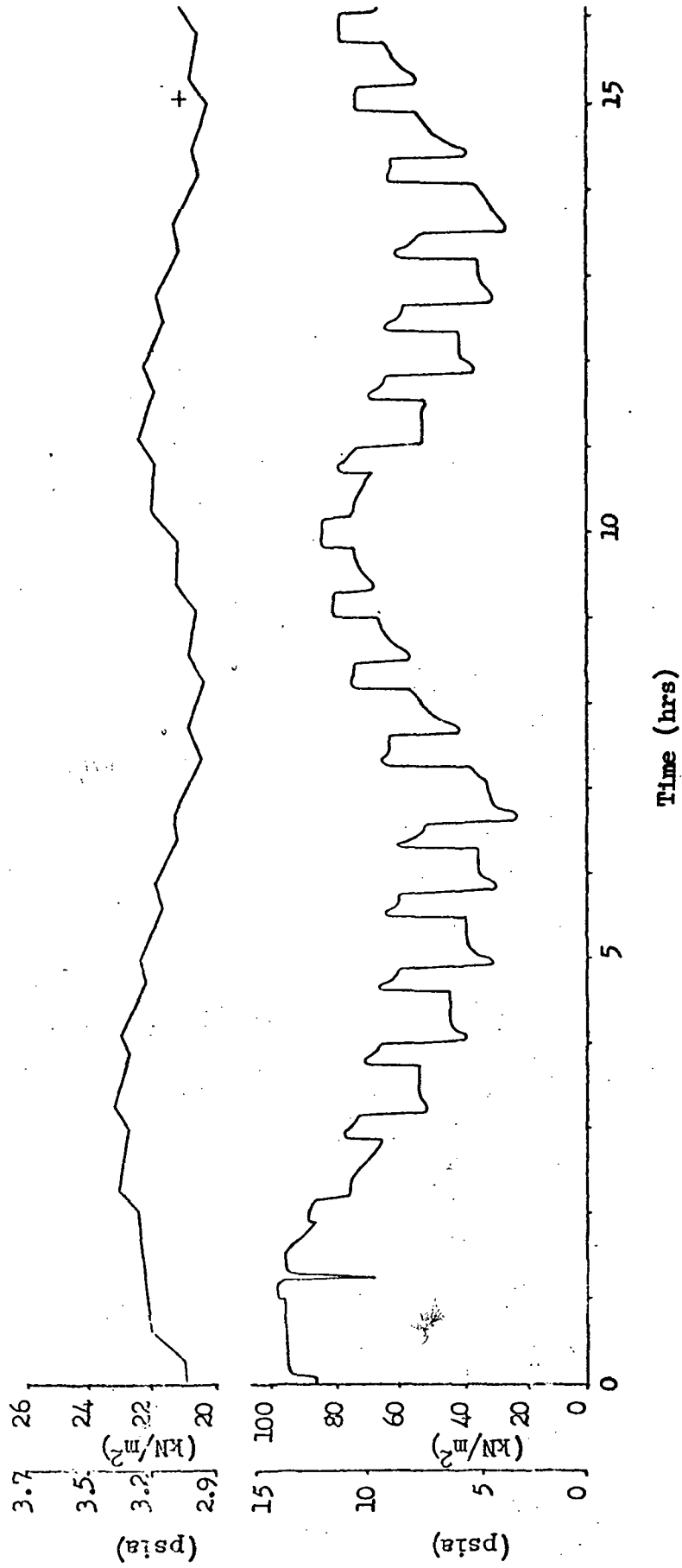


Fig. 19a Test 3 Performance Plot

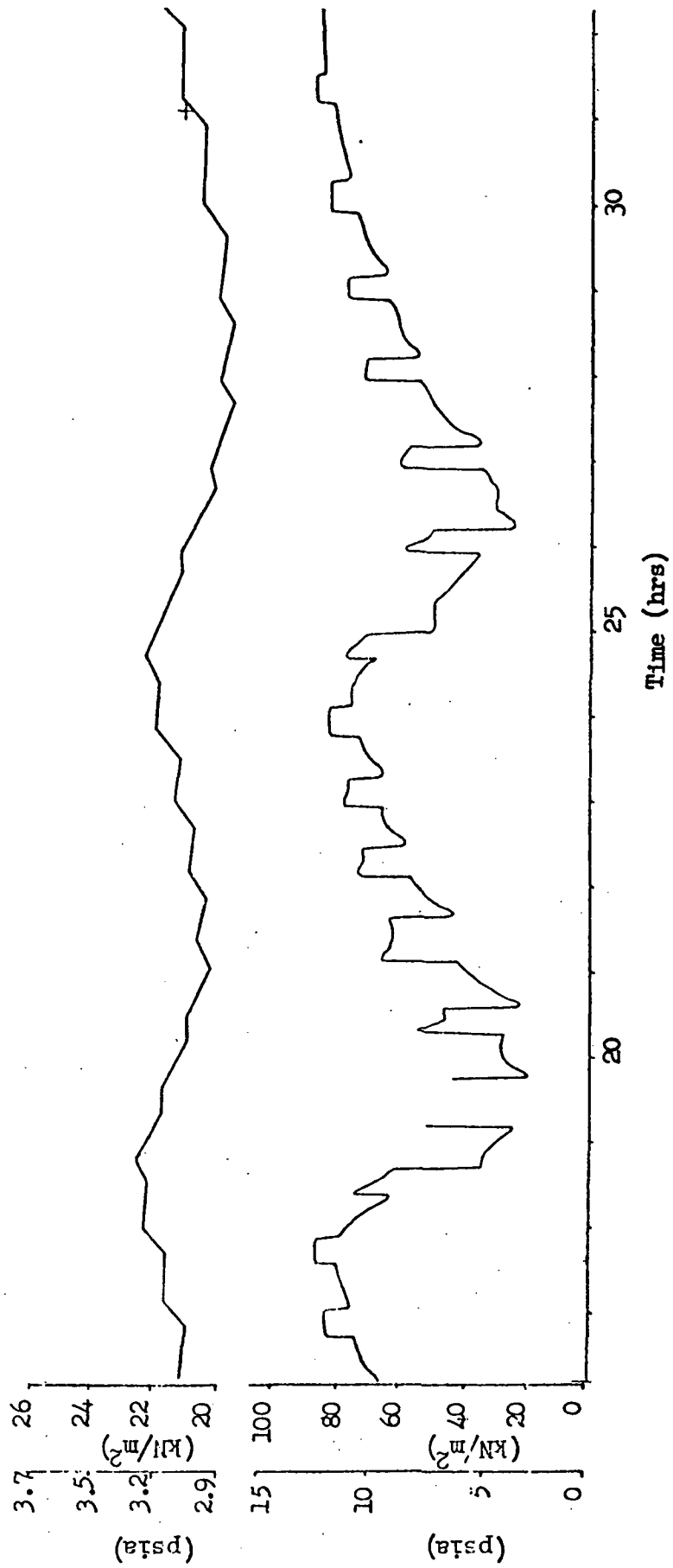


Fig. 19b Test 3 Performance Plot

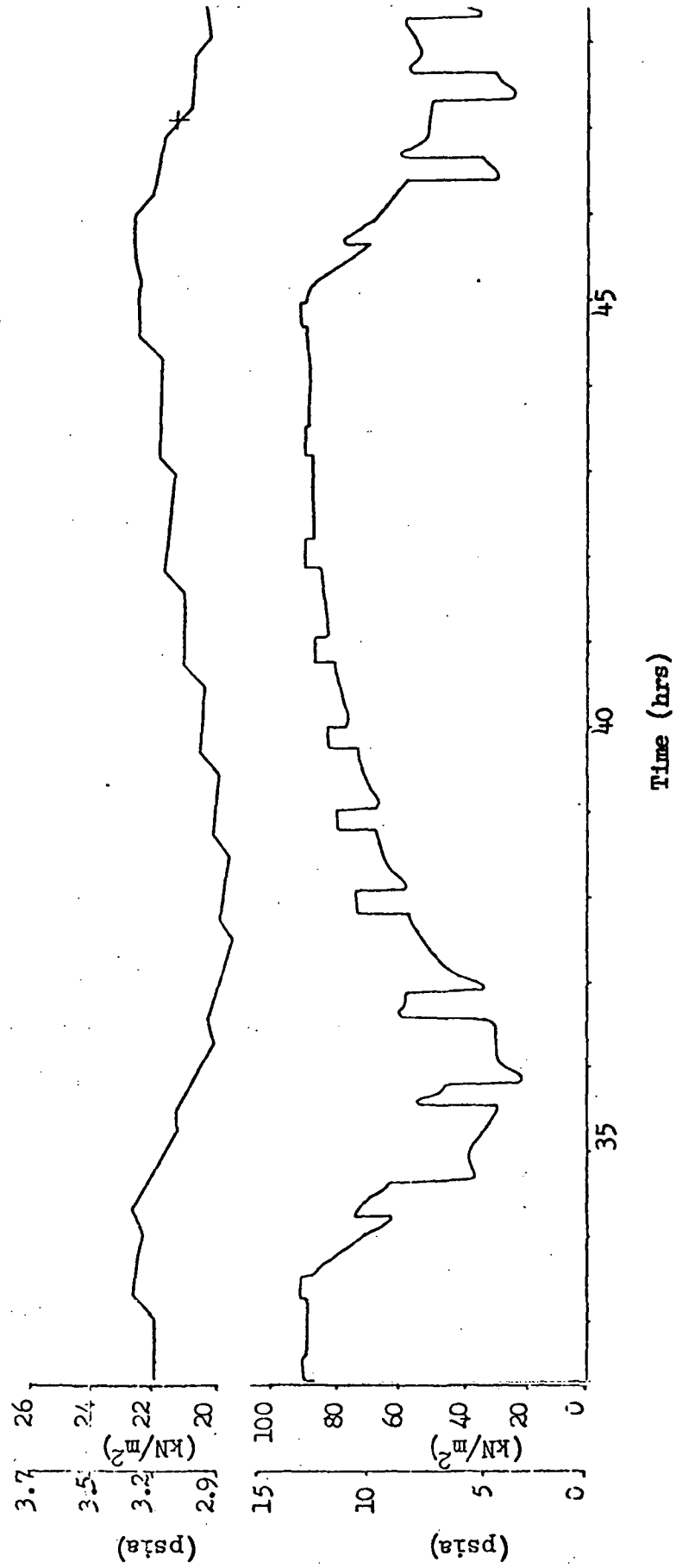


Fig. 19c Test 3 Performance Plot

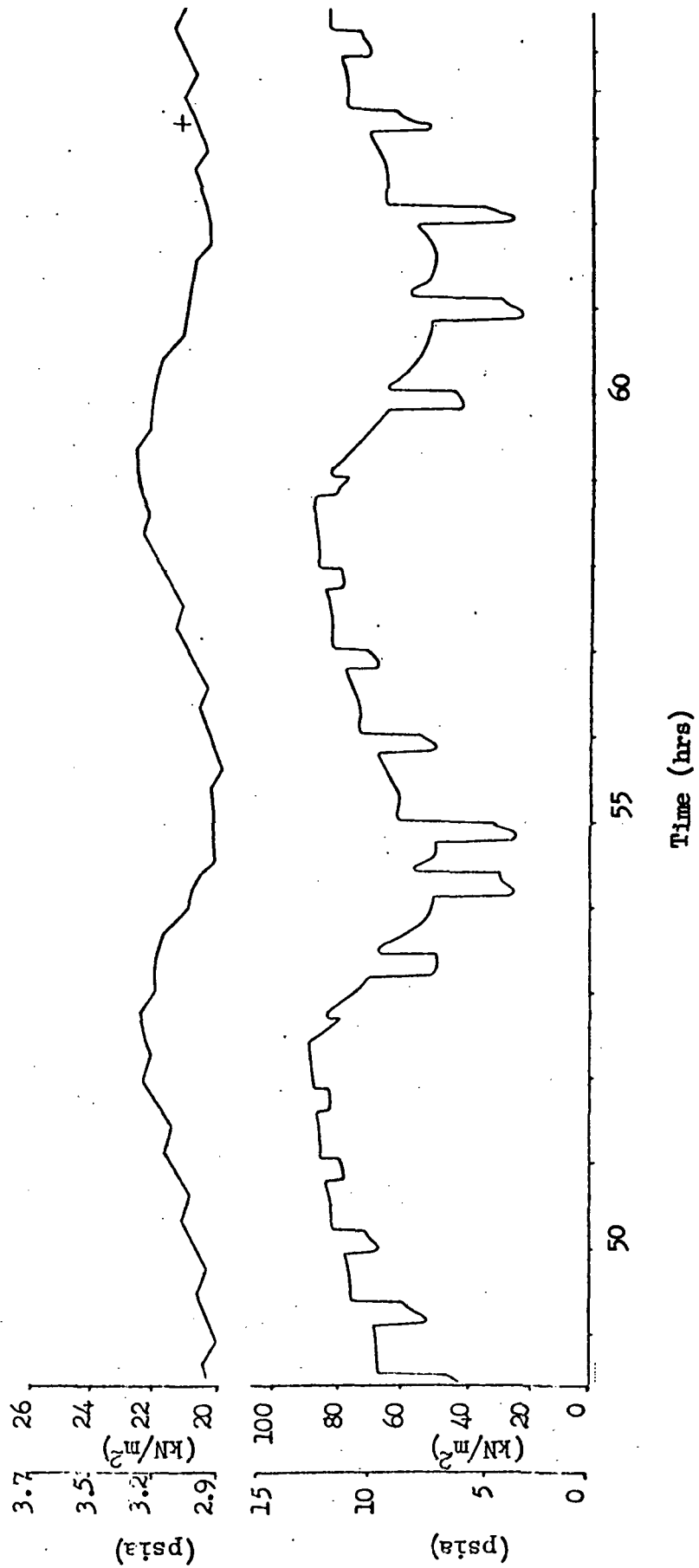


Fig. 19d Test 3 Performance Plot

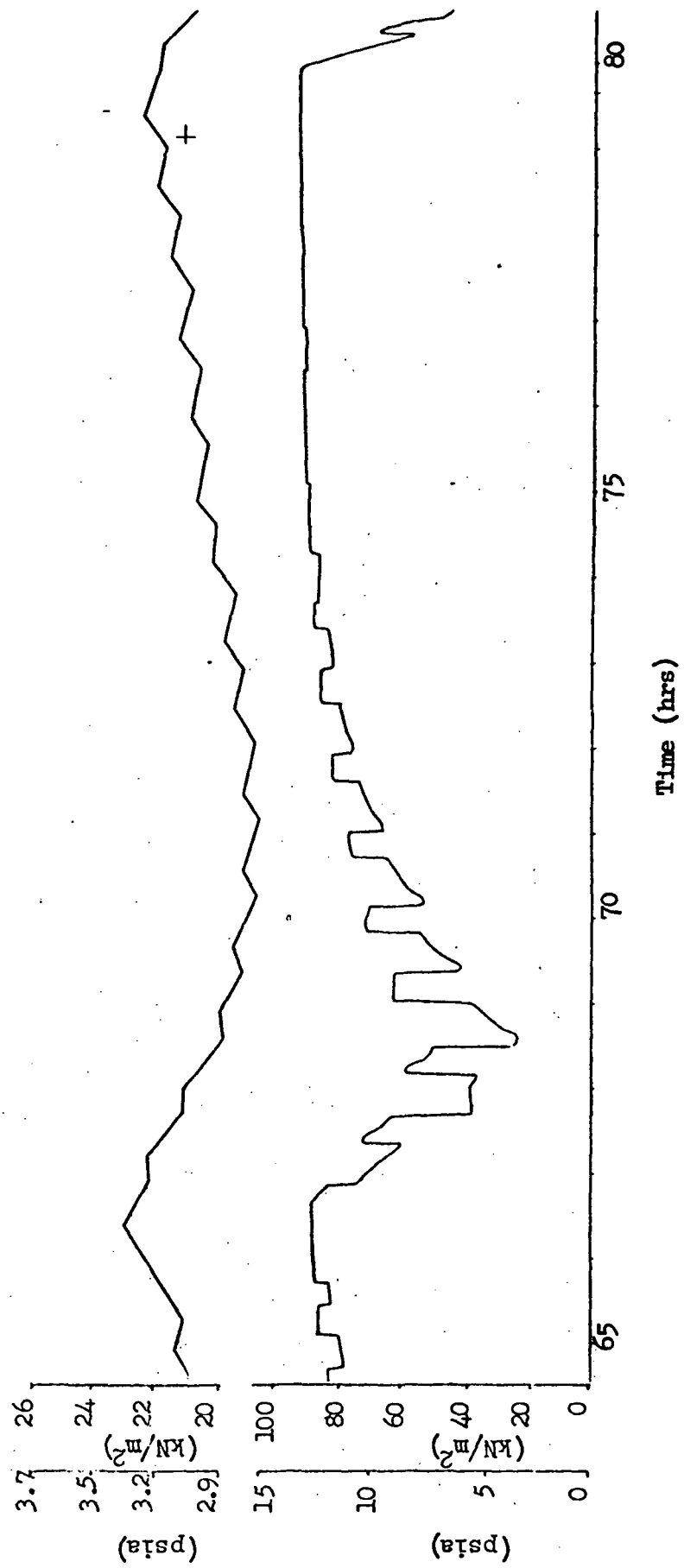


Fig. 19e Test 3 Performance Plot

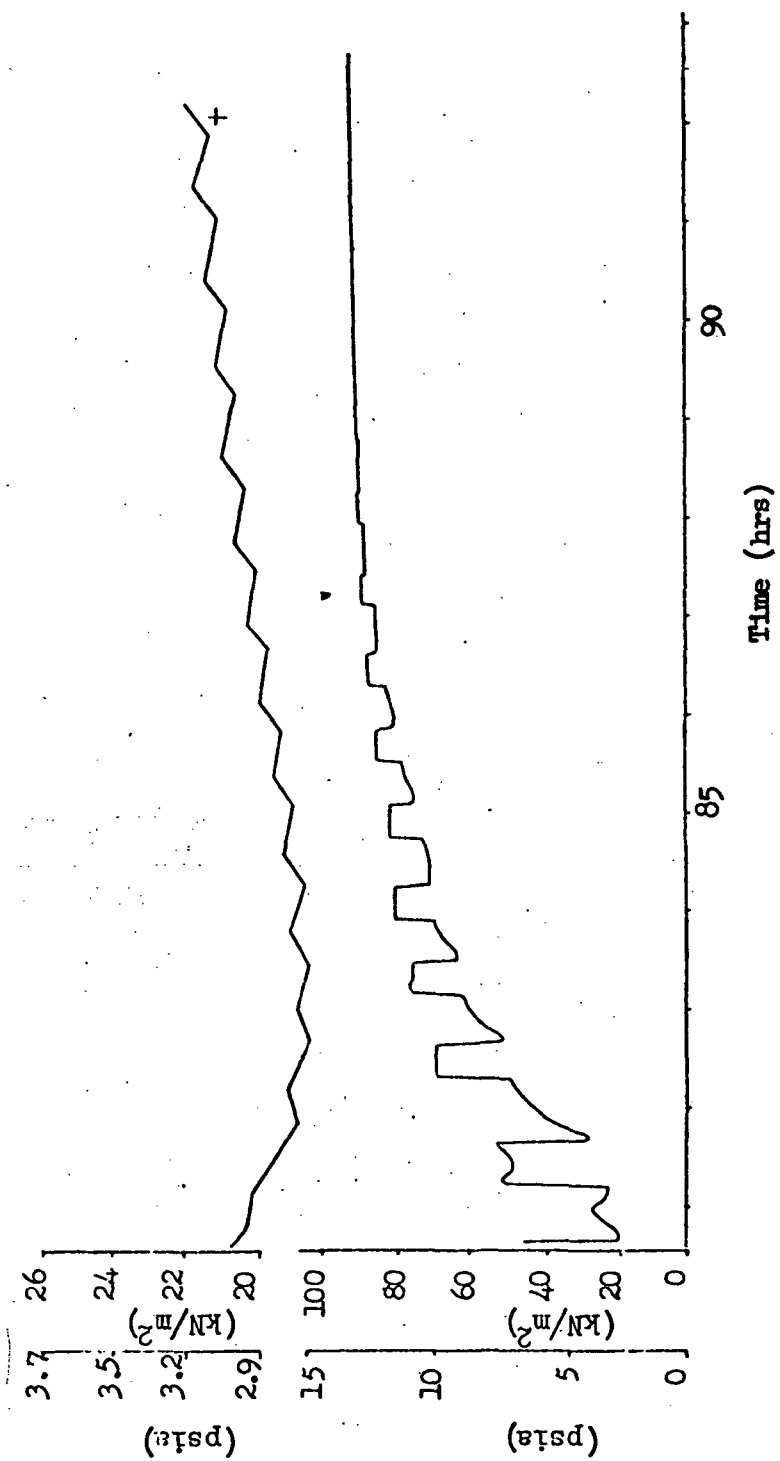


Fig. 19f Test 3 Performance Plot

The following matrix of temperatures and current densities was used in the testing with some duplicate runs made as indicated to determine data scatter.

Temperature (°C)	Current Density (mA/cm <sup>2</sup> )		
	50	100	150
24	2	1	2
29	1	1	1
33	1	2	1

At each set of conditions, an initial charge of hydrazine was added to the electrolyte to bring the hydrazine to approximately 2-3 molar. Electrolyte samples were then analyzed at 1-2 hour intervals, to determine the hydrazine decay rate.  $pO_2$  in the anodic effluent was continuously monitored with a stripchart readout. The raw data on the hydrazine decay rate are shown in Figure 20 and indicate the high precision that was typical throughout the test. These data are an excellent confirmation of the first order reaction mechanism of the hydrazine, i.e., confirming that the reaction rate is  $\frac{dc}{dt} = cm$  where  $m$  is the reaction rate constant.

Similar results were obtained with the  $pO_2$  monitor on the anodic effluent gas as shown in the raw data sampling in Figure 21 (plotted as  $P_T - pO_2 = pN_2$ ). Again, excellent correlation was observed. Cross-plots were made of  $CN_2H_4$  and  $pN_2$  for all the runs and are shown in Figure 22. The current density effect indicated in these results appears reasonable; however, the temperature effect appears anomolous. The raw data showed almost no scatter (as indicated in Figures 20 and 21), and the results were reproducible in the duplicate runs that were made. In carefully reviewing the test conditions, the only difference which was found between individual runs was the manner in which hydrazine was added to the system. In all runs except the 24°C/50 mA/cm<sup>2</sup>, 24°C/150 mA/cm<sup>2</sup>, and 33°C/150 mA/cm<sup>2</sup>, the hydrazine charge was added to the upper reservoir and mixed within 20 minutes. In the 24°C/50 mA/cm<sup>2</sup> and 24°C/150 mA/cm<sup>2</sup> runs, the hydrazine was introduced into the KOH inlet line to the module over a period of 1-2 hours. In the 33°C/150 mA/cm<sup>2</sup> run, hydrazine was added to the upper reservoir but in small increments over a period of an hour.



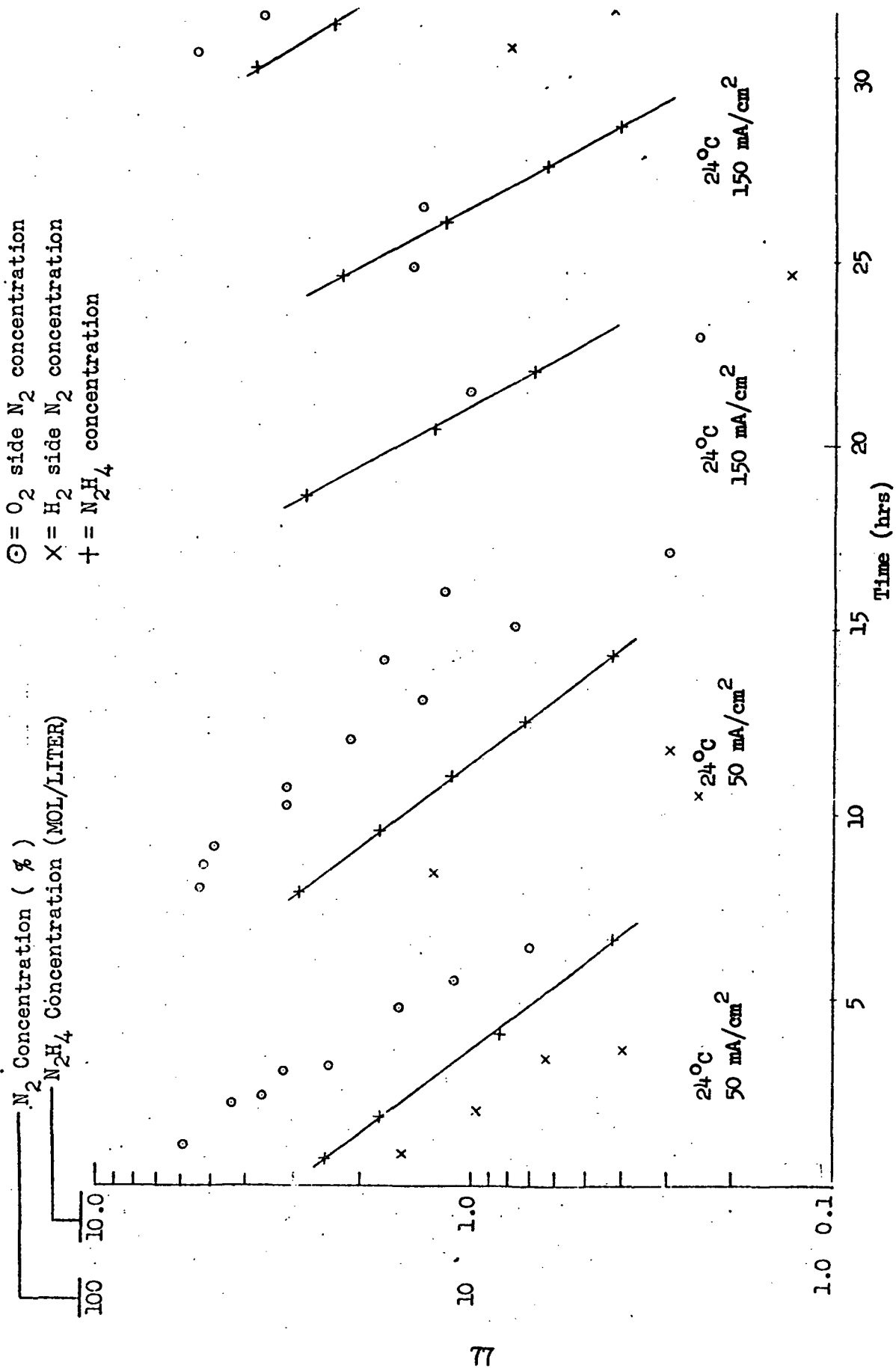


Fig. 20a Hydrazine Reaction Rate - Test 4

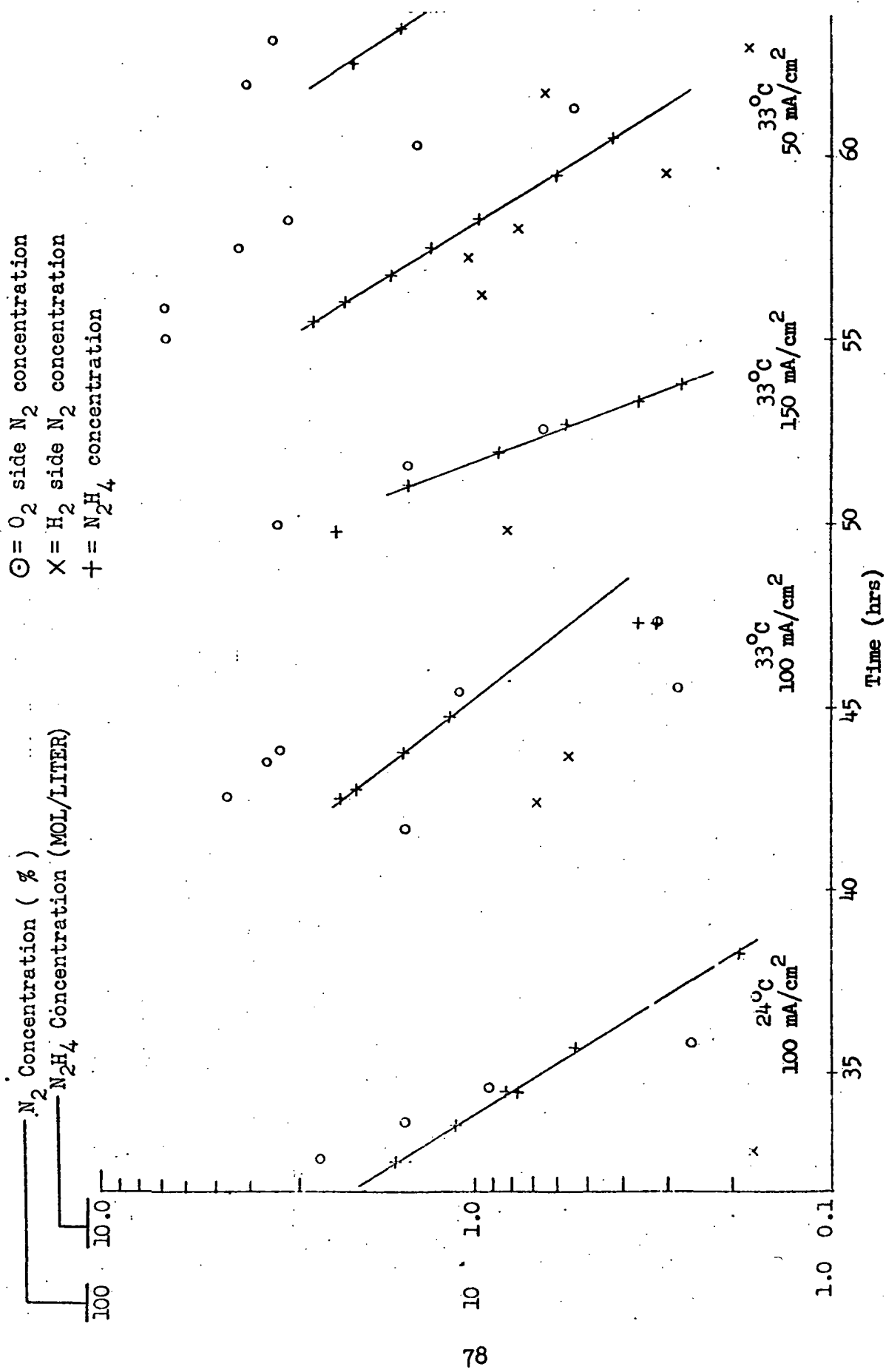


Fig. 20b Hydrazine Reaction Rate - Test 4  
(Continued)

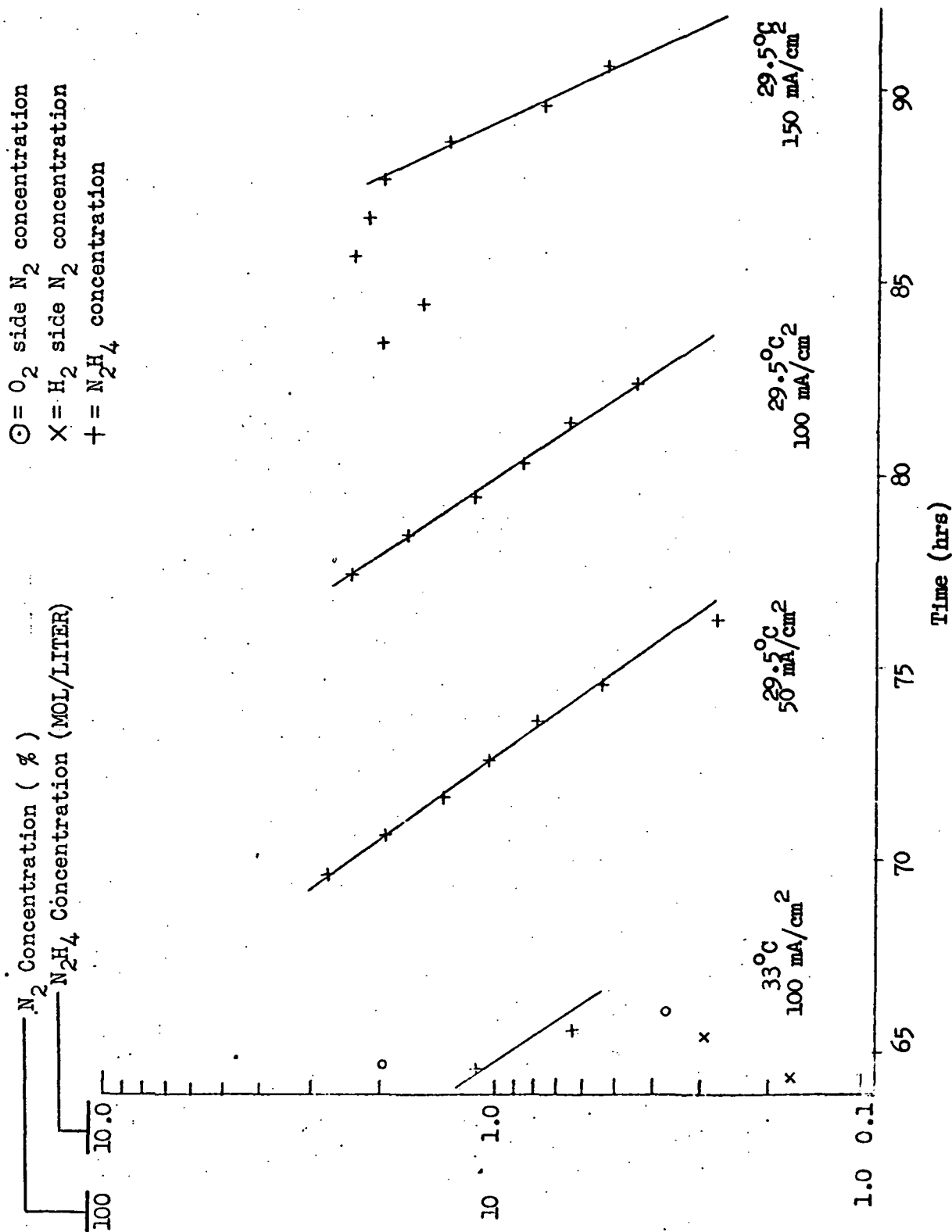


Fig. 20c Hydrazine Reaction Rate - Test 4  
(Continued)

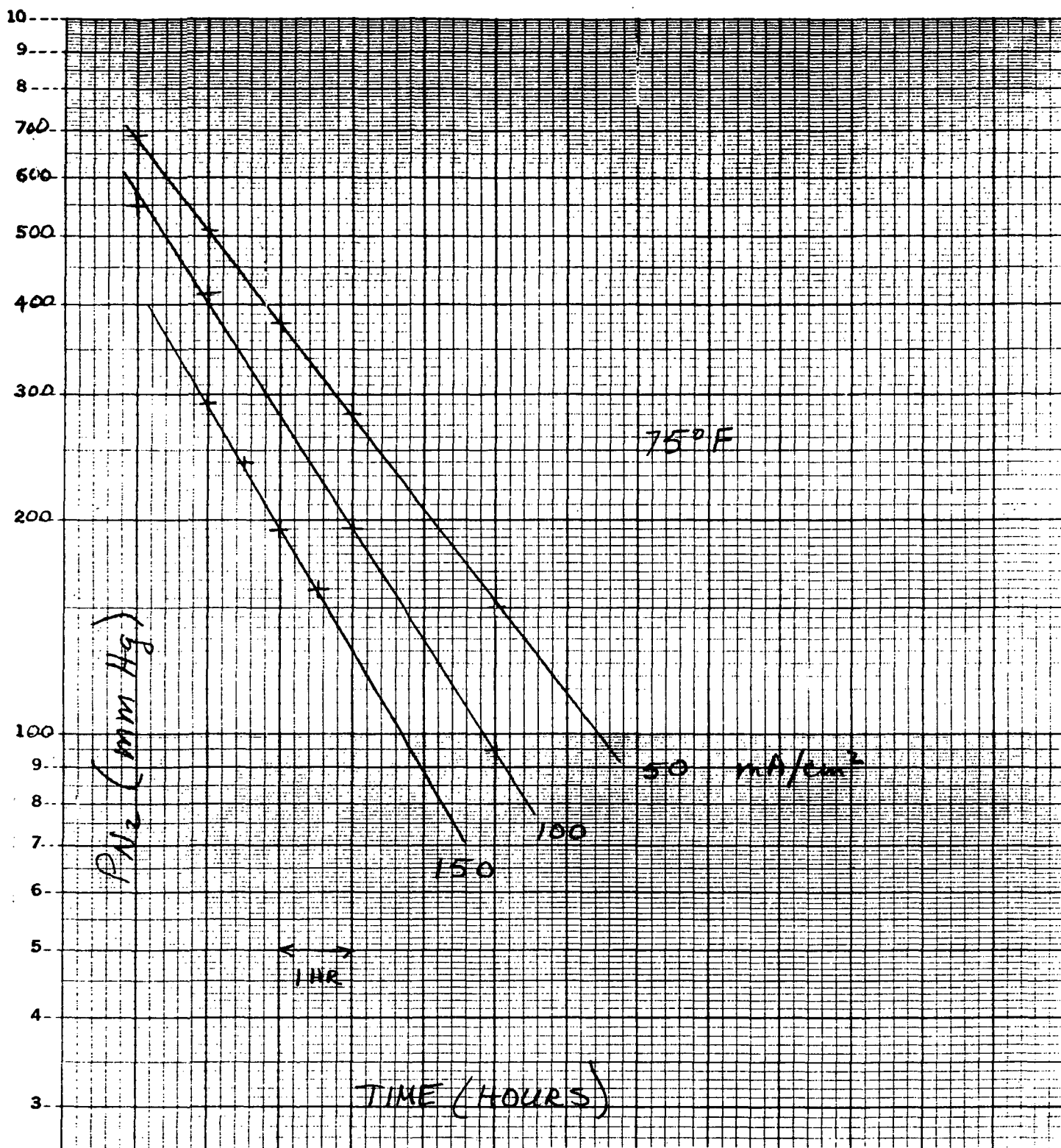


Figure 21 Anodic Gas Composition, Test 4

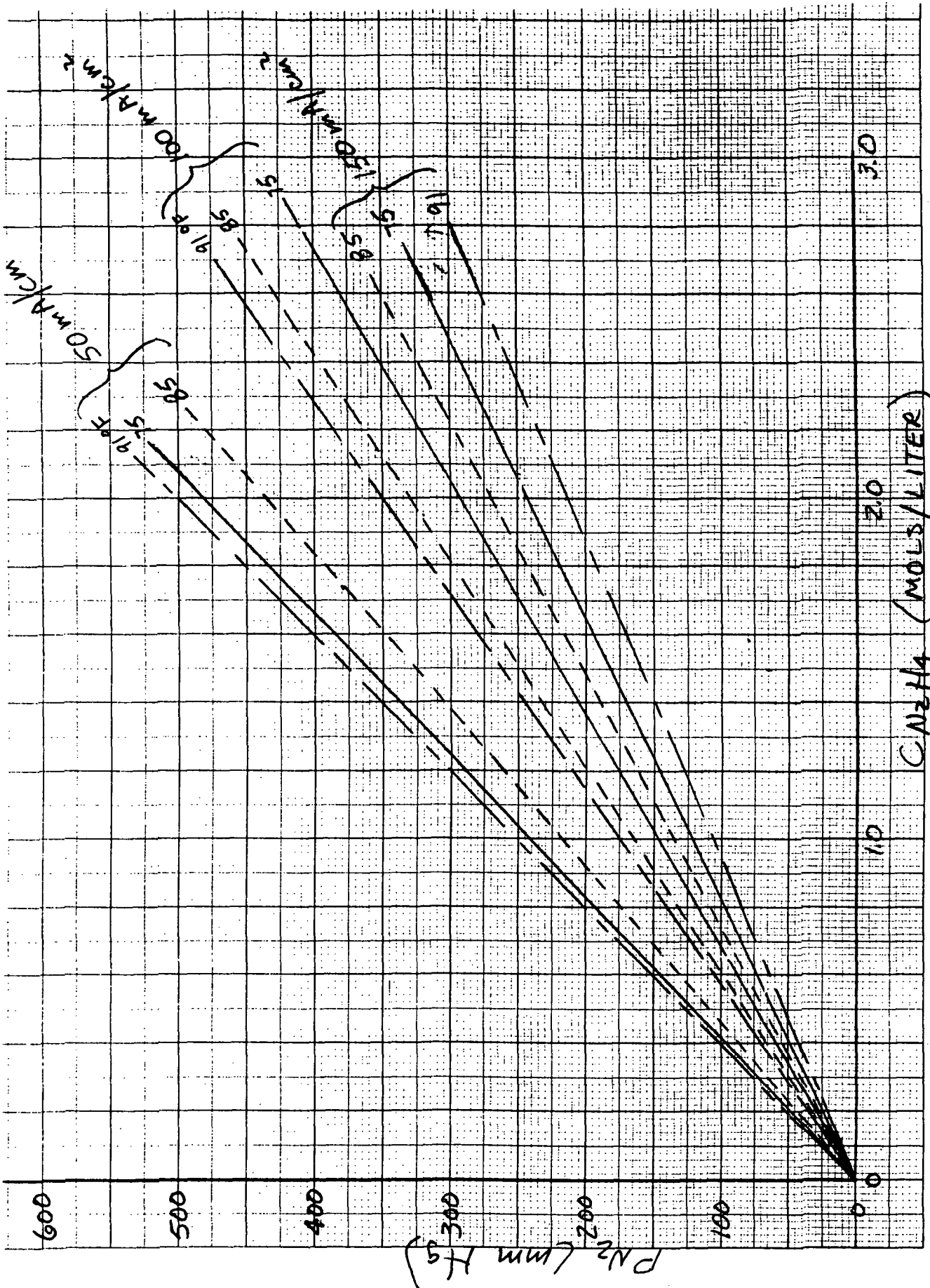


Figure 22 Cross-Plot of Hydrazine and Anodic Gas Data

If the three runs in which the hydrazine was fed over a period of time are disregarded, a trend is observed which shows increased decomposition with temperature. This would be anticipated from the increased kinetics of decomposition with increasing temperature. However, as  $pN_2$  should vary with hydrazine concentration and not with history of feed into the system, it is difficult to rationalize dismissal of this data. In summary, there is not enough data, consistently taken, to draw any definite conclusions.

Considering next the chemical composition of the generated gases, comprehensive analysis techniques including gas chromatography, infrared, and mass spectrometry, were used to establish the levels of trace contaminants in the generated gases and also in the bubble separator discharge. A summary of the results is shown in Table 15. Considering first the hydrogen product gas stream, high oxygen levels in some samples show corresponding high argon levels (indicating room air contamination of these samples) and should be discounted. Trace amounts of  $NO_2$  (< 20 ppm),  $NH_2$  (20-30 ppm), and  $N_2H_4$  derivatives ( $\leq 20$  ppm) were detected.

In the  $N_2/O_2$  gas stream,  $NO_2$  (< 20 ppm),  $N_2O$  (20-30 ppm),  $NH_3$  (30-40 ppm)  $N_2H_4$  derivatives ( $\leq 20$  ppm) and CO (9-10 ppm) were detected. The source of the CO is residual organic material in the commercial electrodes.  $N_2O$  was detected on the mass spectrometer but was not confirmed on the gas chromatograph.

In this test, the vortex bubble separator was used to separate gas from the electrolyte. The gas was withdrawn under a slight vacuum which made sampling difficult. In the samples which showed the least amount of entrained air, as indicated by the argon levels, the following constituents were found:  $O_2$  (20%);  $N_2$  (~78%);  $NO_2$  (< 20 ppm); CO (1 ppm);  $CH_4$  (0.8 ppm), and  $N_2H_4$  derivatives ( $\leq 20$  ppm). No  $NH_3$  or  $H_2$  was detected.

These chemical analysis results are further discussed in Section 2.5.3.2.

Table 15

## CHEMICAL ANALYSIS SUMMARY - TEST 4

Date	Time	Samp. Loc.	Temp/ C.D.	N <sub>2</sub> H <sub>4</sub> Conc.	O (%)	N (%)	CO (ppm)	CH <sub>4</sub> (ppm)	CO (%)	Ar (%)	NO <sub>2</sub> (ppm)	N <sub>2</sub> O (ppm)	NH <sub>3</sub> (ppm)	N <sub>2</sub> H <sub>4</sub> (ppm) Derivatives
3-14-72	11:12AM	H <sub>2</sub>	24/50	0.44	29.3	28.1	--	--	0.18	0.25	<20	--	--	≤20
	1:10PM	O <sub>2</sub>	24/50	~2.0	67.5	31.1	--	--	0.35	<0.02	<20	--	--	≤20
	1:36PM	H <sub>2</sub>	24/50	~3.0	1.0	12.8	--	--	0.07	0.05	<20	--	--	≤20
	1:50PM	B/S	24/50	~3.5	19.0	78.5	--	--	0.02	0.78	<20	--	--	≤20
	2:47PM	O <sub>2</sub>	24/50	4.0	--	--	9	N.D.**	--	--	--	--	--	--
	2:56PM	H <sub>2</sub>	24/50	3.8	--	--	N.D.*	N.D.	--	--	--	--	--	---
3-15-72	4:36PM	B/S	24/150	1.9	--	--	N.D.	0.8	--	--	--	--	--	--
	3:50PM	O <sub>2</sub>	33/100	2.1	--	--	--	--	--	--	--	20-30	30-40	≤20
	4:00PM	H <sub>2</sub>	33/100	1.9	5.1	19.1	--	--	0.06	0.11	<20	--	--	≤20
	4:35PM	B/S	33/100	1.5	20.0	~78	--	--	0.03	<0.9	<20	--	--	≤20
	5:05PM	O <sub>2</sub>	33/100	1.2	58.9	38.5	--	--	0.06	0.11	<20	--	--	≤20
	4:12PM	O <sub>2</sub>	33/100	1.7	--	--	10	N.D.	--	--	--	N.D.	--	--
	3:52PM	B/S	33/100	2.0	--	--	N.D.	N.D.	--	--	--	--	--	--
	4:09PM	H <sub>2</sub>	33/100	1.8	--	--	N.D.	N.D.	--	--	--	--	--	--
3-16-72	12:00M	H <sub>2</sub>	33/100	1.8	--	--	--	--	--	--	--	--	20-30	--
	12:30PM	B/S	33/100	1.5	--	--	1	--	--	--	--	--	15-25	--
	3:04 PM	H <sub>2</sub>	33/100	0.7	--	--	N.D.	--	--	--	--	--	--	--

C.D. - Current Density, mA/cm<sup>2</sup>NO<sub>2</sub> - Lower limit of Detection 20 ppmN<sub>2</sub>H<sub>4</sub> - Lower limit of Detection 20 ppm

\*N.D. - None detected (lower limit of detection: 0.2ppm)

\*\*N.D. - None detected (lower limit of detection: 0.1 ppm)

Test 5.- This test was conducted for the specific purpose of evaluating the long-term performance capability of the prototype vortex bubble separator. After 92 hours of successful operation of the device in Test 4, it was operated for a total of 811 hours in Test 5. Test 5 data was entirely observational. A complete log of observations is presented in the Appendix.

The first 175 hours of operating time were logged on a normal day shift basis. This resulted in 22 start/stop operations and allowed the gas discharge tube inside the device to stand in contact with the system electrolyte for long periods of time, on nights and weekends. The transparent gas discharge tube was visually inspected daily for evidence of electrolyte carryover. Over the one-month period of on/off operation, one small drop (less than  $1 \text{ cm}^3$ ) of liquid collected in the gas discharge line. For use in a full-scale system, the device would need to have a momentary back purge on startup to prevent even such a small amount of liquid carryover.

For the last 636 hours of Test 5, the second reservoir (required for operation with hydrazine) was removed and the primary reservoir was sealed. This modification resulted in a completely closed electrolyte loop as would be required in a full-scale flight system. Operation was continuous with no interruptions during the final 636 hours of testing. A once-a-day check was made to assure that the system was operating properly. No problems occurred with the vortex bubble separator throughout the test. Its performance capability was demonstrated by a cumulative total of 903 hours of successful operation.

#### 2.5.3.2 Data Analysis and Discussion

$pO_2$  Effluent - It was determined in Test 1 that a maximum allowable hydrazine feed rate existed for a given high and low current due to the transient effects occurring in the  $pO_2$  of the generated  $N_2/O_2$  gas mixture when the current switched between high and low. It can be seen in Figure 17 that a transient effect was present in switching current in either direction, high to low, or low to high.



A diffusion model can be used to explain the transient effects. This model is demonstrated graphically in Figure 23. The model assumes two shapes of the equilibrium hydrazine concentration gradient across the hydrophilic matrix separating the anode from the bulk liquid electrolyte in the center of the cell. The shape of the equilibrium gradient depends on whether the current mode is high or low as shown in (a) and (b). This assumption appears reasonable in view of the large difference in the dilution effect of water production and hydroxyl ion consumption for the two cases. When the current is suddenly switched from one mode to the other, the gradient must shift to the new equilibrium condition. As shown in (c), this non-steady state transient results in net excess hydrazine (shown as cross-hatched area) in the case of changing from high to low current; conversely, this area represents a net deficiency in the case of changing from low to high current.

A net excess hydrazine when switching from high to low current would cause the undershoot of the equilibrium effluent  $pO_2$  as shown in (d). Likewise, the net deficiency of hydrazine in switching from low to high current would cause an overshoot of the equilibrium high mode value.

Transients in the effluent  $pO_2$  response to step changes in current were not recognized as such in previous testing in Phase I because the test conditions did not allow equilibrium to be attained in low current mode. The identification in this test program of the existence of the low mode transient is particularly significant. The ability to accurately predict the value of the undershoot will be essential in the scale-up of the process to a full-scale system. It will be necessary to be able to predict the minimum effluent  $pO_2$  for a given  $pO_2$  low limit so that cross-over into the region of hydrogen production does not occur. The model presented above is a very simple one and it is recognized that a more complete quantification of the complex processes occurring in the cells will be a necessary step in the continuing development of the process.

#### $pO_2$ Control Characteristics

It was found that the new  $pO_2$  control technique, which modulates the hydrazine feed at high and low mode  $pO_2$  effluent limits, improved the  $pO_2$  control by increasing its responsiveness. The improvement in  $pO_2$  cycle time

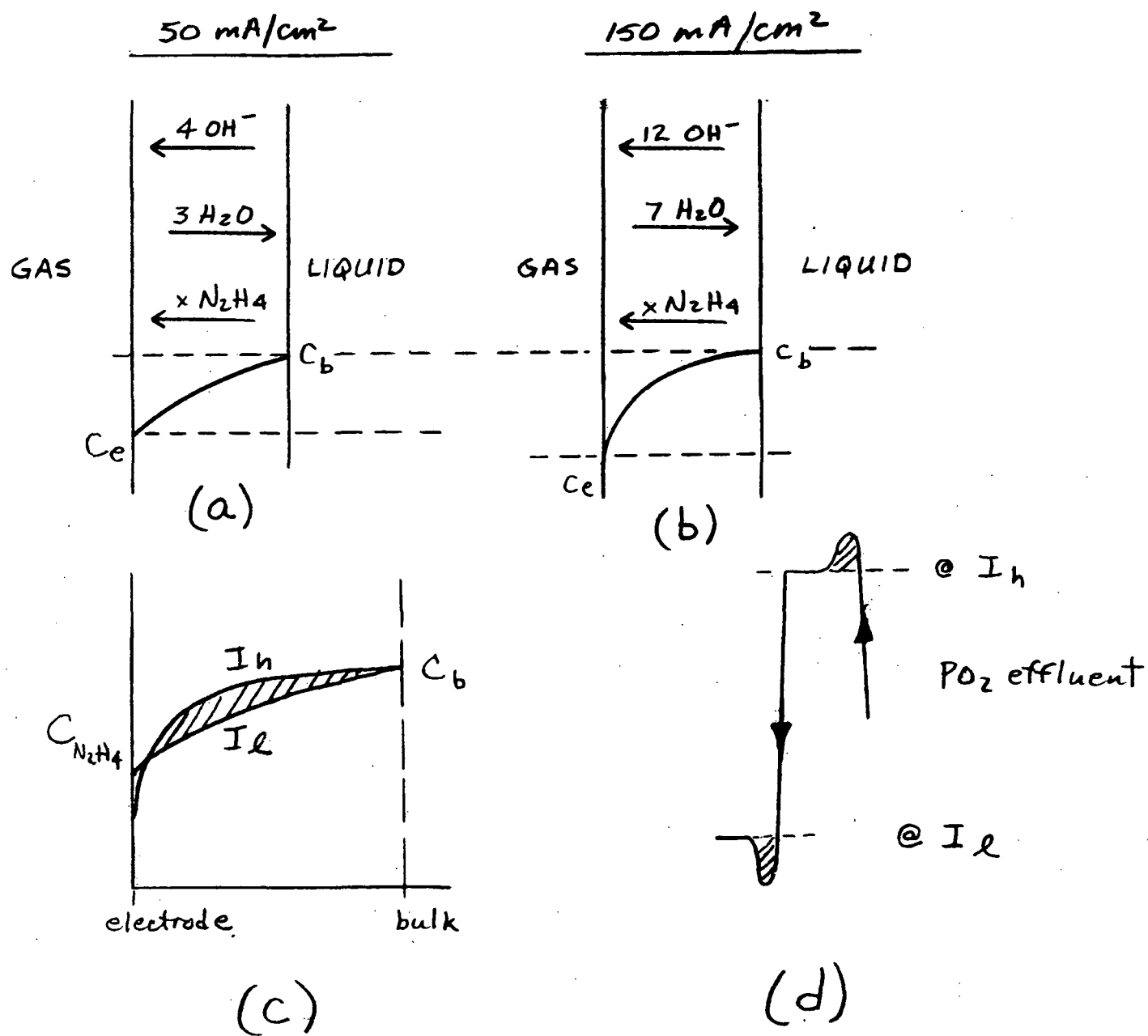


Figure 23 Diffusion Model of Electrolysis Cell

which was achieved by decreasing the control dead band (Tests 1 and 2) indicates that an even more sophisticated control technique, possibly proportional or rate control, might ultimately be considered for this system.

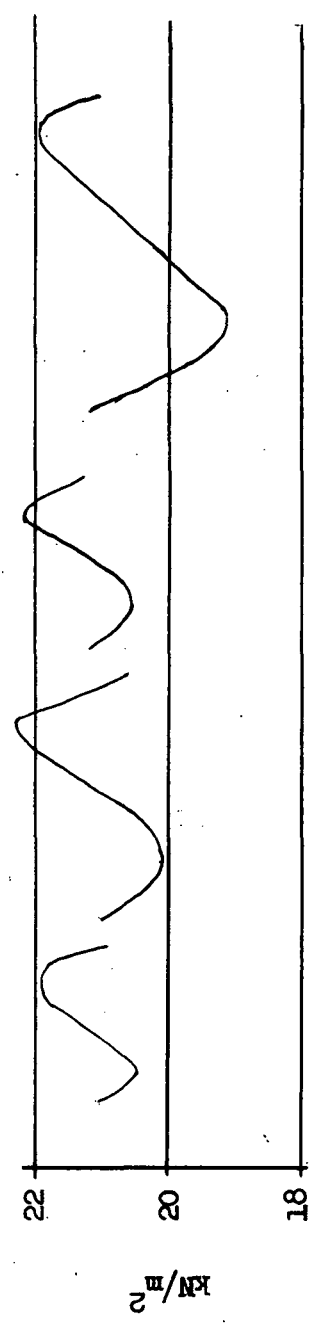
It was demonstrated in Tests 2 and 3 that increasing the low mode current improved the  $pO_2$  control by reducing the cycle time. If there were no other constraints or requirements on the system, it is obvious that the optimum  $pO_2$  control would occur with constant current operation. A manned spacecraft, however, can realistically be expected to have a wide range of metabolic and leakage loads. The  $N_2/O_2$  system must therefore be versatile enough to meet the varying demand by having more than a single current mode. It appears that a reasonable compromise of the conflicting requirements to optimize  $pO_2$  control yet still control the total pressure of the cabin would be to set the low mode current as high as possible, i.e., to provide for minimum metabolic and leakage load, and to set the high mode current at the lowest possible value, i.e., to provide for maximum metabolic and normal leakage. The case of maximum leakage would then be handled by turning on an installed spare module. This approach would allow the high and low mode currents to be set reasonably close together to achieve good  $pO_2$  control and would still allow the maximum demand conditions to be met.

The four cases of metabolic and leakage loads which were run in Test 3 were a good demonstration of the ability of the  $N_2/O_2$  system to respond to step changes in demand without control upset. The  $pO_2$  control characteristics for each case are presented in Figure 24. These data show that as expected, the shortest cycle time and smallest amplitude of  $pO_2$  occurred at the normal design point conditions. The worst response occurred at the conditions of Case IV, where there was a minimum percentage requirement for nitrogen. Here, the high  $N_2/H_2$  feed rate resulted in a large undershoot of the  $pO_2$  control band.

#### Trace Gas Contaminants

Undesirable trace constituents were found in the gases generated by the system in sufficient quantities to require attention. The chemical analysis results of Test 4 are summarized in Table 16 and are considered individually below.

	<u>CASE I</u>		<u>CASE II</u>		<u>CASE III</u>		<u>CASE IV</u>	
METABOLIC LEAKAGE	NORMAL		NORMAL		MAXIMUM		MAXIMUM	
CABIN PO <sub>2</sub>	NORMAL		MINIMUM		NORMAL		MINIMUM	
AMPLITUDE (KN/m <sup>2</sup> )	1.6		2.3		1.7		2.7	
CYCLE TIME (Hrs)	6.4		9.9		6.8		12.3	



	6.2		6.2		6.2		6.2	
CABIN P <sub>Total</sub>	50		59		50		53.5	
AMPLITUDE (KN/m <sup>2</sup> )	40		27.2		67		35	
CYCLE TIME (Min)								
% HIGH MODE								

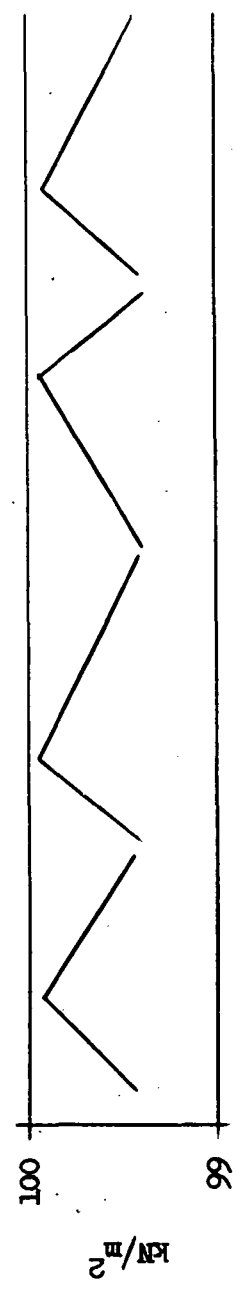


Figure 24 Cabin PO<sub>2</sub> and P<sub>Total</sub> Control Characteristics as a Function of Gas Demand - Typical Cycle

Table 16  
GAS ANALYSIS SUMMARY RESULTS

SAMPLE LOCATION	TRACE CONTAMINANTS (PPM)					
	CO	CH <sub>4</sub>	NO <sub>2</sub>	N <sub>2</sub> O	NH <sub>3</sub>	N <sub>2</sub> H <sub>4</sub> DERIVATIVES
O <sub>2</sub> /N <sub>2</sub>	9 - 10*	N.D.**	20	20 - 30	30 - 40	20
H <sub>2</sub>	N.D.	N.D.	20	N.D.**	20 - 30	20
BUBBLE SEPARATOR (20% O <sub>2</sub> 78% N <sub>2</sub> )	1*	0.8	20	N.D.	N.D.	20
METHOD OF CONTROL	NONE REQD	NONE REQD	H <sub>2</sub> O CHARCOAL OR BASIC SORBENT	H <sub>2</sub> O CHARCOAL	ACID CHARCOAL OR SORBEADS	OXIDATION

\* NO CO EVOLVED FROM EXPERIMENTAL ELECTRODES

\*\* N.D. = NONE DELETED

Carbon monoxide, detected in the  $N_2/O_2$  effluent and the bubble separator effluent, was produced by the slow oxidation of residual organic materials in the commercial electrodes used in the cell stack. This would not be a problem in a spacecraft system because the experimental electrodes being developed as part of this program do not produce CO.

Methane, detected at an extremely low level in the bubble separator gas, would not require special control because of the very low level and the very low gas production rate. It is also very possible, because of the difficulty of obtaining clean gas samples from a reduced pressure point, that the analysis was not correct.

Nitrogen dioxide was indicated by the analyses to be present at all three sample locations. The analysis technique used was not very sensitive for  $NO_2$ ; the presence of  $NO_2$  should be verified in the future by chemiluminescence. If, indeed,  $NO_2$  is being produced by the system, processing of the  $N_2/O_2$  by wet charcoal or a basic sorbent would be necessary in a spacecraft application.

Nitrous oxide was detected in the  $N_2/O_2$  gas by mass spectrometer analysis but was not confirmed by gas chromatography. Its actual presence is questionable, but if present, would require processing with wet charcoal in a spacecraft application.

Ammonia was detected at levels well above the limits of detectability in both the  $N_2/O_2$  and the hydrogen gases. Acid charcoal or sorbeds could be used in a spacecraft application to remove the  $NH_3$  from the  $N_2/O_2$  gas.

Hydrazine derivatives were detected in all sample locations. The  $N_2/O_2$  would require processing by catalytic oxidation to remove this undesirable constituent.

Based on available information concerning trace contaminant control in a manned spacecraft<sup>6</sup>, it appears entirely feasible to process the  $N_2/O_2$  gas directly in the spacecraft contaminant control system without imposing an appreciable excess load on this system. This approach would permit handling of the contaminants at their source (highest concentration) rather than having to process them after dilution to lower concentration in the spacecraft cabin atmosphere.

Neither the hydrogen nor the bubble separator gas would require treatment. The hydrogen would be used in a CO<sub>2</sub> reduction system where the low levels of contaminants would not be expected to interfere. The gas production rate in the bubble separator is low enough not to cause a problem if this gas is dumped directly to the cabin.

## 2.6 PROTOTYPE DESIGN

### 2.6.1 Requirements

The purpose of this task was to define the design of a prototype unit consisting of a replaceable electrolysis module incorporating the modularity concept of the preliminary design effort previously performed in Phase I of the contract. The results of an analysis effort under a separate oxygen-only program<sup>7</sup> form the basis for this task. The detailed component drawings and specifications for the  $N_2/O_2$  system were submitted as a separate item under this contract. This section of the final report covers the additional analyses that were conducted to expand the  $O_2$ -only design to an  $N_2/O_2$  design and briefly describes the functional components of the  $N_2/O_2$  assembly.

### 2.6.2 System Analysis

The  $N_2/O_2$  system is based on the Space Station Prototype (SSP)  $O_2$  system design, with changes only as required to allow the generation of nitrogen and to account for specific mission variations. The basic differences, therefore, lie in the areas of a revised system design point, a revised heat exchanger analysis, and an increase in system electrolyte volume and  $\Delta P$  due to the new reservoir design and other minor changes.

#### 2.6.2.1 System Design Point

The system is designed for SSP cabin leakage and metabolic consumption rates. Each module is designed for operation at a maximum current density of  $150 \text{ mA/cm}^2$  and, therefore, 4 modules with 22 cells per module are required for a 6-man system at the maximum values of metabolic and leak rates. At lesser values, fewer modules are required.

A design point summary of input and output parameters is presented in Table 17. Operation is based on the maximum current density of  $150 \text{ mA/cm}^2$  and a  $N_2H_4$  conversion efficiency of 100%. According to Figure C-6, IMSC/A977498, this requires a cell voltage of 2.2 volts. Total input power is 1195 watts with a controller efficiency of 92% and the total heat rejected is 489 watts. It is assumed that only heat generated in the cell stack is rejected through the electrolyte loop, as there is some convective cooling and the cell controller has a separate heat sink.



Table 17

$\text{N}_2/\text{O}_2$  MAXIMUM POWER DESIGN POINT  
(1 MODULE)

## OUTPUT -

$\text{O}_2$ - (5.10 lb/day)	2.32 kg/day
$\text{N}_2$ - (2.16 lb/day)	0.98 kg/day
eq $\text{O}_2$ - (7.55 lb/day)	3.43 kg/day
$\text{H}_2$ - (0.95 lb/day)	0.43 kg/day

## INPUT -

$\text{H}_2\text{O}$ - (5.72 lb/day)	2.60 kg/day	Equivalent to $\text{H}_2\text{O}$ (4.34 lb/day) 1.97 kg/day
$\text{N}_2\text{H}_4$ - (2.46 lb/day)	1.12 kg/day	$\text{N}_2\text{H}_4 \text{ H}_2\text{O}$ (3.84 lb/day) 1.75 "

## OPERATING PARAMETERS:

Current Density	150 mA/cm <sup>2</sup>
Cell Voltage (Total)	2.2 volts
$\text{N}_2\text{H}_4$ Conversion Eff.	100%

## POWER INPUT:

Cell Controller (92% Eff.)	1140 watts
Pump	35 watts
Other	<u>20 watts</u>
Total	1195 watts

## Q REJECTED:

Cell Stack	344 watts
Cell Controller	90 watts
Pump	35 watts
Valves, etc.	<u>20 watts</u>
Total	489 watts

### 2.6.2.2 Revised Heat Exchanger Analysis

SSP requirements for the  $O_2$  system specify a KOH inlet and water inlet temperature of  $32.6$  and  $18.3^\circ\text{C}$  ( $90.8$  and  $65^\circ\text{F}$ ) respectively. Also, the KOH and water flow rates are respectively  $12$  and  $9.4$  gm/s.

The test heat exchanger had an average of  $670 \text{ J/s m}^2$   $^\circ\text{C}$  ( $118 \text{ BTU/hr ft}^2$   $^\circ\text{F}$ ) (See Section 2.3) and an area of  $0.068 \text{ m}^2$  ( $0.737 \text{ ft}^2$ ). Thus, for the assumed electrolyte loop heat rejection of  $344$  watts, a  $7.4^\circ\text{C}$  ( $13.4^\circ\text{F}$ ) LMTD is required versus the  $5^\circ\text{C}$  ( $9^\circ\text{F}$ ) available for the SSP case. The water inlet temperature or flow rate must, therefore, be slightly modified to allow proper system operation. The easiest solution would be to lower the inlet water temperature  $2.8^\circ\text{C}$  ( $5^\circ\text{F}$ ) and keep the specified low rate.

### 2.6.2.3 System Electrolyte Volume $\Delta P$

Due to the revised reservoir design and other minor changes, accurate electrolyte volume and  $\Delta P$  analyses were run. The results of these analyses are summarized in Tables 18 and 19. The bubble separator pump produces  $34.4 \text{ kN/m}^2$  ( $5 \text{ psi}$ )  $\Delta P$  at the required flow rate, and therefore, can easily supply the required pressure of  $27.9 \text{ kN/m}^2$  ( $4.05 \text{ psi}$ ).

### 2.6.3 Detailed Design

#### 2.6.3.1 General Description of Prototype Unit

As shown in Fig. 25 and schematically in Fig. 26, an  $N_2/O_2$  electrolysis module consists of a cell stack, electrolyte reservoir, pump/bubble separator, electrolyte heat exchanger, base plate assembly, and supporting valves, plumbing, and instrumentation. The detailed drawings which were procured for these components and their specifications are listed in Table 20. All components except the heat exchanger are mounted on one side of the base plate assembly, which serves as the primary mounting structure for the unit. The heat exchanger and quick disconnect electrical and plumbing connections are on the opposite side of the base plate and form the sole interface with the system cabinet. All input, output, and control functions are through this interface.

Table 18  
SYSTEM  $\Delta P$  SUMMARY

Cell stack	7.92 kN/m <sup>2</sup>	(1.15 psi)
H <sub>x</sub>	1.38 kN/m <sup>2</sup>	(0.20 psi)
Reservoir	0.69 kN/m <sup>2</sup>	(0.10 psi)
Valves	9.92 kN/m <sup>2</sup>	(1.44 psi)
Pipe, passages, etc.	7.92 kN/m <sup>2</sup>	(1.15 psi)
Total	27.83 kN/m <sup>2</sup>	(4.05 psi)

Table 19  
SYSTEM VOLUME SUMMARY

Reservoir	23.0 cm <sup>3</sup>	(1.40 in <sup>3</sup> )
Cell Stack	1100.0 cm <sup>3</sup>	(67.00 in <sup>3</sup> )
P Regulator	2.7 cm <sup>3</sup>	( 0.12 in <sup>3</sup> )
Cell Stack Header and Tube	0.8 cm <sup>3</sup>	( 0.05 in <sup>3</sup> )
Base Plate	49.2 cm <sup>3</sup>	( 3.00 in <sup>3</sup> )
Heat Exchanger	60.7 cm <sup>3</sup>	( 3.70 in <sup>3</sup> )
Pump/Bubble Sep.	88.5 cm <sup>3</sup>	( 5.40 in <sup>3</sup> )
3-Way Solenoid Valve	14.7 cm <sup>3</sup>	( 0.90 in <sup>3</sup> )
Check Valves	2.7 cm <sup>3</sup>	( 0.12 in <sup>3</sup> )
Total	1342.3 cm <sup>3</sup>	(82.64 in <sup>3</sup> )

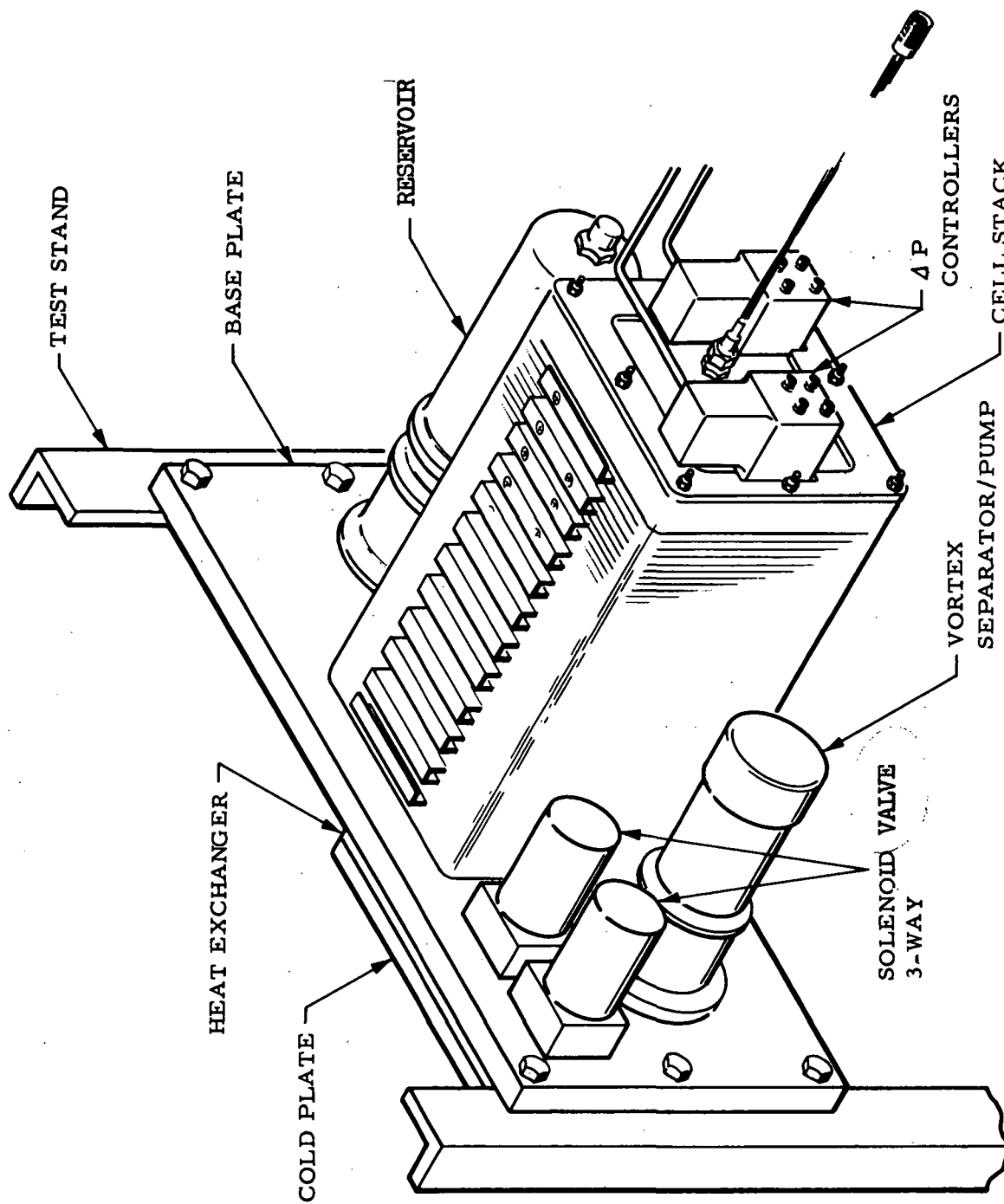


Figure 25 Prototype Unit Assembly

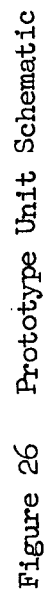


Figure 26 Prototype Unit Schematic

Table 20  
PROTOTYPE UNIT DRAWING LIST

<u>ENGINEERING</u>		<u>PROCESS SPECIFICATIONS</u>
BEH 20001	Schematic - N <sub>2</sub> /O <sub>2</sub> Generation Module	
BEH 20006	Template - Base Plate Passages	
BEH 20007	Base Plate Assy. Gas Electrolysis Cell	MS 33646 LAC-3601
BEH 20008	Spacer - Gas Electrolysis Cell	
BEH 20009	Closure, Bottom, Base Plate, Gas Electrolysis Cell	LAC-3601
BEH 20010	Spacer, Electrolyte- Electrolysis Cell	
BEH 20011	Main Body, Base Plate Gas Electrolysis Cell	LAC-3601
BEH 20012	Spacers, Base Plate, Gas Electrolysis Cell	MS 33646 LAC-3601
BEH 20013	Screen Assembly, Matrix Support- Electrolyte Spacer	
BEH 20014	Spacer Assy., Electrolyte- Electrolysis Cell	
BEH 20015	Frame, Electrode Gas Electrolysis Cell	
BEH 20016	Screen, Catalyst Support Electrode Gas Electrolysis Cell	
BEH 20017	Electrode Support Screen Gas Electrolysis Cell	
BEH 20018	Electrode Assembly N <sub>2</sub> /O <sub>2</sub> Electrolysis Cell	
BEH 20020	Reservoir Assy. N <sub>2</sub> /O <sub>2</sub>	LAC-3601 LAC-0581
BEH 20021	Base Reservoir	LAC-3601

Table 20 (Continued)

DRAWING LIST  
(Continued)

<u>ENGINEERING</u>		<u>PROCESS SPECIFICATIONS</u>
BEH 20022	Housing Reservoir	LAC-3601
BEH 20023	Support Assy., Transducer Reservoir	DS 8988 LAC-3853 LAC-3601
BEH 20024	Case Assy. Reservoir	AND 10050-4 LAC-3853 LAC-3601
BEH 20025	Adjuster Details Reservoir	LAC-3601
BEH 20026	Piston Reservoir	LAC-3601
BEH 20027	Cap, Piston Reservoir	LAC-3601
BEH 20028	Clamp, Transducer Reservoir	LAC-3601
BEH 20029	Support, Piston Reservoir	LAC-3601
BEH 20030	Spring, Reservoir	
BEH 20031	Bushing Support Reservoir	LAC-3601
<u>CONTROL</u>		
2-113	Pump/Bubble Separator	

Operationally, the unit consists of the electrolyte circuit, the nitrogen circuit, the gas supply, the water feed, and instrumentation.

Electrolyte Circuit - The electrolyte is completely sealed within the unit and circulates through all major components. Water and hydrazine enter at the reservoir, which accommodates changes in electrolyte volume and also controls the water and hydrazine feed rates. Water and hydrazine feed modes are separate, and are selected by the control system. During the water feed mode, as water is consumed, the system water volume decreases and sensors in the reservoir activate the water feed solenoid valve. When the volume is restored, the water feed is terminated. In the hydrazine feed mode, the water feed solenoid is deactivated and the reservoir sensor controls hydrazine feed. The water and hydrazine feed systems are introduced into the reservoir to assure complete mixing with the potassium hydroxide electrolyte before passing into the cell stack. The location of the reservoir immediately upstream of the cell stack is considered optimum, as this location presents the minimum potential for free gas accumulation and the reservoir serves to dampen potential electrolyte pressure pulses within the cell stack. In addition, this location provides for close pressure control close to the cell stack which is desirable for setting of gas/liquid pressure differences and the absolute pressure levels.

The electrolyte flows from the reservoir into the cell stack where it provides water for the electrolysis process and cooling of the stack. In the cell stack, the liquid volume is reduced as water is consumed, causing some gas which entered the system dissolved in the feed water, to come out of solution. The cell stack is designed to assure that the free gas formed is separated from the stack by the circulating electrolyte.

The electrolyte containing the free gas then passes into the bubble separator and into the pump. The bubble separator and pump are combined in a single housing and are driven by a common motor. This is a new design for the prototype system. The liquid and gas mixture first enters the cylindrical chamber where a rotating blade creates a vortex. The liquid collects on the outer wall of the chamber where it is directed to the centrifugal circulating pump impeller. The gas separates from the liquid and collects in the center



of the vortex where it is removed by a gas pick up probe. Gas removal is controlled by a sensor which controls the liquid level in the vortex chamber.

The electrolyte leaving the pump is at its highest temperature having picked up heat in the cell stack and in the pump/bubble separator. The liquid then passes through a temperature control valve which either selects a route through the heat exchanger or through a bypass line and back to the reservoir, as determined by temperature sensors at the cell stack inlet. The heat exchanger is of nickel construction and is coated with Kynar. The heat exchanger transfers heat to a cold plate by direct conduction through a mechanical interface. Contact is assured by bolting the heat exchanger and cold plate together. All portions of the circulating electrolyte are either plastic, Kynar coated, or elastomers to assure that no bi-polar electrodes are developed that would produce gas in the electrolyte circuit.

Nitrogen Circuit - The pressure level of the electrolysis system is controlled by the nitrogen pressurization system. Differential pressure regulators set the nitrogen pressure on the back side of the reservoir bellows. A spring in the reservoir which is adjusted to a minus  $13.8 \text{ kN/m}^2$  (2 psi) assures that the liquid pressure will always be less than gas pressure when the module is inactive. This  $13.8 \text{ kN/m}^2$  (2 psi) differential will allow adequate gas pressure for nitrogen purge to inert the modules on shutdown. The absolute pressure of the electrolyte will be  $103 \text{ kN/m}^2$  (15 psig) to prevent possible condensation of water from the effluent oxygen and hydrogen streams under all operating conditions. The nitrogen also serves two other functions. During normal shutdown of the electrolysis system, nitrogen pressurization solenoid valves at the inlet to the hydrogen and oxygen sides of the module are open and the hydrogen and oxygen shut-off valves at the outlet are closed. The nitrogen then feeds slowly into the cell stack to prevent pressure decay as the hydrogen and oxygen are slowly consumed by fuel cell effects in the absence of electrolysis power. A pressure decay could result in flooding. A second nitrogen use is the inerting of the modules during total shutdown and change of a module. In this case, the nitrogen purge and shut-off valves will both be open and hydrogen and oxygen will be purged from the stack by flowing nitrogen. For a predetermined time interval, the module shut-off valves are then closed off and the module is inerted.

Gas Supply - During electrolysis operation, oxygen, nitrogen, and hydrogen are generated in the cell stack. In order to prevent flooding, the gas pressure in the stack must be greater than the electrolyte pressure. Thus, differential pressure regulators are provided which back pressure the effluent gases in the module to a level of  $2.49 \text{ kN/m}^2$  (10 in. water) over an electrolyte pressure reference. Gases passing through the regulators then pass out of the module through shut-off valves.

Water Feed - When the reservoir volume sensor registers low volume, a water feed valve is actuated which restores the electrolyte volume. Back flow of electrolyte is prevented by a check valve in the water feed line.

#### 2.6.3.2 Component Descriptions

Cell Stack - The cell stack design was not modified extensively in this program effort (Ref. 7). One variation from the basic  $\text{O}_2$  only design was that the composition of the electrodes was changed to reflect the design performance improvements indicated in Sections 2.1 and 2.2 of this report. These design changes included the use of the reduced-catalyst cathodes and the iridium-additive experimental anodes. In addition, a high bubble point hydrophilic membrane with an in-situ deposited asbestos matrix combination was substituted for the discrete asbestos sheets used in the previous design to improve the resistance of the cells to gas breakthrough at high gas/liquid differential pressures.

Reservoir - The electrolyte reservoir is provided to accommodate small changes in electrolyte volume due to normal pressure and temperature fluctuations, to provide mixing of the electrolyte and water during a water feed cycle, to compensate for changes in the electrolyte volume due to the consumption of water or hydrazine in the electrolysis process, and to allow the addition of relatively large amounts of hydrazine to the electrolyte when  $\text{N}_2$  generation is desired. In addition, the reservoir controls both water and hydrazine feed, controls the system electrolyte pressure, and provides system safety signals.

The unit consists of a base and housing which support the ethylene propylene and dacron bellofram diaphragm, a guided piston and the piston support, the transducer and transducer support, a spring and spring adjuster assembly, and the outer case assembly. The bellofram divides the unit into separate electrolyte and gas chambers, and the electrolyte interface to the base plate is through face "O" ring seals. All metal components are stainless steel, while seals are ethylene propylene rubber.

The gas side chamber is formed by the outer case assembly and the housing. It has a maximum operating pressure of 15 psi, and contains the piston and support assembly, the pressurizing spring and adjuster, and the transducer assembly. The piston is supported in Delron AF (a mixture of Teflon and Delron) bushings which assure a low coefficient of friction and minimum wear. The coil spring assures a high load with a minimum installed length, and the pressure on the bellofram is easily adjusted by inserting two rods through the slot in the transducer support assembly and rotating the adjustment nut relative to the adjustment sleeve. The hollow support shaft allows the transducer to be placed inside the shaft to minimize external case dimensions.

The transducer itself is a DC input, DC output differential transformer with a built-in carrier oscillator and phase sensitive demodulator. It provides a DC output proportional to linear displacement, and is extremely accurate. It assures long life as the only moving part of the assembly is the transducer core. Electrical feedthroughs are made by a hermetically sealed connector in the outer case.

During operation, the unit is used to control both water and hydrazine feed. Water feed is normally controlled to  $\pm 1\%$  of total system volume, while a hydrazine feed of up to  $17.7\%$  of the nominal system volume can be accommodated. If, during the water feed mode, system volume exceeds  $\pm 3\%$  of the nominal system volume, high or low electrolyte level safety signals are initiated. Also, if during the hydrazine feed mode, the hydrazine feed limit is exceeded by  $2\%$  of the nominal system volume, a safety signal is initiated. Volume control functions are summarized in Table 21.

Table 21  
RESERVOIR VOLUME CONTROL FUNCTIONS SUMMARY

Control positions and nominal percentages of system volume:

- o Low electrolyte volume limit - 3% below nominal system
- o Water feed on point - 1% below nominal system
- o Water feed off point - 1% above nominal system
- o H<sub>2</sub>O feed high electrolyte volume limit - 3% above nominal system volume.
- o N<sub>2</sub>H<sub>4</sub> feed safety limit - 20.7% above nominal system volume
- o High electrolyte volume limit - 22.7% above nominal system volume.

An additional function of the reservoir is to provide system electrolyte pressure control, both during storage and during system operation. At the nominal volume point, the reservoir provides a differential pressure of  $13.8 \text{ kN/m}^2$  (2 psi) between the gas and liquid sides of the system, with the higher pressure on the gas side. This pressure is allowed to fall as low as  $3.4 \text{ kN/m}^2$  (0.5 psi) at the hydrazine feed high limit point. Total system pressure is controlled by pressurizing one side of the reservoir with nitrogen gas. During storage, gas sealed in the reservoir maintains the electrolyte system pressure at  $13.8 \text{ kN/m}^2$  (2 psi). During operation,  $117 \text{ kN/m}^2$  (17 psi) nitrogen is applied to the accumulator, resulting in a nominal system pressure of  $103 \text{ kN/m}^2$  (15 psi).

Pump/Bubble Separator - The pump/bubble separator is manufactured by the Fluid Dynamics Corporation. It combines the functions of electrolyte pump and gas/liquid separator into one unit driven by one motor. It is, therefore, used to circulate electrolyte through all fluid components, and to remove gas bubbles which are formed in the cell stack.

The unit consists of a vortex section and sensing impeller, a pump section, and a magnet drive and motor assembly. The unit mounted to the polysulfone base plate, which in turn mounts to the electrolysis unit main base plate.

The vortex section consists of a polysulfone impeller mounted on the central stainless steel shaft. This shaft also passes through the pump impeller and is attached to the inner magnet drive. A vortex core diameter sensing wheel is free-floating on the central shaft, and consists of a plastic paddle wheel with internally imbedded toothed nickel wheel. Adjacent to this wheel in the housing, is a magnetic proximity detector.

The pump section is between the vortex section and motor, and plastic impeller, which also is attached to the central shaft. The end of the shaft is attached to the inner magnet drive assembly.

The outer magnet drive assembly and motor attach to the end of the pump section. The motor is air cooled and operates on 1 phase, 60 Hz, 115 volt power. The motor case is anodized aluminum and contains space for control electronics. The motor and outer magnet drive are easily replaceable

as a unit, as they are held in place in the housing with a snap ring.

The whole separator unit weighs less than 1.6 kg (3.5 lb) and consumes 35 watts of power. The case is designed for a maximum of  $240 \text{ kN/m}^2$  (35 psi) internal pressure. During operation, the motor drives the central shaft through the magnet drive assembly. Liquid enters through the base and passes into the vortex generator where the spinning vortex wheel creates a liquid vortex with a cylindrical gas core, thus separating any entrained gas from the liquid. The size of the gas core is controlled by the vortex sensing wheel and proximity detector. As the gas core expands, the wheel is less immersed in liquid and slows down. This is detected by the sensor and the associated electronics opens the gas vent valve. As the core shrinks, the wheel speeds up and the valve is shut. In excess of  $10 \text{ cm}^3/\text{hr}$  of gas can be removed.

Gas free electrolyte then passes from the vortex chamber into the pump stage where a centrifugal impeller pumps it through the system. The pump can deliver  $12 \text{ cm}^3/\text{s}$  (12 GPH) at  $27.6 \text{ kN/m}^2$  (4 psid) at  $24^\circ\text{C}$  ( $75^\circ\text{F}$ ).

Heat Exchanger - The prototype heat exchanger, designed and fabricated in a separate phase of this program (see Section 2.3), was design verification tested and found to be suitable for use in this prototype unit.

Base Plate - The  $\text{O}_2$ -only base design was modified only to the extent necessary for use in an oxygen-nitrogen unit assembly. It was modified to accept the prototype heat exchanger discussed above.

Supporting Equipment - Supporting equipment such as valves, plumbing, and most of the instrumentation were not considered in this effort because the design was directed to an early prototype assembly utilizing laboratory support equipment, rather than to a full-flight prototype unit.

#### 2.6.4 Process Specifications

Standard good practice, manufacturing specifications, both IMSC and MIL specs, were identified for those components that would be expected to be fabricated by the IMSC R&D machine shop. For those components or parts of components which are still in the development phase, e.g., electrodes,

catalyst materials, and baseplate, process specifications were indicated as TBD (To Be Determined).

## 2.7 RELIABILITY ANALYSIS

A formal reliability program was not required by the contract. Therefore, other than the reliability inherent in good engineering judgment, there was no attempt to invoke the reliability principles that would be normal for a flight article.

With regard to the breadboard system, the long-term performance test of the vortex bubble separator did provide useful reliability data, indicating the need to incorporate in the design a reliable means of preventing liquid carryover.

In the detailed design of the prototype unit, the reliability analysis conducted in the preliminary design effort in Phase I was enforced.<sup>2</sup>

In developing the water electrolysis system, it was decided that the optimum approach was to avoid breaking into the electrolyte circuit to perform any maintenance tasks. This approach eliminated the necessity for handling the electrolyte in zero gravity and could be implemented with no significant weight penalty. The maintenance concept that was evolved consisted of providing individual self-contained hydraulic assemblies with no electrolyte connections. A reliability analysis was then conducted to determine the optimum size and number of these individual assemblies.

Preceding page blank

### Section 3

#### CONCLUSIONS

##### 3.1 CATALYST ADDITIVES

Substantial improvements in the long-term performance stability of electrolysis cell anodes was achieved through the use of catalyst additives, in particular iridium black, and through improvements in the electrode fabrication and processing techniques. This order of magnitude of performance improvement would be reflected in a full-scale system design, e.g., the 12-man preliminary design of Phase I, as a 10 to 20 percent reduction in power requirement (a savings of 0.78 to 1.57 KW) and approximately 50 percent reduction in cooling requirement (2 KW).

##### 3.2 CATHODE DEVELOPMENT

Reduced catalyst loading of the electrolysis cell cathodes was demonstrated experimentally to be a feasible means of improving the hydrazine reaction efficiency in the cells. Even though reduced catalyst loading increased the cell voltage to a full-scale total equivalent weight (TEW) tradeoff shows a potential savings of 20 percent in TEW resulting when the conflicting parameters of power and cooling are compared to fixed weight savings in hydrazine storage.

##### 3.3 PROTOTYPE HEAT EXCHANGER

The prototype heat exchanger conceived for the 12-man preliminary design effort in Phase I of the program was successfully fabricated and tested. Its performance was demonstrated to be better than the original analysis had predicted. Analysis of the test results indicated that this unit would be acceptable for use in a prototype module assembly.

##### 3.4 SYSTEM TESTING

Over 1000 hours of cumulative operating time were logged on the one-man breadboard system under various test conditions. The tests that were conducted have led to a more complete characterization of the hydrazine/water electrolysis process in the following specific areas:



- o A new cabin  $pO_2$  control technique was successfully demonstrated. The use of this technique, coupled with more optimum control band and current level settings, resulted in achieving a cabin  $pO_2$  cycle time of 6 hours as compared to approximately 12 hours in Phase I.
- o The ability of the system to respond without control upset to a wide range of cabin gas demands was demonstrated.
- o A closed-loop test of laboratory prototype zero-gravity components, i.e., a vortex bubble separator and bellofram reservoir, was successfully conducted.
- o A series of parametric tests in which current density and temperature were varied were carried out. The data indicate that increasing temperature increases the hydrazine decomposition rate. However, results are not conclusive because of differences in method of hydrazine feed to the system and the range of temperatures investigated was not sufficiently large to give a clear trend.
- o A comprehensive analysis of the chemical composition of the generated gases led to the conclusion that processing of the generated  $N_2/O_2$  mixture to remove trace nitrogen compounds will be necessary in a spacecraft application.

### 3.5 PROTOTYPE UNIT DESIGN

Engineering drawings and specifications sufficient to fabricate/procure the necessary components of a prototype  $N_2/O_2$  electrolysis module were completed.

## Section 4

### REFERENCES

1. Greenough, B.M., "The Development of a Non-Cryogenic Nitrogen/Oxygen Supply Technique", NASA CR-114912, May 17, 1971.
2. Greenough, B.M., "Preliminary Design of a Space Station Electrolytic Oxygen-Nitrogen Generator", IMSC/A977498, March 5, 1971.
3. Greenough, B.M., "Design, Development and Fabrication of a Water Electrolysis System for a 90-Day Manned Test", NASA CR-111911, June 21, 1971.
4. Greenough, B.M., "Status of the IMSC Circulating Electrolyte Water Electrolysis System", ASME Paper 71-AV-20, SAE/ASME/AIAA Life Support and Environmental Control Conference, San Francisco, California, July 12-14, 1971.
5. NASA Contract NAS9-11848, "Water Electrolysis System Refurbishment and Testing", Document MSC 07383.
6. Olcott, T.M., "Development of a Sorber Trace Contaminant Control System including Pre- and Post-Sorbers for a Catalytic Oxidizer", NASA CR-2027, May 1972.
7. "Space Station Electrolytic Oxygen Generator, Preliminary Design", IMSC/A981656, January 1, 1971.

LIBRARY CARD ABSTRACT

A development program was conducted concerned with the use of a hydrazine/water electrolysis technique to provide both the metabolic-oxygen for crew needs and the oxygen and nitrogen for spacecraft cabin leakage make-up. Anode stability was improved with catalyst additives and improved processing techniques. The hydrazine conversion efficiency was improved by using reduced-catalyst loading of the cathodes. Over 1000 hours of testing of a one-man breadboard  $O_2/N_2$  system provided data for characterization of the hydrazine/electrolysis process and for improvement in system control. Detailed design of a prototype modular unit was conducted including fabrication and design verification testing of the internal heat exchanger, which is a component of the unit.

Preceding page blank

## APPENDIX

### TEST DATA LOGS

#### CATALYST ADDITIVE TEST DATA

The following section presents the raw data taken on electrodes in the testing of various anode compositions. Data are presented for the most promising electrodes only. Many of the electrodes built up were not subject to cell testing due to mechanical defects. A discussion of these data is presented in Section 2.1 of the text.

## WATER ELECTROLYSIS DATA SHEET

Cell No. 71-7

Date 11-15-71 Operator Kopp-rnik Sheet 1 of       

Cell Description:                      Size\_\_\_\_\_

Anode  $\text{Ti} = 25\% \text{ Teflon}, 50\% \text{ Jaquer}, 20\% \text{ Pt}, 5\% \text{ Rhodium}$

Cathode 69-11 note Rh 20% of catalyst

Matrix

Assembly Standard

Electrolyte 30% KOH

Test Description:

Test Analysis:

Total Operating Time\_\_\_\_\_

Reason for Stopping Test \_\_\_\_\_

Remarks \_\_\_\_\_

OPERATOR Keppel Sheet 3 of 3 Cell No. 21-7 Test st<sub>2</sub> #12

Date	Time	Elap. Time Meter Time	Accum. Curr. Time	Voltage		Flow Rate		Gas Analysis		
				Cell	H <sub>2</sub>	O <sub>2</sub>	H <sub>2</sub>	O <sub>2</sub>	H <sub>2</sub>	O <sub>2</sub>
11/25	11:00		0	2.7	1865	189	1.09			
	11:01 AM		3	2.7	1879	189	1.687			
	11:02 AM		5	2.7	1879	191	1.679			
11/26	8:00 AM		21	2.7	1885	189	1.709			
	8:20 AM		23.5	2.7	1919	209	1.710			
	11:20 AM		26.5	2.7	1919	199	1.710			
	11:30 AM		29.5	2.7	1919	207	1.710			
11/27	8:00 AM		45	2.7	1939	219	1.729			
	11:00 AM		77	2.7	1942	210	1.727			
	11:30 AM		50.5	2.7	1939	209	1.729			
	11:30 AM		53.5	2.7	1919	201	1.719			
11/28	8:00 AM		69	2.7	1939	209	1.729			
	10:00 AM		71	2.7	1939	209	1.729			
	11:00 AM		74	2.7	1930	209	1.727			
	3:30 PM		76.5	2.7	1927	209	1.720			
11/29	8:00 AM		93	2.7	1949	209	1.730			
11/22	8:30 AM		165.5	2.7	1960	189	1.739			
	12:00 PM		170.0	2.7	1959	179	1.729			
	11:30 AM		173.5	2.7	1959	179	1.729			
11/23	8:00 AM		189	2.7	1909	179	1.739			
	3:30 PM		196.5	2.7	1909	179	1.740			
11/24	8:00 AM		213	2.7	1980	179	1.757			
11/25	8:00 AM		333	2.7	1979	159	1.757			
	1:00 PM		339	3.8	2189	219	1.879			
	1:05 PM		338	2.7	2009	159	1.777			
11/30	8:00 AM		357	2.7	2100	170	1.799			
	1:30 PM		362.5	2.7	2000	139	1.770			

~~11/23~~ KOH level is low - H<sub>2</sub>O Fed not working  
added H<sub>2</sub>O manually

OPERATOR

Sheet 2 of 3

Cell No. 71-7

STA. #2

Date	Time	Elap. Time	Accum. Time	Curr.	Voltage		Flow Rate		Gas Analysis	
					Cell	H <sub>2</sub>	H <sub>2</sub>	O <sub>2</sub>	H <sub>2</sub>	O <sub>2</sub>
11/30	4:30 PM		365.5	2.7	2.00	199		1787		
12/1	8:00 AM		381	2.7	1990	199		1789		
	11:00 AM		384	2.7	1989	199		1789		
	2:00 PM		387	2.7	1989	199		1789		
	4:00 PM		389	2.7	1989	199		1789		
12/2	8:00 AM		405	2.7	1989	199		1789		
	4:20 PM		413.5	2.7	1999	199		1791		
12/3	8:00 AM		429	2.7	2.00	199		1800		
	4:20 PM		437.5	2.7	2.00	199		1809		
12/6	8:00 AM		501	2.7	2.00	199		1804		
"	Shut		Cell down							
"	9:45 AM		501	New	sat	8:30			29% KOH -	
	12:30 PM		503.5	2.7	1943	189		1729	Restarted cell	
	4:20 PM		507.5	2.7	1969	191		1751	29%	
12/7	8:30 AM		523.5	2.7	1950	189		1749		
	4:30 PM		531.5	2.7	1960	199		1759		
12/8	6:00 AM		546	2.7	2.00	219		1791		
	4:30 PM		554.5	2.7	2.01	219		1769		
12/9	8:00 AM		570	2.7	2.030	229		1803		
	4:20 PM		578	2.7	2.000	209		1789		
12/10	8:00 AM		594	2.7	2.009	209		1799		
	3:30 PM		601.5	2.7	1.979	199		1779		
12/13	8:00 AM		601.5	Cell	shut	down			even weekend	
	9:00 AM		601.5	Cell	back	on			26.6	
	1:00 PM		605.5	Restarted	KOH	back on			fine 1.05	
	2:00 PM		606.5	2.7	1944	200		1781		
	4:30 PM		609	2.7	1928	180		1724		

Le Reservoir & H<sub>2</sub>O Ford eff. - 50% low

power supply failed  
334 g/L - 26.6% KOH

Sheet 3 of 3 Cell No. 71-7 JTH #2-

Cell No. 171-7

3 of 3

Sheet\_\_\_\_\_

**OPERATOR**

Date	Time	Flap. Time Meter	Accum. Curr. Time	Voltage		Flow Rate		Gas Analysis		
				Cell	H <sub>2</sub>	O <sub>2</sub>	H <sub>2</sub>	O <sub>2</sub>	H <sub>2</sub>	O <sub>2</sub>
12/14	8:00 AM		64.5	2.7	1.942	1.72	1.740			36.4 g/L KOH
	11:30 AM			2.7	1.931	1.69	1.739			
12/15	8:00 AM			2.7	1.982	1.79	1.769			36.3 g/L KOH
	11:30 AM			2.7	1.982	1.79	1.769			
	4:00 PM			2.7	1.978	1.79	1.769			
12/20	8:30 AM			2.7	1.961	1.89	1.775			
	12/21	8:30 AM		2.7	2.02	2.03	1.816			
	11:30 AM			2.7	2.009	1.94	1.810			
12/22	9:00 AM			2.7	2.019	1.99	1.819			34.8 g/L KOH
	10:00 AM				OFF					



WATER ELECTROLYSIS DATA SHEET

Test Sta. #1

Cell No. 71-8

Date 12/6 Operator \_\_\_\_\_ Sheet 1 of \_\_\_\_\_

Cell Description:

Size \_\_\_\_\_

Anode ~~69-11~~ #10 25% Teflon - 50% Jaguar, 20% Pt, 5% Ruth

Cathode 69-11 Ni Le Re 20% Pt

Matrix \_\_\_\_\_

Assembly Standard

Electrolyte 30% KOH

Test Description:

Test Analysis:

Total Operating Time \_\_\_\_\_

Reason for Stopping Test KOH solution turned amber color

Remarks Analysis showed Ruthenium was major component in dilute solution of KOH  
effluent

[illegible]

To B. Greenough  
from F. Smith

Subject: Metal Components in Electrolytic Cell H<sub>2</sub>O

12-7-71

Components

Ru  
Fe  
Ni  
K  
V

Amount

major  
trace  
trace  
minor to trace  
trace

The presence of Vanadium is questionable due to  
a ~~2nd~~ secondary iron line lying very close to this V  
analysis line

F. C. Smith

WATER ELECTROLYSIS DATA SHEET

Cell No. 71-9

Date 12 Operator \_\_\_\_\_ Sheet 1 of \_\_\_\_\_

Cell Description: Size 18 cm<sup>2</sup>

Anode #11 25% Teflon, 50% Jaguar, 20% Pt, 5% Iridium

Cathode Ni-L Tr 20% of Cat

Matrix \_\_\_\_\_

Assembly Standard

Electrolyte 30% KOH

Test Description:

Test Analysis:

Total Operating Time \_\_\_\_\_

Reason for Stopping Test \_\_\_\_\_

Remarks \_\_\_\_\_



WATER ELECTROLYSIS DATA SHEET

Test Sta. #2

Cell No. 71-410

Date 12/22 Operator \_\_\_\_\_ Sheet 1 of \_\_\_\_\_

Cell Description:

Size 18<sup>2</sup> CM

Anode #15 25% Teflon 50% aquar 20% Pt 5% Rhodium

Cathode 69-11 Ni-Rh 5% of cat

Matrix \_\_\_\_\_

Assembly Standard

Electrolyte 30% KOH

Test Description:

Test Analysis:

Total Operating Time \_\_\_\_\_

Reason for Stopping Test \_\_\_\_\_

Remarks \_\_\_\_\_

210-2  
Test Sta #2

Cell No. 171-1C

Sheet 1 of

OPERATOR

Date	Time	Elec. Meter Time	Accum. Time	Curr.	Voltage		Flow Rate			Gas Analysis		
					Cell	H <sub>2</sub>	O <sub>2</sub>	H <sub>2</sub>	C <sub>2</sub>	Moisture	H <sub>2</sub>	O <sub>2</sub>
12/22	12:00			2.7	2.019	439	1582					
12/23	8:00 AM			2.7	2.119	119	1.99					
	11:00 AM			2.7	2.109	189	1.907			28%		
	3:00 PM			2.7	2.099	159	1.87					
	4:30 PM			2.7	2.109	199	1.907					
12/24	8:00 AM			2.7	2.129	187	1.929					
	9:45 AM			Increased	pressure							
				Cell off								
1/3/72	2:30 PM			Cell restarted								
4/4/72	4:30 PM			Re assembled cell								
				Anode side to								
				increase pressure								
7/5/72	1:30			Cell line								
4/30/71				2.7	1.907	209	1.699					
4/6/72	8:00 PM			2.7	1.959	229	1.719					
	3:30 PM			2.7	1.959	229	1.709					
4/7/72	8:00 AM			2.7	1.949	229	1.719					
4/8/72	8:00 AM			2.7	1.929	219	1.709					
4/9/72	8:00 AM			2.7	1.929	219	1.709					
4/10/72	8:00 AM			2.7	1.939	213	1.714					
	9:00 AM			Shut down								
	2:15 PM			Start up								
4/12/72	1:00 PM			2.7	1.920	199	1.729					
4/12/72	3:00 PM			2.7	1.940	209	1.729					
	3:45 PM			Back on								
4/12/72	4:00 PM			2.7	1.920	199	1.706					
4/12/72	8:00 PM			2.7	1.949	209	1.739					
7/3/72	1:00			2.5	1.940	209	1.729					

355 7/2 11/11

355 7/2 11/11

shut down cell to repair H-X

STN #2

Cell No. 21-10

OPERATOR \_\_\_\_\_ Sheet 2 of \_\_\_\_\_

Date	Time	Flap. Time	Accum. Curr. Time	Voltage		Flow Rate		Gas Analysis	
				Cell	H <sub>2</sub> O <sub>2</sub>	H <sub>2</sub> O <sub>2</sub>	Moisture	H <sub>2</sub> O <sub>2</sub>	
4/14/72	10:50 AM		42.0	2.7	1945	2.7			
4/14/72	4:00 PM		45.0	2.7	1940	2.7			
4/17/72	8:30 AM		114.0	2.7	1993	2.29	7.2		403 g/L = 31% KOH
4/18/72	4:30 PM		136.5	2.7	1987	2.29			
4/18/72	8:30 AM		4.0	2.7	1979	2.19			
4/19/72	8:00 AM		160.0	2.7	1974	2.19			
4/20/72	4:30 PM		184	2.7	1949	2.09			
4/21/72	8:30 AM		208	2.7	1963	2.09	7.2		312 g/L = 30% KOH
4/24/72	8:30 AM		230.5	2.7	1955	2.09			
4/25/72	4:30 PM		254.5	2.7	1949	2.09			
4/26/72	4:30 PM		279.0	2.7	1942	2.09			
4/27/72	8:00 AM		303.5	2.7	1933	2.11			
4/28/72	4:30 PM		328.0	2.7	1942	2.20			
4/29/72	8:00 AM		352.5	2.7	1956	2.01			
5/1/72	4:30 PM		377.0	2.7	1965	2.09			
5/2/72	8:00 AM		401.5	2.7	1949	1.99			
5/3/72	4:30 PM		426.0	2.7	1953	1.99			
5/4/72	8:00 AM		450.5	2.7	1949	1.99	6.72		318 g/L = 29.5% KOH
5/5/72	4:30 PM		475.0	2.7	1952	1.99			
5/6/72	8:00 AM		500.0	2.7	1959	2.09			
5/7/72	4:30 PM		524.5	2.7	1969	2.19			
5/8/72	8:00 AM		549.0	2.7	1959	2.09			
5/9/72	4:30 PM		573.5	2.7	1959	2.09			



Cell No. 77-1c

OPERATOR \_\_\_\_\_ Sheet 3 of \_\_\_\_\_

Date	Time	Elap. Time Meter	Accum. Time	Curr.	Voltage		Flow Rate		Gas Analysis					
					Cell	H <sub>2</sub>	O <sub>2</sub>	H <sub>2</sub>	O <sub>2</sub>	M <sub>air</sub>	H <sub>2</sub>	O <sub>2</sub>		
5/9/72	4:30 PM			2.7	1.979	2.21	1.593							
5/9	4:30			2.7	1.979	2.29	1.209							
5/10	8:00 AM			2.7	1.981	2.85	1.191							
5/17	10:30 AM			5.167	down	cell	for modification							

Test sta. #1

WATER ELECTROLYSIS DATA SHEET

Cell No. 71-11

Date 12/23 Operator \_\_\_\_\_ Sheet 1 of \_\_\_\_\_

Cell Description: Size 18" CM

Anode #16 25% Teflon, 50% Invar, 20% Pt, 5% Iridium

Cathode 69-11 Note Ir 5% of Cat

Matrix \_\_\_\_\_

Assembly Standard

Electrolyte 30% KOH

Test Description:

Test Analysis:

Total Operating Time \_\_\_\_\_

Reason for Stopping Test \_\_\_\_\_

Remarks \_\_\_\_\_

Start

Cell No. 71-11

Sheet 1 of

OPERATOR

Date	Time	Flap. Time Meter	Accum. Curr. Time	Voltage		Flow Rate		Gas Analysis		
				Cell	H <sub>2</sub>	O <sub>2</sub>	H <sub>2</sub>	C <sub>2</sub>	Molar	O <sub>2</sub>
12/23/71	11:04 AM		2.7	1969	1079	879				Start Test
	3:00 PM		2.7	1960	859	1079				
	4:30 PM		2.7	1959	779	1179				
12/24	8:00 AM		2.7	1969	729	1159				
12/27	6:30 PM		Cell found off - reason unknown							
	6:45									
	6:45		2.7	1889	1169	1719				
12/30	10:30 AM		2.7	2009	209	1825				
1/3	11:30 AM		2.7	2033	199	1819			5.45	306 g/L $\Rightarrow$ 25%
	1:30 PM		add 2 gms KOH							to electrolyte (-vol. change)
	1:40 PM		2.7	2009	209	1799				
	2:00 PM		2.7	2009	199	1798				
1/4	10:00 AM		2.7	2019	219	1819				
1/5	8:00 AM		2.7	2049	219	1830				
1/7	8:00 AM		2.7	2019	209	1828				
1/10	8:00 AM		2.7	2060	209	1819				
1/11	8:30 AM		2.7	2069	199	1860				
1/12	8:00 AM		2.7	2071	199	1859				
1/13	8:00 AM		2.7	2149	209	1826				
1/14	8:00 AM		2.7	2175	209	1999				
	4:30 PM		2.7	2159	199	1949				
1/17	4:30 PM		2.7	2219	209	2000				
1/18	8:30 AM		2.7	2229	209	2010				
1/19	8:30 AM		2.7	2242	209	2007				
2/1/72	11:30 AM		2.7	2339	219	2107			5.18	296.6 g/L = 23.6% KOH
2/2/72	1:45 PM		Replaced & Replenished H <sub>2</sub> X with Young Red Co. H <sub>2</sub> X							
	1:45 PM		black						6.62	371 g/L = 24%

STA 21

Cell No. 71-11

Sheet 2 of       

OPERATOR       

Date	Time	Flap. Time Meter	Accum. Curr. Time	Voltage		Flow Rate		Gas Analysis		
				Cell	H <sub>2</sub>	O <sub>2</sub>	H <sub>2</sub>	M <sub>1</sub> /min	H <sub>2</sub>	O <sub>2</sub>
2/3/72	8:30 AM			2.7	1.996	2.57				
2/4/72	11:00 AM			2.7	2.009	2.37				
2/11/72	10:00 AM			2.7	2.017	2.01				
2/25/72	9:00 AM			2.7	2.103	1.519				
	9:10			O.C.	1.309	1.139				
4/4/72	Cleaned out									
	replaced			40 H	31 d					
1/15/72				2.7	1.869	1.19		6.9		
4/5/72	4:30 PM		2.2	2.7	1.937	2.67				
4/6/72	8:00 AM		4.07	2.7	1.957	2.67				
4/6/72	4:00 PM		5.07	2.7	1.937	2.67				
4/7/72	5:00 AM		6.07	2.7	1.957	2.67				
4/8/72	4:00 PM		1.07	2.7	1.947	2.67				
4/10/72	8:00 AM		1.07	2.7	1.969	2.67				
4/11/72	5:00 AM		2.07	2.7	1.957	2.67				
4/11/72	9:00 AM		3.07							
2/10/72										
4/12/72	3:30 PM		11.5	2.7	1.969	2.77				
4/12/72	5:00 AM		2.0	2.7	1.969	2.77				
4/12/72	4:30 PM			2.7	1.977	2.77				
4/12/72	11:00 AM		5	2.7	1.969	2.67				
4/12/72	7:00 PM			2.7	1.969	2.67				
4/12/72	2:00 AM		12	2.7	2.007	3.19				
4/12/72	4:15 PM			Cell	1.5	6.100				

57A #1

Cell No. 71-11

Sheet 3 of 3

OPERATOR

Date	Time	Elap. Time	Accum. Time	Curr.	Voltage			Flow Rate		Gas Analysis		
					Cell	H <sub>2</sub>	O <sub>2</sub>	H <sub>2</sub>	Mobility	H <sub>2</sub>	O <sub>2</sub>	
4/20/72	2:30 PM	Rebuild	0:00	0.00	2.07	2.89	1.789	11.0	0.26	0.26	0.26	Matrix
4/21/72	8:30 AM		0:00	2.7	2.09	2.99	1.769					
4/22/72	4:30 PM		0:00	2.7	2.09	2.99	1.759					
4/23/72	8:30 AM		0:00	2.7	2.09	3.09	1.749					
4/24/72	4:30 PM		0:00	2.7	2.09	3.19	1.752					
4/25/72	4:30 PM		0:00	2.7	2.09	3.29	1.764					
4/26/72	4:30 PM		0:00	2.7	2.09	3.09	1.749					
4/27/72	4:30 PM		0:00	2.7	2.09	3.09	1.749					
4/28/72	4:30 PM		0:00	2.7	2.09	3.19	1.749					
4/29/72	8:30 AM		0:00	2.7	2.09	3.10	1.749					
4/29/72	8:30 AM		0:00	0.00	0.00	0.00	0.00	0.00	0.00	0.00	0.00	Matrix

#### CATHODE DEVELOPMENT DATA

A series of four tests were run on cathodes having different platinum loadings as described in Section 2.2 of the text. The test data for these electrodes is presented in the following pages. The basis for analysis was taken as a hydrogen flow rate of 1.70 cc/min at a current of 13.5 amps and no hydrazine. Calculations of increased hydrogen flow considered the difference between the measured flow at each molarity and the 1.70 cc/min base.

WATER ELECTROLYSIS DATA SHEET

Cell No. 71-2

Date 8-9-71 Operator B. Heenough Sheet 1 of 1

Cell Description: Size 90 cm<sup>2</sup>

Anode old electrode from EONS

Cathode C-1 experimental electrode 2.5 mg/cm<sup>2</sup> Pt

Matrix ACCO

Assembly Standard

Electrolyte 30% KOH

Test Description:

Hydrazine conversion efficiency vs cathode voltage - first of three tests with various H loadings

Test Analysis:

Total Operating Time 55 Hrs.

Reason for Stopping Test Stopped after 55 Hrs with

Remarks approx. 2 molar initial hydrazine loading  
cell operation remained fairly good no  
excessive gassing noted

STATION

Cell No. 71-2OPERATOR Greenough Sheet 2 of 2  
cc/sec

Date	Time	Elap. Time Water Meter	Accum. Time	Curr.	Voltage		Flow Rate		Gas Analysis	
					Cell	H <sub>2</sub>	O <sub>2</sub>	H <sub>2</sub>	O <sub>2</sub>	H <sub>2</sub>
8-9	10 am		-0-	13.5						
8-11	6 pm		56	13.5	2.200	.115	2.029			
8-12	5:30 pm		86	13.5	2.229	.171	2.050			
8-13	5:30 pm		104	13.5	2.249	.179	2.069			
8-14	8:30 am		cell turned off							
9-8	3:45 PM		-0-	13.5	1.859	.239	1.617	1.741	.870	
9-8	4:30		1	13.5	1.829	.179	1.709	1.744	.890	
9-9	8:00 AM		100	13.5	2.130	.179	1.949	1.726	.890	
9-9	10:00 AM		150	13.5	2.130	.179	1.959	1.726	.890	
"	11:00		190	13.5	2.139	.179	1.952	1.726	.890	
"	1:00 PM		210	13.5	2.139	.179	1.959	1.726	.890	
"	2:00 PM		220	13.5	2.139	.179	1.959	1.726	.890	
"	3:00 PM		230	13.5	2.139	.179	1.959	1.726	.890	
"	4:00 PM		240	13.5	2.139	.179	1.959	1.726	.890	
"	4:45 PM		24.75	13.5	2.131	.179	1.959	1.711	.881	
9-10	8:00 AM		420	13.5	2.169	.179	1.989	1.800	.871	
"	9:00 AM		410	13.5	2.159	.179	1.980	1.612	.877	
"	10:00 AM		420	13.5	2.179	.179	2.000	1.612	.877	
"	11:00		420	13.5	2.179	.179	2.000	1.612	.877	
"	12:00		440	13.5	2.179	.177	2.000	1.612	.877	
"	1:00 PM		450	13.5	2.169	.179	1.992	1.612	.877	
"	2:00 PM		460	13.5	2.169	.179	1.989	1.612	.881	
"	3:00 PM		470	13.5	2.169	.177	1.989	1.612	.877	
"	4:00 PM		480	13.5	2.169	.174	1.989	1.612	.881	
"	4:30 PM		430		2.160	.179	1.989	1.612	.881	
"	6:35 PM		cell turned off							

reference not working

bottom of H<sub>2</sub> SP controller



OPERATOR C. Greenough Sh. 3 of 7 Cell No. 11-2 57A1

Date	Time	Elap. Time Meter	Accum. Curr. Time	Voltage		Flow Rate			Gas Analysis			
				Cell	H <sub>2</sub>	O <sub>2</sub>	H <sub>2</sub>	O <sub>2</sub>	MUAR	H <sub>2</sub>	O <sub>2</sub>	
9/29	1:45		13.5				4.2					Started cell added 16.2 H <sub>2</sub> ~ 2 molar
	5:00	24	13.5	1.989		824	3.2		1.75	3.10		500 cc, 1.75 H <sub>2</sub> 1.754 M
	5:30		13.5	2.073			4.2		1.10			
9-30	5:00		13.5	2.356			3.6		1.05			300 gmo H <sub>2</sub> 6.019 molar
	10:00		13.5	2.350			3.1		3.07			320 gmo O <sub>2</sub> 6.019 molar
	1:30		13.5	2.359			3.1		3.07			100 "
	1:00		13.5	2.348			3.07		1.60			
	2:00		13.5	2.338			3.04		3.07			
	11:00		13.5	2.342			3.04		3.07			
10-1	8:00		13.5	2.420			3.00		3.07			11.2 gmo H <sub>2</sub> 1.754 M
	9:30		13.5	2.341			1.83		1.61			1.754 M (1.754 M)
	11:00		13.5	2.308			1.82		1.61			
	1:30		13.5	2.395			1.82		1.61			
	2:00		13.5	2.382			1.82		1.44			
	10:30		13.5	2.380			1.82		1.61			
10-4	9:30	0	13.5									Started Cell added 16.2 H <sub>2</sub> 1.754 molar
	10:30		13.5	2.059			2.00		1.81			
	11:30	2.0	13.5				2.00		1.81			
	1:00	3.5	13.5	2.126			2.03		1.73			
	3:00	5.5	13.5	2.279			2.05		1.56			
	4:30	7.0	13.5	2.325			2.02		1.56			
10-5	5:00	10.0	13.5	2.349			1.93		1.03			
	10:30	12.0	13.5	2.356			1.89		1.86			
	11:30	14.0	13.5	2.363			1.90		1.86			
	1:00	15.5	13.5	2.361			1.89		1.97			
	2:30	17.0	13.5	2.369			1.90		1.88			

Cell No. 71-2

Sheet 4 of       

OPERATOR Greenough

~~22511~~

WATER ELECTROLYSIS DATA SHEET

Date 11/20/71 Operator Kopennik Cell No. E-2-71-3 Sheet 1 of 1

Cell Description: Size 40 CM<sup>2</sup>

Anode \_\_\_\_\_

Cathode C-2 Experimental Cathode

Matrix ACCO

Assembly Standard

Electrolyte 30% KOH

Test Description:

2nd in series testing Hydrazine conversion  
efficiency vs cathode voltage

Test Analysis:

Total Operating Time \_\_\_\_\_

Reason for Stopping Test \_\_\_\_\_

Remarks \_\_\_\_\_

OPERATOR Kepernik Sheet 1 of 1 Cell No. 71-3

Test cell C-2

Date	Time	Blap. Time Meter	Accum. Curr. Time	Voltage		Flow Rate		Gas Analysis		
				Cell	H <sub>2</sub>	O <sub>2</sub>	H <sub>2</sub>	O <sub>2</sub>	H <sub>2</sub>	O <sub>2</sub>
10/20	2:20 PM		Cell put on							
	2:25 PM		13.5 1.879	1.039			1.5	1.87		
	2:30 PM		13.5 1.819	1.009			1.5	1.80		
	2:35 PM		13.5 1.900	1.009			1.5	1.88		
10/21	8:30 AM		13.5 2.029	1.009			1.45	1.86		
	10:00 AM		13.5 2.013	1.009			1.40	1.87		
	11:00 AM		13.5 2.019	1.009			1.40	1.87		
	2:00 PM		13.5 2.002	1.009			1.40	1.88		
	4:00 PM		13.5 1.944	1.009			1.40	1.88		
10/22	8:20 AM		13.5 1.999	1.009			1.40	1.88		
			Cell was off							
	10:25 AM		Cell was on							
	11:00		13.5 1.939	1.009			1.40	1.85		
	3:00 PM		13.5 1.959	1.009			1.40	1.85		
	4:30 PM		13.5 1.969	1.009			1.40	1.85		
11/25	8:00 AM		13.5 2.009	1.009			1.40	1.84		
	10:00 AM		13.5 2.002	1.009			1.40	1.84		
	10:30 AM		Cell was on							
			Cell was off							
	11:20 AM		13.5 1.910	1.009			1.40	1.80		
	1:00 PM		13.5 1.919	1.009			1.40	1.80		
	2:30 PM		13.5 1.922	1.009			1.40	1.82		
	4:30 PM		13.5 1.929	1.009			1.40	1.80		
11/26	8:00 AM		13.5 1.971	1.009			1.40	1.80		
	10:00 AM		13.5 1.970	1.009			1.40	1.80		
	11:00 AM		13.5 1.965	1.009			1.40	1.80		

Cell No. 7/-3

Date	Time	Elap. Time Meter	Accum. Curr. Time	Voltage		Flow Rate		Gas Analysis				
				Cell	H <sub>2</sub>	O <sub>2</sub>	H <sub>2</sub>	C <sub>2</sub>	H <sub>2</sub>	O <sub>2</sub>		
1/26	1:45		13.5	1963	770	759	1.82	84	1.82		1963	1963
	5:45		13.5	1961	820	759	1.81	85			1961	1961
	4:30 PM		13.5	1959	809	759	1.81	84	1.78		1959	1959
1/27	5:25 PM		13.5	1974	820	789	1.75	84	1.63		1974	1974
	6:00 PM		13.5	1999	809	759	1.75	84			1999	1999
	1:00 PM		13.5	1974	860	869	1.75	84	1.7		1974	1974
	2:00 PM		Turned	Cell	off						111	234

WATER ELECTROLYSIS DATA SHEET

C-4

Cell No. 71-4

Date 11/28 Operator Keepernik Sheet 1 of 1

Cell Description: Size 90 cm<sup>2</sup>

Anode \_\_\_\_\_

Cathode C-4 Experimental Cathode

Matrix ACCO

Assembly Standard

Electrolyte 30% KOH

Test Description:

3RD in series Testing Hydrazine  
conversion efficiency vs cathode voltage

Test Analysis:

Total Operating Time 50 hrs

Reason for Stopping Test \_\_\_\_\_

Remarks \_\_\_\_\_



C. 2

Cell No. 71-5  
Date 11/2/71 Operator Boenik Sheet 1 of 1

Assembly Standard

Test Description:  
4th in series testing Hydrazine  
conversion efficiency vs cathode voltage

Remarks \_\_\_\_\_



6552

Greenough

OPERATOR Kepeyink Sheet 1 of 1

Cell No. 71-5

Date	Time	Elap. Time Meter	Accum. Time	Curr.	Voltage		Flow Rate		Gas Analysis		
					Cell	H <sub>2</sub>	O <sub>2</sub>	H <sub>2</sub>	O <sub>2</sub>	H <sub>2</sub>	O <sub>2</sub>
11/2	2:15 PM			13.5		Cell		on	11.0		
	2:30 PM			13.5	2.130	960	1.179	1.08	.84		14.6
	4:00 PM			13.5	2.144	669	1.479	1.07	.84		23.3
11/3	5:00 PM			13.5	2.225	529	1.679	1.07	.84		11.7
	6:00 PM			13.5	2.234	614	1.609	1.04	.84		11.6
	11:30 PM			13.5	2.221	519	1.679	1.07	.84		11.7
	2:00 PM			13.5	2.219	529	1.689	1.07	.85		11.5
	4:30 PM			13.5	2.212	519	1.689	1.07	.85		23.1
11/4	8:00 AM			13.5	2.247	539	1.709	1.07	.84		11.4
	9:15 AM			Added	480	c		N <sub>2</sub>	Flow		23.3
	10:30 AM			13.5	2.230	310	1.789	1.05	.85	Section	11.2
	1:00 PM			13.5	2.234	300	1.809	1.05	.85		11.1
	3:00 PM			13.5	2.239	300	1.799	1.05	.85		23.1
	4:30 PM			13.5	2.252	303	1.849	1.05	.86	1.46	11.2
11/5	8:00 AM			13.5	2.289	339	1.939	1.04	.84	1.24	11.3
	10:00 AM			13.5	2.293	339	1.959	1.04	.84		11.3
	11:30 AM			13.5	2.291	339	1.959	1.04	.84		23.4
	1:30 PM			13.5	2.286	350	1.909	1.04	.84		11.3
	3:30 PM			13.5	2.279	359	1.969	1.04	.84	.94	23.2
11/6	2:00 PM			Cell	740	div	c				
	3:00 PM			Cell	100	1.057	d	1.7	unimp	on	
	4:00 PM			13.5	2.204	1570	1.60	1.74	.84		11.5
	5:00 PM			13.5	2.226	1615	1.59	1.74	.84		11.5
11/9	5:00 PM			13.5	2.306	173	1.849	1.69	.84		11.6
	6:45 AM			Added	500	c		N <sub>2</sub>	Flow	Section	23.3
	10:00 AM			13.5	2.205	557	1.709	1.13	.79	2.08	11.4
	11:00 AM			13.5	2.204	557	1.69	1.13	.80		24.4

Correspondence

Sheet 2 of 2

Cell No.

[illegible]

PRECEDING PAGE BLANK NOT FILMED

SYSTEM TEST DATA

The following section presents the log sheets of the five system tests which were run in this program. A description appears in Section 2.5 of the text.

TEST NO. 1 - CHECKOUT TEST SYSTEM STATUS

START AT 9:30am 1/19/72

DATE	TIME	ELAPSED TIME (HRS)	HYDROGEN OUTPUT METER	POWER INPUT		PRESSURE (PSIG)				COOLANT TEMP (°F)	FLOW RATE				GAS ANALYSIS		
				HIGH VOLTS	LOW VOLTS	MOD	PT	IN. H <sub>2</sub> O	OUT. H <sub>2</sub> O		KOH UNIT	UNIT	UNIT	UNIT	N <sub>2</sub> -O <sub>2</sub>	TEMP	CURRENT
1/19	10:00	0.5		V A	V A	PSI	IN. H <sub>2</sub> O	IN. H <sub>2</sub> O	IN. H <sub>2</sub> O	°F	UNIT	UNIT	UNIT	UNIT	LIQUIDS	MOD-B	
	11:00	1.5		28.2	20.5	1.7	11.0	16.8	4.5	5.0	8.0	8.0	8.0	8.0	10.15	25.1	33.86
	12:00	2.5		28.2	21.0	2.0	10.0	17.8	4.5	5.5	8.0	8.0	8.0	8.0	38.1	33.92	11.21
	1:00	3.5		28.2	21.5	2.0	10.0	18.1	4.5	5.5	8.0	8.0	8.0	8.0	47.3	33.92	11.34
	2:00	4.5		28.2	21.8	2.1	10.0	17.6	4.5	5.5	8.0	8.0	8.0	8.0	57.2	34.23	34.55
	3:00	5.5		28.2	21.8	2.1	10.0	17.6	4.5	5.5	8.0	8.0	8.0	8.0	66.0	11.35	11.42
	3:20			High make currents seem to be drifting higher - adjusted to 33.8mv													
	4:00	6.5				2.1	11.0	16.9	4.0	4.5	8.0	8.0	8.0	8.0	82.0	33.92	33.81
	5:00	7.5				2.1	11.0	16.5	4.0	4.5	8.0	8.0	8.0	8.0	91.0	33.97	33.81
	6:00	8.5		28.2	21.5	2.0	9.5	16.4	4.0	4.8	8.0	8.0	8.0	8.0	95.1	33.92	33.84
	7:00	9.5		28.2	21.5	2.0	11.0	16.2	4.0	4.8	8.0	8.0	8.0	8.0	104.0	11.33	11.42
	8:00	10.5		28.2	21.5	1.9	10.5	15.9	4.0	4.8	8.0	8.0	8.0	8.0	118.0	33.91	33.84
	9:00	11.5		28.2	21.5	1.8	11.5	15.7	4.3	4.8	8.0	8.0	8.0	8.0	122.0	34.12	33.94
	9:21			7.57													
	10:00	12.5		28.2	21.5	1.8	11.8	15.6	4.3	4.8	8.0	8.0	8.0	8.0	132.0	34.02	33.84
	10:11			4.20	Feed												
	11:00	13.5				28.2	6.0	1.7	10.5	4.8	8.0	8.0	8.0	8.0	140.0	11.25	11.35
	10:57			4.60	Feed												
1/20	18:00	14.5		28.2	21.5	2.0	10.5	16.3	4.5	4.8	8.0	8.0	8.0	8.0	150.4	34.03	33.83
	12:00	15.5		28.2	21.5	2.0	10.5	16.3	4.5	4.8	8.0	8.0	8.0	8.0	150.4	34.03	33.83
	1:00	16.5		28.2	21.5	2.0	10.5	16.3	4.5	4.8	8.0	8.0	8.0	8.0	150.4	34.03	33.83
	2:00	17.5		28.2	21.5	2.0	10.5	16.3	4.5	4.8	8.0	8.0	8.0	8.0	150.4	34.03	33.83
	3:00	18.5		28.2	21.5	2.0	10.5	16.3	4.5	4.8	8.0	8.0	8.0	8.0	150.4	34.03	33.83
	3:45			18.00	off	18.00	off	18.00	off	18.00	8.0	8.0	8.0	8.0	150.4	34.03	33.83
	3:50			19.00	off	19.00	off	19.00	off	19.00	8.0	8.0	8.0	8.0	150.4	34.03	33.83
	4:00	19.5		28.2	21.5	2.0	10.5	16.3	4.5	4.8	8.0	8.0	8.0	8.0	150.4	34.03	33.83
	5:00	20.5		28.2	21.5	2.0	10.5	16.3	4.5	4.8	8.0	8.0	8.0	8.0	150.4	34.03	33.83
	5:10			28.2	21.5	2.0	10.5	16.3	4.5	4.8	8.0	8.0	8.0	8.0	150.4	34.03	33.83
	5:20			28.2	21.5	2.0	10.5	16.3	4.5	4.8	8.0	8.0	8.0	8.0	150.4	34.03	33.83
	5:30			28.2	21.5	2.0	10.5	16.3	4.5	4.8	8.0	8.0	8.0	8.0	150.4	34.03	33.83
	5:40			28.2	21.5	2.0	10.5	16.3	4.5	4.8	8.0	8.0	8.0	8.0	150.4	34.03	33.83
	5:50			28.2	21.5	2.0	10.5	16.3	4.5	4.8	8.0	8.0	8.0	8.0	150.4	34.03	33.83

DATE	TIME	ELAPSED TIME (HRS)	HYDROGEN OUTPUT METER	POWER INPUT		PRESSURE (PSIG)				COOLANT TEMP (°F)	FLOW RATE			GAS ANALYSIS	
				HIGH VOLTS	LOW VOLTS	MOD	PT	PO2	CAL		KOH	CHART	N2	N2 - O2	ANALYSIS
1/20	6:00	20.5	—	28.2	22.0	1.9	11.5	16.8	45	4.8	8.0	—	OFF 12.5	2070	34.12
	6:10	N <sub>2</sub> H <sub>4</sub>	Back to 0			1.8	11.0	16.6	45	4.8	8.0	—	OFF 12.5	2163	34.00
	7:00	21.5		28.2	20.0	1.8	11.0	16.6	45	4.8	8.2	—	OFF 12.5	2163	11.39
	7:05	P6	weight mud feed			783 gm					4.0	—	OFF 12.5	2163	11.45
	7:10	N <sub>2</sub> H <sub>4</sub>	Back to 10 flow rate								4.0	—	OFF 12.5	2163	11.45
	8:00	22.6		28.2	20.0	1.8	12.2	16.2	46	4.8	8.0	—	OFF 12.5	2260	11.35
	9:00	23.5		28.2	21.8	1.7	12.5	15.8	45	4.8	8.0	—	OFF 12.5	2348	34.07
	9:10	H <sub>2</sub> O	FEED; N <sub>2</sub> H <sub>4</sub> FEED			OFF	AT	161 mm	on	LEN chart	8.0	—	OFF 12.5	2348	33.95
	9:50	Recharged N <sub>2</sub> H <sub>4</sub> tank									8.0	—	OFF 12.5	2443	11.32
	10:00	24.5		28.2	20.0	1.8	13.0	15.7	44.5	4.5	8.0	—	OFF 12.5	2541	11.31
	11:00	25.5		28.2	20.0	1.7	12.0	16.0	45	4.8	8.0	—	OFF 12.5	2630	34.13
	12:00	26.5		28.2	21.5	1.8	12.0	16.3	45	4.8	8.0	—	OFF 12.5	2739	11.23
	12:50	N <sub>2</sub> H <sub>4</sub>	FEED ON			1.7	11.0	16.0	45	4.8	8.0	—	OFF 12.5	2739	11.35
	1:00	27.5		28.0	20.0	1.7	11.0	17.0	45	4.8	8.0	—	OFF 12.5	2846	34.24
	2:00	28.5		28.2	21.5	2.1	13.0	17.0	45	4.8	8.0	—	OFF 12.5	2904	11.37
	2:40	Changed high mud Pz	offluent limit to 470 mm								8.0	—	OFF 12.5	3006	34.10
	3:00	29.5		28.2	22.0	2.1	11.5	16.6	44.5	4.7	7.7	—	OFF 12.5	3097	11.49
	4:00	30.5		28.2	22.0	2.1	11.5	16.4	45	4.7	7.7	—	OFF 12.5	3185	11.45
	5:00	31.5		28.2	20.0	1.8	11.0	16.2	45	4.7	7.7	—	OFF 12.5	3287	34.20
	6:00	32.5		28.2	20.0	1.8	11.0	16.2	45	4.7	7.7	—	OFF 12.5	3384	11.37
	6:55	N <sub>2</sub> H <sub>4</sub> Feed	off								7.7	—	OFF 12.5	3467	11.37
	7:00	33.5		28.2	22.0	2.1	12.5	15.7	45	4.6	7.7	—	OFF 12.5	3552	34.02
	8:00	34.5		28.2	20.0	1.7	12.5	16.0	44	4.6	7.7	—	OFF 12.5	3648	11.27
	9:00	35.5		28.2	20.0	1.7	13.0	16.4	44	4.7	7.7	—	OFF 12.5	3742	11.37
	10:00	36.5		28.2	22.0	1.7	13.5	16.7	44	4.7	7.7	—	OFF 12.5	3840	11.37
	10:05	N <sub>2</sub> H <sub>4</sub> Feed	on								7.7	—	OFF 12.5	3936	11.37
	11:00	37.5		28.2	20.0	1.8	12.5	17.2	44	4.7	7.7	—	OFF 12.5	4032	11.37
	12:00	38.5		28.2	20.0	2.0	13.0	17.2	44	4.7	7.7	—	OFF 12.5	4128	11.37
	12:05	Low Pz	set point shifted								7.7	—	OFF 12.5	4224	11.37

③

④





TEST NO. 2

SYSTEM STATUS

PAGE 1 OF 1

DATE	TIME	ELAPSED TIME (HRS)	HYDROGEN OUTPUT METER	POWER INPUT		PRESSURE (PSIG)			COOLANT TEMPERATURE	KOH	FLOW RATE		GAS ANALYSIS	
				HIGH VOLTS	LOW VOLTS	MOD	PT	PO2	CAL	NH3	Q	N2	N2-O2	H2
1/24	2:30	0-0			282 6.0	2.1	9.0	162	445	4.7	80	OFF	530	11.27
	3:00	0.5		280 21.0		1.9	11.0	161	44	4.9	80	OFF	578	33.43
	4:00	1.5			282 6.0	2.2	10.0	169	44	4.9	80	OFF	672	11.18
	5:00 PM	2.5			282 6.0	2.2	9.0	171	44	4.9	3082	8.5	786	11.23
	6:00 PM	3.5			282 6.0	2.2	9.5	170	44	4.9	3084	8.0	894	11.24
	7:00 PM	4.5			282 21.5	2.2	10.5	166	44	4.9	3086	8.5	942	33.88
	8:00 PM	5.5			282 6.0	2.2	9.0	165	44	4.9	3090	8.5	1045	11.25
	9:00 PM	6.5			282 22.0	2.2	10.5	162	44	4.9	3092	8.5	1159	33.88
	10:00 PM	7.5			282 6.0	1.8	9.0	160	44	4.9	3095	8.0	1228	11.26
	9:00	N2 H4		FF								OFF		11.29
	11:00 PM	8.5			282 6.0	1.8	9.5	160	44	4.9	3098	8.0	1315	11.21
	12:00	9.5			282 22.0	1.8	8.5	162	44	4.9	3100	8.0	1437	33.64
1/25	12:00			N2 H4 feed on				165	170.5	4.7		9.0		
	1:00	10.5			282 6.0	1.8	8.0	167	45	4.8	3013.2	8.0	1497	11.16
	2:00	11.5			282 21.5	2.0	10	167	44.5	4.8	3015.4	8.0	1582	33.2
	3:00	12.5			282 5.8	2.0	7.5	170	45	4.8	3019.0	7.8	1687	11.45
	4:00	13.5			280 22.0	2.0	8.0	166	45	4.8	3022.0	8.0	1784	34.11
	4:10			Adg										
	5:00	14.5			282 6.0	1.75	8.0	164	44.5	4.7	3024.8	8.0	1874	11.22
	6:00	15.5			282 21.8	2.0	10	163	44.5	4.7	3028.2	7.9	1970	11.23
	7:00	16.5			282 22.0	2.0	8.0	159	44.5	4.8	3031.0	7.9	2060	33.85
	7:20			N2 H4				158	114.4	4.7				
	8:00	17.5			282 6.0	1.7	7.0	160	45.0	4.7	3034.2	7.9	2157	11.22
	9:00	18.5			282 21.5	1.8	7.5	160	45.0	4.7	3039.2	7.9	2252	33.83
	9:12	N2 H4												
	10:00	19.5			282 6.0	1.9	8.0	165	45	4.7	3039.5	7.9	2342	11.17
	11:00	20.5			282 6.0	1.9	7.0	168	45	4.7	3042.5	7.6	2433	11.21
	12:00	21.5			282 23.0	2.1	8.0	166	45	4.8	3045.2	7.7	2530	33.92
	1:00 PM	22.5			280 6.0	2.0	8.0	165	45	4.8	3048.2	7.8	2620	11.23
	2:00	23.5			280 6.0	1.7	6.5	163	45	4.8	3051.6	7.5	2715	11.44
	3:00	24.5			282 22.2	4.6	7.5	160	45	4.8	3054.5	7.7	2808	34.19
3:30														33.95



TEST NO. 2SYSTEM STATUS FlowmeterPAGE 2 OF —

DATE	TIME	ELAPSED TIME (HRS)	HYDROGEN OUTPUT METER	POWER INPUT			PRESSURE (PSIG)			COEFFICIENT TEMPERATURE	KOH	FLOW KATE			GAS ANALYSIS		
				HIGH VOLTS	LOW VOLTS	AMPS	MOD	PT.	PO2	CAL	NIN	COM	N2	ME	N2-O2	CABIN	H2
1/25	4:00 PM	25.5			28	6.0	1.8	8.0	159	45	4.8	off	12.6	9.2	2899	11.22	11.19
	5 PM	26.5			28.2	6.0	1.8	7.0	162	45	4.8	OFF	12.6	9.2	2897	11.16	11.15
	6 PM	27.5		28.2	22.0		1.8	7.5	164	45	4.8	OFF	12.6	9.2	2899	11.16	11.15
	6:07 PM		N2 H4					7.0	170	45	4.8	OFF	12.6	9.2		11.16	11.15
	7:00 PM	28.5			28.2	6.0	1.7	9.0	170	45	4.8	8.5	12.6	9.2	190	34.09	33.87
	8:00 PM	29.5		28.2	22.0		1.8	9.0	168	45	4.8	8.5	12.6	9.2	270	11.34	11.25
	9 PM	30.5			28.2	6.0	1.6	7.0	168	45	4.6	8.5	12.6	9.2	369	34.10	33.93
	10 PM	31.5			28.2	6.0	1.6	7.0	164	45	4.6	8.5	12.6	9.2	468	11.41	11.25
	11 PM	32.5			28.2	6.0	1.8	8.0	165	45	4.8	OFF	12.6	9.2	570	33.95	33.80
	12 PM	33.5		28.2	22.0		1.8	9.0	162	45	4.8	OFF	12.6	9.2	642	11.25	11.21
	1:00 PM	34.5			28.2	6.0	1.8	9.0	161	44.5	4.7	9.0	12.6	9.2	741		
11	1:42				164.5	164.5	159										
	2:00	35.5		28.2	22.0		1.9	8.3	160	44.5	4.8	OFF	12.6	9.2	833	34.35	34.07
	3:00	36.5			28.2	5.8	2.0	9.0	160	45.0	4.7	OFF	12.6	9.2	926	11.21	11.17
	4:00	37.5		28.2	22		1.8	8.0	163	45.0	4.8	OFF	12.6	9.2	1016	34.00	33.95
12	4:20				170.0	170.0	165										
	5:00	38.5		28.2	22.0		2.2	10.0	164	45.0	5.0	8.5	12.6	9.2	1112	34.23	33.93
	6:00	39.5			28.2	6.0		8.5	165	45.0	4.8	10.0	12.6	9.2	1206	11.23	11.21
	7:00	40.5		28.2	22.2		2.1	9.0	163	45	4.9	8.5	12.6	9.2	1295	34.41	34.08
	8:00	41.5			28.1	5.9	1.9	9.8	162	45	4.9	8.5	12.6	9.2	1393	11.24	11.24
	9:00	42.5			28.0	6.0	1.8	9.0	161	45	4.9	8.5	12.6	9.2	1485	11.47	11.34
	10:00	43.5		28.2	22.0		1.9	10.0	159	45	4.9	8.9	12.6	9.2	1578	34.37	34.05
13	11:00	44.5			28.0	5.9	1.7	10.0	159	45	4.8	OFF	12.6	9.2	1671	11.24	11.21
	12:00 PM	45.5		28.2	22.0		1.9	8.0	162	45	4.9	OFF	12.6	9.2	1763	11.20	11.17
	1 PM	46.5		28.2	22.0		1.9	9.0	163	45	4.9	OFF	12.6	9.2	1887	34.14	33.85
	2 PM	47.5			28.2	6.0	2.0	9.0	168	45	4.9	8.5	12.6	9.2	1950	11.21	11.19
	3 PM	48.5			28.2	5.9	2.0	7.5	169	45	4.9	9.0	12.6	9.2	2042	11.26	11.27
	4 PM	49.5		28.2	22.5		2.0	8.5	166	45	4.9	OFF	12.6	9.2	2149	34.69	34.27
	5 PM	50.5			28.2	6.0	1.8	8.5	166	45	4.9	8.5	12.6	9.2	2225	11.24	11.23
	6 PM	51.5		28.2		28.2	6.0	1.5	8.0	165	45	8.5	12.6	9.2	2323	11.27	11.31
	7 PM	52.5		28.2	6.0	1.8	2.0	9.0	163	45	4.9	8.5	12.6	9.2	2418	11.24	11.22

SYSTEM STATUS

DATE	TIME	ELAPSED TIME (HRS)	HYDROGEN OUTPUT METER	POWER INPUT		PRESSURE (PSIG)		COOLANT TEMP (°F)	FLOW RATE		GAS ANALYSIS	
				HIGH VOLTS AMPS	LOW VOLTS AMPS	MOD	PT		KOH	CONCENTRATION	WETA	BUB SEP
1/26	8PM	53.5		28.2 22.0		1.7	7.5	4.9	3140.4	8.0	8.0 12.6 9.2	
	9PM	54.5			28.2 22.0	2.2	12.0	4.9	3143.2	8.5	8.0 12.6 9.2	
	10PM	55.5		28.2 22.0		2.0	8.0	4.9	3146.2	8.0	OFF 12.6 9.2	
	11PM	56.5			28.2 22.0	2.0	9.0	4.9	3149.5	8.5	8.0 12.6 9.2	
	11:40 PM		N <sub>2</sub>	0 FF								
	12 PM	57.5		28.2 22.0		1.8	8.0	4.9	3152.1	8.5	OFF 12.6 9.2	
1/27	12:43		Note much higher blacklight you note 33.8									
	1:00	58.5	Atty High	28.2 21.8		2.1	9.0	4.9	3154.5	8.1	OFF 12.6 9.1	
	1:08		add 25cc	28.2 21.8		1.7	6.5	4.9	3166.8	7.8	8.5	
	1:18		add 25cc	28.2 21.8		2.0	8.5	4.9	3169.5	8.0	8.5	
	2:00 PM	59.5		28.2 21.8		2.1	8.0	4.9	3173.2	7.9	9.0 12.6 9.1	
	3:00	60.5		28.2 21.8		2.0	9.5	4.9	3163.5	8.1	9.0 12.6 9.1	
	4:00	61.5		28.2 21.8		1.7	6.5	4.9	3166.8	7.8	9.0 12.6 9.1	
	5:00	62.5		28.2 21.8		2.0	8.5	4.9	3169.5	8.0	9.0 12.6 9.1	
	6:00	63.5		28.2 21.8		2.0	8.5	4.9	3169.5	8.0	9.0 12.6 9.1	
	6:46		add 20cc KOH	28.2 21.8		1.7	7.5	4.9	3173.2	7.9	9.0 12.6 9.1	
	7:00	64.5		28.2 21.8		1.9	9.0	4.9	3176.0	8.0	9.0 12.6 9.1	
	8:00	65.5		28.2 21.8		1.9	9.5	4.9	3179.4	7.9	9.0 12.6 9.1	
	9:00	66.5		28.2 21.8		1.8	7.5	4.9	3182.5	7.9	9.0 12.6 9.1	
	10:00	67.5		28.2 21.8		1.9	11.0	4.9	3185.2	8.0	9.0 12.6 9.1	
	11:00	68.5		28.2 21.8		1.9	9.5	4.9	3188.5	8.0	9.0 12.6 9.1	
	12:00	69.5		28.2 21.8		1.8	10.5	4.9	3191.4	7.5	9.0 12.6 9.1	
	1 PM	70.5		28.2 21.8		1.8	10.5	4.9	3191.4	7.5	9.0 12.6 9.1	
	1:40		Swapped high limit on Cabin P02 down - also reduced effluent P02 limit from 56.5 to 55.0 on trip									
	2 PM	71.5		28.2 21.8		1.8	10.0	4.9	3193.8	7.5	9.0 12.6 9.1	
	3:00	72.5		28.2 21.8		1.8	10.0	4.9	3196.3	7.5	9.0 12.6 9.1	
	4:00 PM	73.5		28.2 21.8		2.0	11.0	4.9	3199.0	7.5	9.0 12.6 9.1	
	5:00 PM	74.5		28.2 21.8		1.8	11.0	4.9	3203.1	7.8	9.0 12.6 9.1	
	6 PM	75.5		28.2 21.8		1.8	10.5	4.9	3206.2	7.8	9.0 12.6 9.1	
	7 PM	76.5		28.2 21.8		1.8	12.8	4.9	3209.3	7.8	9.0 12.6 9.1	

FIGURE 2-31

TEST NO. 2

SYSTEM STATUS

PAGE 4 OF 4

DATE	TIME	ELAPSED TIME (HRS)	HYDROGEN OUTPUT METER	POWER INPUT		PRESSURE (PSIG)			COOLANT TEMPERATURE (°F)	FLOW RATE		GAS ANALYSIS				
				HIGH VOLTS AMPS	LOW VOLTS AMPS	MOD PT	PO2	CAL		NH4	KOH	CONV N2H4	META	N2	BUB SEP	N2-O2
1/20/76	8:00 AM	77.5		28.2	6.0	1.8	10.5	162	45	4.8	3212.3	7.5	9.2/12.5	1767	11.43	11.64
	8:21		H4	OFF			18.2	158	45				OFF			
	9:00 AM	78.5		28.2	6.0	1.6	12.2	156	45	4.6	3214.5	7.0	OFF	12.5	9.5	11.22
	10:00 AM	79.5		28.2	6.0	1.6	11.0	160	45	4.8	3217.5	7.4	OFF	12.5	9.5	11.14
	11:00 AM	80.5		28.2	21.5	2.0	12.5	161	45	4.9	3219.5	6.8	OFF	12.5	9.5	11.19
1/20/76	12:00 PM	81.5		28.2	22.0	2.0	12.5	162	45	4.9	3222.1	8.0	OFF	12.5	9.5	11.22
	12:00 AM		N2 H4	ON		1.70	15.0	165					OFF	12.5	9.5	11.22
	12:05			28.2	22.0	2.0	13.5	167	45	4.9	3224.0	8.0	9.5	12.6	9.2	11.32
	1:00 AM	82.5		28.2	22.0	2.0	13.5	171	45	4.9	3227.2	8.0	7.0	12.6	9.1	11.23
	2:00	83.5		28.2	22.4	2.0	13.5	170	45	4.8	3230.8	8.1	4.8	12.6	9.1	11.23
	3:00	84.5		28.2	22.4	2.0	13.5	170	45	4.8	3230.8	8.1	4.8	12.6	9.1	11.23
	4:00	85.5		28.2	22.4	2.0	13.5	170	45	4.8	3230.8	8.1	4.8	12.6	9.1	11.23
	4:05			28.2	22.4	2.0	13.5	170	45	4.8	3230.8	8.1	4.8	12.6	9.1	11.23
	5:00	86.5		28.2	22.4	2.0	13.5	170	45	4.8	3230.8	8.1	4.8	12.6	9.1	11.23
	6:00	87.5		28.2	22.4	2.0	13.5	170	45	4.8	3230.8	8.1	4.8	12.6	9.1	11.23
	7:00	88.5		28.2	22.4	2.0	13.5	170	45	4.8	3230.8	8.1	4.8	12.6	9.1	11.23
	8:00	89.5		28.2	22.4	2.0	13.5	170	45	4.8	3230.8	8.1	4.8	12.6	9.1	11.23
	9:00	90.5		28.2	22.4	2.0	13.5	170	45	4.8	3230.8	8.1	4.8	12.6	9.1	11.23
	9:50	91.5		28.2	22.4	2.0	13.5	170	45	4.8	3230.8	8.1	4.8	12.6	9.1	11.23
	10:00	92.5		28.2	22.4	2.0	13.5	170	45	4.8	3230.8	8.1	4.8	12.6	9.1	11.23
	11:00	93.5		28.2	22.4	2.0	13.5	170	45	4.8	3230.8	8.1	4.8	12.6	9.1	11.23
	12:00 PM	94.5		28.2	22.4	2.0	13.5	170	45	4.8	3230.8	8.1	4.8	12.6	9.1	11.23
	1:00 PM	95.5		28.2	22.4	2.0	13.5	170	45	4.8	3230.8	8.1	4.8	12.6	9.1	11.23
	2:30	96.0		28.2	22.4	2.0	13.5	170	45	4.8	3230.8	8.1	4.8	12.6	9.1	11.23

TEST NO. 3

SYSTEM STATUS

UNIT 1-D

DATE	TIME	ELAPSED TIME (HRS)	HYDROGEN OUTPUT METER		POWER INPUT		PRESSURE (PSIG)			COOLANT TEMP (°F)	FLOW RATE		BUB SEP	GAS ANALYSIS						
			HIGH VOLTS	LOW VOLTS	HIGH AMPS	LOW AMPS	MOD	PT	PD2		CAL	NH3		COIL	N2	META	N2	META	N2	
2-7-72	6:00	0	3277.0		280	8.5	1.8	10.5	158	45	5.0		8.0	✓	off	12.5	9.2	334	15.60	15.65
	6:10	10																		
	6:33																			
	6:35																			
	7:00	1:00	3279.2		280	8.0		9.0	166	44	5.0		8.0	✓	off	12.5	10.0	426	15.66	15.70
	7:01																			
	7:10		3279.5		280	8.5	2.0	9.0	166	44.5	5.0		8.0	✓	off	12.6	9.2	435	15.75	15.75
	8:00	2:00	3280.8		280	210	2.1	10.5	168	45	5.1		8.0	✓	off	12.7	9.2	496	33.78	33.81
	9:00	3:00	3283.5		280	210		2.2	10.5	169	44.5	5.0	7.8	✓	off	12.6	9.3	588	33.45	33.47
	10:00	4:00	3286.5		280	215		2.2	9.5	170	44.5	5.0	8.0	✓	off	12.6	9.2	680	33.45	33.50
	11:00	5:00	3289.5					2.1	9.0	168	44.5	5.0	8.0	✓	off	12.6	9.2	772	15.81	15.85
2-8-72	12:00	6:00	3293.5		280	8.5	2.2	9.0	165	45.0			8.0	✓	off	12.6	9.2	861	15.78	15.83
	1:55	Changed	N2 H2					to	1.0	272	Flow meter									
	12:30																			
(1)	12:33																			
	1:00 AM	7	3296.3		280	8.5	2.2	9.5	158	450	5.0		8.0	✓	off	12.7	9.2	960	15.80	15.88
	1:00																			
	2:00 AM	8	3299.5		280	8.5	2.2	9.5	157	450	5.0		8.0	✓	off	12.7	9.2	1054	15.71	15.81
	3:00 AM	9	3302.5		280	9.0	2.2	10.0	157	450	5.0		8.0	✓	off	12.7	9.2	1144	15.68	15.77
	4:00 AM	10	3305.5		280	220		1.7	9.0	162	44.5	5.0	8.0	✓	off	12.7	9.2	1245	33.70	33.84
	4:10 AM																	1338	15	
	5:00 AM	11	3308.5		280	8.5	2.2	8.5	168	44.5	5.0		8.0	✓	off	12.7	9.2		15.84	15.81
	6:00 AM	12	3311.0		280	8.5	2.2	9.0	165	450	5.0		8.0	✓	off	12.7	9.2	1434	15.87	15.85
	7:00 AM	13	3314.2		280	8.5	2.2	9.0	162	44.5	5.0		8.0	✓	off	12.7	9.2	1527	15.94	15.89
	7:44 AM																			
	8:00 AM	14	3317.5		280	8.5	2.2	10.0	157	150	5.0		8.0	✓	off	12.7	9.2	1647	16.01	15.91
(2)	9:00	15	3320.2	280	21.8			2.0	11.0	155	45	5.0	8.0	✓	off	12.6	9.3	1704	33.98	33.85
	10:00	16	3323.1	280	21.8			1.7	9.5	158	45	5.0	7.5	✓	off	12.6	9.3	1897(?)	33.78	33.92
	11:00	17	3325.9	280	21.8			1.9	8.5	162	45	5.0	7.7	✓	off	12.7	9.3	1894	33.57	33.71
	11:41																			

TEST NO. 3

SYSTEM STATUS

PAGE 2 OF 4

DATE	TIME	ELAPSED TIME (HRS)	HYDROGEN OUTPUT METER	POWER INPUT		PRESSURE (PSIG)		COOLANT TEMP (°F)	FLOW RATE		GAS ANALYSIS	
				HIGH VOLTS	LOW VOLTS	MOD	PT		KOH	COOLANT N <sub>2</sub> H <sub>2</sub>	ANALYST	PERCENT R
2-8-72	12 noon	18	3328.1	—	28.0	8.8	2.0	8.5	167	45	5.0	
	1:00	19	3331.3	—	28.0	8.5	2.0	9.0	167	45	5.0	
	2:00	20	3338.6	—	28.0	8.5	2.1	9.0	161	45	5.0	
(3)	2:01		N <sub>2</sub> H <sub>4</sub>	feed off	28.0	8.5	2.0	9.5	156	45	4.9	
	3:00	21	3338.0	28.0	21.5	—	2.0	9.5	156	45	4.9	
	4:00	22	3341.7	28.0	22.0	—	1.9	7.5	158	45	4.9	
	5:00	23	3344.2		28	8.5		8.0	162	45	5.0	
	5:42		N <sub>2</sub> H <sub>4</sub>	on	28	8.5	2.1	8.0	165	45	4.9	
	6:00	24	3346.8		28	8.5	2.0	8.5	165	45	5.0	
	7:00	25	3349.5		28	8.5	2.1	8.0	165	45	4.9	
(4)	7:24		N <sub>2</sub> H <sub>4</sub>	off				16.5	165	45	4.9	
	8:00	26	3352.8		28.0	8.5	2.1	7.5	159	45	4.9	
(5)	8:00		N <sub>2</sub> H <sub>4</sub>	on	28	8.5	2.0	8.5	165	45	5.0	
	9:00	27:00	3355.8		28	8.5	1.9	8.0	154	45	4.9	
	10:00	28:00	3358.5		28	8.5	1.9	8.0	153	45	4.9	
	11:00	29	3361.2		28	8.5	1.9	8.0	153	45	4.9	
	12:00	30:00	3363.5		28	8.5	2.0	7.5	157	45	4.9	
24/72	1:00 PM	31:00	3365.0	28.0	22.0		2.1	7.5	158	45	4.9	
	2:00 PM	32:00	3368.2	28.0	22.0		2.0	8.5	161	45	4.9	
	3:00 PM	33:00	N <sub>2</sub> H <sub>4</sub>	on								
	3:00 PM	33:00	3370.5	28.0	22.0		2.0	8.0	167	45	4.9	
	4:00 PM	34	3373.5	28.0	22.0		2.0	8.0	167	45	4.9	
	5:00 PM	35	3375.8		28.0	8.5	2.0	8.0	162	45	4.9	
(6)	5:57 AM		N <sub>2</sub> H <sub>4</sub>	off								
	6:00 AM	36	3378.8		28.0	8.5	2.0	8.0	155	45	4.9	
	7:00 AM	37	3382.2		28.0	8.5	2.0	8.5	150	45	4.7	
	8:00 AM	38	3384.8		28.0	8.5	2.0	8.5	150	45	4.7	
	9:00	39	3387.0	—	28.0	8.5	2.0	8.5	152	45	4.9	
	10:00	40	3389.5	—	28.0	8.5	1.9	8.0	155	45	4.9	

TEST NO. 3

## SYSTEM STATUS

PAGE 2 OF 2

DATE	TIME	ELAPSED TIME (HRS)	HYDROGEN OUTPUT METER	POWER INPUT		PRESSURE (PSIG)		COOLANT TEMP (°F)	FLOW RATE		GAS ANALYSIS	
				HIGH VOLTS	LOW VOLTS	MOD	PT		KOH	N <sub>2</sub> H <sub>2</sub>	N <sub>2</sub> O <sub>2</sub>	H <sub>2</sub>
12-9	11am	41	3392.2	—	280	8.5	2.0	8.0	158	45	4.9	15.77
12-9	12noon	42	3393.7	—	280	8.5	2.1	7.0	161	45	4.9	15.75
12-9	12:45		Low current cycle is run 70 minutes	—	—	—	—	—	—	—	—	—
1pm	43		—	—	280	8.5	2.0	6.0	161	45	5.0	34.35
2pm	44		—	—	280	8.5	2.1	7.0	162	45	5.0	15.75
2:18			N <sub>2</sub> H <sub>2</sub> feed on	—	—	—	—	—	—	—	—	—
3:00	45		Changed conditions to max. temp / normal leak	—	—	—	—	—	—	—	—	—
3:00			3399.8	—	280	8.5	2.2	7.5	167	45	4.9	15.83
4:00	46		3403.8	—	280	8.5	2.2	7.5	165	45	4.8	15.87
5:00	47		3408.0	—	280	8.5	2.2	8.5	159	45	4.8	15.95
5:04			N <sub>2</sub> H <sub>2</sub> off	—	—	—	—	—	—	—	—	—
6:00	48		3411.8	—	280	8.5	2.2	8.0	153	45	4.9	33.85
7:00	49		3415.2	—	280	8.5	2.0	7.0	153	45	4.9	33.84
8:00	50		3419.0	—	280	8.5	2.2	6.5	157	45	4.8	33.71
9:00	51		3422.0	—	280	8.5	1.9	6.0	161	45	4.9	33.82
9:45			N <sub>2</sub> H <sub>2</sub> on	—	—	—	—	—	—	—	—	—
10:00	52		3424.8	—	280	8.5	2.1	8.0	166	45	4.9	15.74
11:00	53		3428.0	—	280	8.5	2.0	8.5	164	45	4.8	34.08
12:00	54		3433.2	—	280	8.5	2.2	6.5	157	45	4.7	33.86
12:10			3437.0	—	280	8.5	2.0	7.0	154	45	4.8	33.93
1:00pm	55		3440.0	—	280	8.5	2.0	7.0	156	45	4.8	33.84
2:00pm	56		3443.8	—	280	8.5	2.0	6.5	160	45	4.8	33.87
3:00pm	57		3446.8	—	280	8.5	2.1	7.0	165	45	4.9	33.93
4:00pm	58		N <sub>2</sub> H <sub>2</sub> off	—	—	—	—	—	—	—	—	—
4:03pm			3450.0	—	280	8.5	2.2	7.0	169	45	4.8	33.96
5:00pm	59		3454.5	—	280	8.5	2.0	7.5	165	45	4.8	34.09
6:00pm	60		3458.8	—	280	8.5	2.0	8.0	158	45	4.9	34.10
7:00pm	61		N <sub>2</sub> H <sub>2</sub> off	—	—	—	—	—	—	—	—	—
7:06pm			3462.5	—	280	8.5	2.0	8.0	155	45	4.9	34.02
8:00pm	62		3466.0	—	280	8.5	2.0	8.0	155	45	4.9	34.45
9am	63			—	—	—	—	—	—	—	—	—

TEST NO. 3

SYSTEM STATUS

PAGE 4 OF 4

DATE	TIME	ELAPSED TIME (HRS)	HYDROGEN OUTPUT METER	POWER INPUT		PRESSURE (PSIG)			COOLANT TEMP (°F)	FLOW RATE			GAS ANALYSIS						
				HIGH VOLTS	LOW VOLTS	MOD	PT	POL		CAL	NH <sub>3</sub>	KOH	CO <sub>2</sub>	N <sub>2</sub>	META	W <sub>2</sub>	N <sub>2</sub> -O <sub>2</sub> META	CABIN/COMP	A
2-10	10am	64	3469.3	28.0	22.0	—	2.0	8.0	158	45	4.9	8.0	✓	OFF	17.0	12.8	1224	33.93	34.38
2-10	11am	65	3472.2	—	28.0	8.5	1.8	7.5	160	45	4.9	8.0	✓	OFF	17.0	12.8	1337	15.78	15.78
	Note: sometime between 10:45/11am N <sub>2</sub> supply cylinder pressure changed - N <sub>2</sub> flow rate high										213.5	—	—	—	—	—	—	—	—
	12am	66	3475.3	28.0	22.0	—	2.0	7.5	166	45	4.9	8.0	✓	11.0	17.0	12.8	1471	33.75	33.75
2-10	11:50	—	N <sub>2</sub> -H <sub>4</sub>	ON	—	—	—	—	—	—	—	—	—	—	—	—	—	—	—
2-10	12:10	—	Changed	condition	—	—	—	—	—	—	—	—	—	—	—	—	—	—	—
2-10	1pm	67	3478.2	28.0	22.0	—	2.1	7.5	166	45	4.9	8.0	✓	11.0	16.0	12.8	1609	33.87	33.95
2-10	2pm	68	3482.0	28.0	22.0	—	1.9	7.0	159	45	4.9	8.0	✓	OFF	16.0	12.8	1720	33.95	34.07
2-10	2:02	—	N <sub>2</sub> -H <sub>4</sub>	OFF	—	—	—	—	—	—	—	—	—	—	—	—	—	—	—
2-10	3pm	69	3485.2	—	28.0	9.0	2.0	7.0	151	45	4.9	7.8	✓	OFF	16.0	12.8	1854	15.89	15.92
2-10	4pm	70	3488.0	—	29.0	8.5	2.0	8.0	147	45	4.9	8.0	✓	OFF	15.85	12.7	1986	15.86	15.87
2-10	4:05	70.5	3488.0	28.0	21.5	—	2.0	8.0	145	45	5.0	8.0	✓	OFF	15.95	12.7	2008	15.87	15.89
2-10	5:00	71	3490.8	—	29.2	9.8	2.0	8.5	145	45	4.9	8.0	✓	20	15.90	12.4	2109	15.84	15.88
2-10	6:00	72	3493.2	28.0	21.8	—	1.9	9.0	145	44.5	4.9	8.0	✓	20	15.85	12.4	2228	34.06	33.85
2-10	7:00	73	3495.8	28.0	22.0	—	2.0	8.0	149	44.5	4.9	8.0	✓	20	15.85	12.4	2353	33.87	33.98
2-10	8:00	74	3498.2	28.0	22.0	24	2.2	7.5	151	44.5	4.5	8.0	✓	20	15.85	12.8	2475	33.79	33.83
2-10	9:00	75	3500.8	—	29.2	9.5	2.0	8.0	156	45	4.9	7.9	✓	20	15.85	12.5	2526.05	15.80	15.79
2-10	10:00	76	3502.0	—	29.2	8.8	2.1	8.5	157	45	4.9	8.0	✓	20	15.85	12.4	2730	15.82	15.79
2-10	11:00	77	3505.0	—	29.1	8.7	1.9	9.5	158	45	4.9	8.0	✓	20	16.0	12.5	2854	15.79	15.87
2-10	12:00	78	3507.5	—	29	9.0	2.0	10.0	161	45	4.9	8.0	✓	20	16.0	12.7	2999	15.79	15.81
2-11	1:00	79	3501.0	28.0	22.0	—	2.0	9.5	166	45	4.9	8.0	✓	20	16.0	12.45	1121	34.30	34.41
2-11	2:00	80	3513.0	28.0	22.0	—	2.0	8.5	165	45	4.9	8.0	✓	20	16.0	12.6	2268	33.71	33.83
2-11	3:00	81	3516.8	28.0	22.0	—	2.0	8.0	155	45	4.9	8.0	✓	20	16.0	12.65	3620	33.96	33.98
2-11	4:00	82	3510.0	28.0	22.0	—	2.0	8.7	149	45	4.9	8.0	✓	20	16.0	12.60	4221	34.98	34.06
2-11	5:00	83	3522.8	—	28.0	9.0	2.0	9.1	146	45	4.9	8.0	✓	20	15.95	12.60	5115	15.84	15.86
2-11	6:00	84	3525.2	—	28.0	9.0	2.0	10.0	146	45	4.9	8.0	✓	20	15.95	12.60	7144	15.83	15.87
2-11	7:00	85	3528.0	28.0	22.0	—	1.9	11.0	147	45	4.9	8.0	✓	20	15.95	12.60	7283	33.73	33.75
2-11	8:00	86	3531.0	28.0	22.0	—	2.0	9.5	150	45	4.9	8.0	✓	20	15.95	12.6	7883	33.62	33.68
2-11	9:00	87	3533.0	—	28.0	8.5	2.1	10.0	152	45	4.9	7.8	✓	OFF	15.85	12.7	0990	15.78	15.81
2-11	10:00	88	3535.0	—	28.0	8.5	2.1	10.5	154	45	4.9	7.8	✓	OFF	15.85	12.7	1230	15.78	15.81

TEST NO. 3

SYSTEM STATUS

PAGE 2 OF —

DATE	TIME	ELAPSED TIME (HRS)	HYDROGEN OUTPUT METER	POWER INPUT		PRESSURE (PSIG)					COOLANT TEMP (°F)	FLOW RATE				GAS ANALYSIS			
				HIGH VOLTS AMPS	LOW VOLTS AMPS	MOD	P.T.	PO <sub>2</sub>	CAL	N <sub>2</sub> H <sub>4</sub>		KOH	(COUNT)	N <sub>2</sub> H <sub>4</sub>	META	N <sub>2</sub>	BUB. SEP.	META	WTA
2-11	11am	89	3547.1	—	280 8.5	2.0	11.0	156	45	4.8		7.7	✓	OFF	15.9	12.75	1343	15.78	15.81
(2)	12noon	90	3539.5	280 22.0	—	2.0	11.0	157	45	4.9		7.8	✓	OFF	15.9	12.75	1479	15.78	15.82
	1pm	91	3541.5	—	280 8.5	2.1	11.0	158	45	4.9		7.8	✓	OFF	15.9	12.75	1590	15.77	15.81
	2pm	92	3543.7	280 22.0	—	2.0	10.0	161	45	4.9		7.8	✓	OFF	15.95	12.75	1716	34.28	34.23
	2:10		END OF TEST	— N <sub>2</sub> H <sub>4</sub> ON		@ 2.08					PO <sub>2</sub> 165								
			Final calibration:			Cabin					PO <sub>2</sub> -C 140								
											PO <sub>2</sub> -D 141								
						TOTAL					14.83								
						Barometer					765.4								
						PO <sub>2</sub> EFFLUENT													



SYSTEM STATUS

TEST NO. 4

DATE	TIME	ELAPSED TIME (HRS)	POWER INPUT		PRESSURE (PSIG)		COOLANT TEMP (°F)	FLOW RATE		GAS ANALYSIS	
			VOLTS	AMPS	MOD	PDZ		KOH	N <sub>2</sub> H <sub>4</sub>	N <sub>2</sub> -O <sub>2</sub>	H <sub>2</sub>
3-14-70	7:37 PM	0	28.0	5.5	2.1	780	4.7	8.0	9.0		
	9:00 PM	1.5	28.0	6.0	2.1	290	4.6	8.0	12.0		
	9:30 PM	2.0			off						
	9:35 PM										
	9:40 PM										
	9:50 PM										
	10:40 PM	3.25									
	12:00 PM	4.5	28.0	5.5	2.1	520	4.6	7.5	-		
3-14	12:00 AM		28.0	5.5	2.1	600	4.8	7.5	-		
	2:00	6.5	28.0	5.5	2.1	645	4.8	7.5	-		
	3:00	7.5	28.0	6.0	2.0	695	4.8	7.5	-		
	3:30	8.0	End Flight Cycle								
	3:30		5.4	6.0		710					
	4:00	8.5	28.0	6.0	2.1	660	4.7	7.5	19.5		
	5:00	9.5	28.0	5.5	2.2	90	5.2	7.0	8.0		
	6:00	10.5	28.0	6.0	2.1	290	5.2	7.5	8.0		
	7:00	11.5	28.0	6.0	2.1	435	4.8	7.5	8.0		
	8:00	12.5	28.0	6.0	2.1	530	4.8	7.3	8.0		
	9:00	13.5	28.0	6.0	2.0	600	4.8	7.4	8.0		
	10:00	14.5	28.0	6.0	1.9	640	4.8	7.2	8.0		
	11:00	15.5	28.0	6.0	1.6	695	4.8	7.0	8.0		
3-14	12:00 PM	16.5	28.0	6.0	1.6	696	4.8	7.0	8.0		
			END OF CYCLE								
	12:40		N <sub>2</sub> H <sub>4</sub> VALVE OPENED FOR NEXT CYCLE								
	1:00	17.5	28.0	6.0	1.9	680	4.8	7.0	8.0		
	2:00	18.5	28.0	6.0	2.0	523	4.85	7.0	8.0		
	3:00	19.5	28.0	6.0	2.0	270	4.90	7.0	8.0		
	3:31	START CYCLE 3 (TIME ZERO)									
	4:35	21.0	28.0	21.0	2.1	560	4.9	7.5	off		
	5:25	22.5	28.0	21.0	1.6	630	4.9	7.2	off		

N<sub>2</sub>H<sub>4</sub> SAMPLE TAKEN - SWITCHED TO 150 mA/cm<sup>2</sup> / N<sub>2</sub>H<sub>4</sub> OFF

SYSTEM STATUS

TEST NO. 4

MM H<sub>2</sub>

DATE	TIME	ELAPSED TIME (HRS)	HYDROGEN OUTLET PRESSURE	POWER INPUT		PRESSURE (PSIG)		T <sub>amb</sub> TEMP (°F)	COOLANT TEMP (°F)	FLOW RATE		GAS ANALYSIS	
				HIGH VOLTS	LOW VOLTS	MOD	PD <sub>2</sub>			KOH COUNT	N <sub>2</sub> H <sub>4</sub> MFL	N <sub>2</sub> -O <sub>2</sub>	H <sub>2</sub>
3/4	6:55 PM	23.5	650	280	210	1.9	695	4.9		7.2	OFF		
	6:55 PM	23.5	N <sub>2</sub> H <sub>2</sub>	Sample		1.6	740	4.9		7.0	OFF		
	8:10 PM	24.5	650	280	210	1.6	740	4.9		7.0	OFF		
	8:12 PM	24.5	650	Cycle		1.6	740	4.9		7.0	OFF		
	9:00 PM	25.5	650	280	210	2.1	410	4.9		7.1	OFF		
	9:30 PM	26.5	N <sub>2</sub> H <sub>2</sub>	Sample		1.6	740	4.9		7.0	OFF		
	9:35 PM	26.5	N <sub>2</sub> H <sub>2</sub>	Sample		1.6	740	4.9		7.0	OFF		
	10:00 PM	27.2	650	280	205	1.6	740	4.9		7.2	OFF		
	11:00 PM	28.2	650	280	205	1.6	740	4.9		7.2	OFF		
	11:25 PM	28.2	650	280	205	1.6	740	4.9		7.2	OFF		
3/5	12:00	28.2	650	280	211	1.6	690	4.9		6.8	—		
	12:30	29.2	630	280	215	1.6	730	4.8		7.5	—		
	1:30 AM	30.2	640	280	215	1.7	745	4.8		7.5	—		
	2:00 AM	31.2	645	280	210	2.2	120	4.8		7.5	—		
	3:20	32.2	645	280	210	2.1	320	4.8		7.5	—		
	4:10 AM	33.2	650	280	210	2.1	520	4.9		7.0	—		
	5:00 AM	34.2	655	280	210	1.9	535	4.9		8.0	—		
	6:00 AM	35.2	645	280	210	1.9	660	4.9		7.8	—		
	7:00 AM	36.2	645	280	210	1.8	710	4.9		7.7	—		
	8:00 AM	37.2	650	280	210	2.0	740	4.9		7.7	—		
	9:00 AM	38.2	654	280	210	1.7	758	4.9		7.5	—		
	10:00 AM	39.2	654	280	210	1.5	760	4.9		7.5	—		
	11:30	40.2	645	280	210	1.5	760	4.9		7.5	—		

SYSTEM STATUS

TEST NO. 4 Dia Pump  
MIN HO

DATE	TIME	ELAPSED TIME (HRS)	HYDROGEN PRESSURE	POWER INPUT		PRESSURE (PSIG)		TANK NIMH	COOLANT TEMP (°F)	FLOW RATE		GAS ANALYSIS	
				HIGH VOLTS	LOW VOLTS	MOD	PO2			KOH	CHLORINE NIMH	CHLORINE SET	CHLORINE NIMH
3/15	1:00		6.65	28.0	13.0	1.25	760	4.9		5.9	off	22.33/22.34	1740
	2:00		6.25	28.0	12.5	1.75	760	4.9		7.3	off	22.30/22.31	1690
	3:00		6.45	28.0	13.0	2.00	480	4.9		7.2	off	22.43/22.39	1728
	3:20	START	CYCLE	6	at 9:00 F	100	100	4.9					
	4:00		6.50	28.0	13.0	2.0	450	4.9		7.3	off		1755
	5:00		6.50	28.0	12.5	2.0	540	4.9		7.5	off		1787
	5:20		N <sub>2</sub> H <sub>4</sub>	Sample									
	6:00		6.50	28.0	12.5	1.5	600	4.9		7.5	off		1820
	7:00		6.50	28.0	12.5	1.5	600	4.9		7.5	off		1860
	8:00		6.50	28.0	12.5	1.6	710	4.9		7.2	off		1893
	8:15		N <sub>2</sub> H <sub>4</sub>	Sample									
	9:00		6.50	28.0	12.5	1.8	730	4.9		7.2	off		1924
	10:00		6.50	28.0	6.0	2.0	315	4.9		7.2	off		1950
	10:45	START	Cycle	7.9	at 9:10 F	4	150	4.9					
	11:00		N <sub>2</sub> H <sub>4</sub>	Sample									
	11:07		6.50	28.0	20.0	2.0	520	4.9		7.2	off		1946
3/16	12:00	midnight	6.50	28.0	20.5	1.7	595	4.9		7.0	—	3303/33.74	2021
	11:57			N <sub>2</sub> H <sub>4</sub>	Sample								
	12:35			N <sub>2</sub> H <sub>4</sub>	Sample								
	1:00 AM		6.50	28.0	21.0	1.8	675	4.9		7.6	—	3377/33.75	2082
	1:40			N <sub>2</sub> H <sub>4</sub>	Sample								
	2:00 AM		6.55	28.0	21.0	1.5	725	4.9		7.6	—	3377/33.75	2137
	3:00		6.45	28.0	21.0	1.7	730	4.8		7.6	—	3377/33.75	2137
	3:25		Switch	to low current									
	4:30		1st N <sub>2</sub> H <sub>4</sub>	Sample									
	5:00		6.35	28.0	5.5	2.1	160	4.9		7.3	—	3377/33.75	2247
	6:00		6.35	28.0	5.5	2.0	240	4.9		7.3	—	3377/33.75	2262
	7:00 AM		6.30	28.0	5.5	2.0	480	4.9		7.2	—	3377/33.75	2279
	8:00 AM		6.30	28.0	5.5	2.0	570	4.9		7.2	—	3377/33.75	2296
	9:00 AM		6.30	28.0	6.0	1.75	645	4.9		7.3	—	3377/33.75	2340

TEST NO. 4

SYSTEM STATUS

PAGE 1 OF 1

Dia Pump  
MIM No

DATE	TIME	ELAPSED TIME (HRS)	HYDROGEN PRESSURE		POWER INPUT		PRESSURE (PSIG)		COOLANT TEMP (°F)	FLOW RATE			GAS ANALYSIS			
			HIGH VOLTS	LOW VOLTS	AMPS	MOD	PT	PDZ		CAL	NiH <sub>2</sub>	Temp	N <sub>2</sub>	COG SEP	ANALYST	TEST NO.
3/16	10:00		635	280	6.0		1.7		690		7.3	off		11:22/11:23	2331	1812
	11:00		635	280	6.0		2.0		340		7.2			11:27/11:27	2400	1644
	12:00		640	280	12.5		2.0		460		7.3			22:48/22:30	2444	1668
	1:00		650	280	12.0		2.0		560		7.2			22:17/22:20	2490	1761
	2:00		648	280	12.0		1.8		635		7.0			22:15/22:14	2442	1821
	3:00		647	280	12.0		1.5		680		7.2			22:12/22:09	2475	1923-
	4:00		650	280	12.0		2.0		720		7.0			22:09/22:08	2511	1995
	5:00		650	280	12.0		1.7		720		7.0			22:08/22:09	2544	2067
CHANGED TO 85 OF THERMO BAYLES																
3/16	5:20	START N <sub>2</sub> H <sub>4</sub> ADDITION														
3/16	6:30	START N <sub>2</sub> H <sub>4</sub> ADDITION														
3/16	6:30	PM	650	280	6.5		2.1		105		7.1			12:32/13:00	2569	2181
3/16	6:40	AT CURRENT							1					11:27/11:28		
3/16	7:00		650	280	5.5		2.0		140		7.0			11:21/11:24	2519	2184
3/16	8:00		650	280	5.7		2.0		330		7.0			11:27/11:24	2576	2244
3/16	9:00		655	280	5.7		2.1		460		8.0			11:22/11:22	2613	2298
3/16	10:00		650	280	5.5		2.1		545		8.1			11:21/11:21	2629	2346
3/16	11:00	PM	655	280	5.7		1.9		610		8.1			11:21/11:25	2640	2388
3/17	12:00	midnight	650	280	5.7		1.7		650		8.1			11:24/11:25	2666	2440
3/17	1:00		650	280	5.5		1.7		690		8.1			11:24/11:25	2681	2471
3/17	1:15	PM	N <sub>2</sub> H <sub>4</sub> sample added													
3/17	1:45	PM	Added													
3/17	2:00	4:11	650	280	13.0		2.1		450		8.1			22:00/22:44	2712	2538
3/17	2:15	PM	N <sub>2</sub> H <sub>4</sub> sample added											22:24/22:42		
3/17	3:00	PM	650	280	13.0		2.1		470		8.1			22:37/22:42	2744	2631
3/17	4:00	PM	650	280	13.0		1.8		570		8.1			12:49/12:07	2781	2756
3/17	5:00	PM	650	280	13.0		2.0		670		8.1			22:56/22:57	2814	2806
3/17	6:00	PM	650	280	13.0		2.0		690		8.1			22:49/22:49	2850	2886
3/17	7:00	PM	650	280	13.0		2.0		720		8.1			22:47/22:50	2883	2957
3/17	8:00	PM	650	280	13.0		1.8		730		8.1			22:41/22:41	2920	3036



Tues March 21 1972

Test #5

1) ReFilled system with fresh  
KOH  $M = 6.9$

Bottle + Liquid water Fill	3687
Bottle + Liquid residue	372
Total H <sub>2</sub> O Added To System	3295

Hydrozine + Bottle Weight	1337
Bottle + Liquid residue	409
Total NaH <sub>2</sub> in System	928

Test 5 Start at 2pm Wed March 22

Circuit Breaker Cut all power at 2:47 PM Closed all  
Switches and Started Module again 2:57

Monday March 27, 1972

1) started cell on low current  
mode — 9:25 A.M.

2) Cell voltage reset to  $13.8 \text{ mV} = \text{low}$   
 $33.8 \text{ mV} = \text{high}$

TUESDAY MARCH 28, 1972

START SYSTEM — LOW MODE — 9:00 am

stop

4:30 PM

Wednesday March 29, 1972

Start system low mode - 8:30 AM

stop system - 5:00 PM

Thursday March 30, 1972

Start system low mode - 8:00 AM

Stop System - 4:45 PM

FRIDAY March 31, 1972

started system low mode 8:00 AM

Stop ~~system~~ system - 4:30 PM

Monday April 3, 1972

1) Started cell - low mode 8:15 AM

Stop cell at 4:30 PM

Tuesday April 4, 1972

1) Started cell - low mode 8:00 AM

2) Stop cell 4:30 PM

Wednesday April 5, 1972

1) Start cell - low mode 8:15 AM

Molarity Check 7.5 420.75 g/L

2) Stop Cell 4:30 PM

Thursday April 6 1972

1) Start Cell - low mode 8:00 AM

2) Stop Cell 4:30 PM

Friday April 7 1972

1) Start Cell - low mode 8:00 AM

Bottle & H<sub>2</sub>O drained 1548 gm  
Bottle empty H<sub>2</sub>O 370 gm  
(3-21-72) 3295 gm  
1178  
2117 gm H<sub>2</sub>O consumed

Friday April 7, 1972 - (cont.)

New Charge H<sub>2</sub>O + Bottle 3910 gm  
residual & ~~H<sub>2</sub>O~~ Bottle 480  
new charge H<sub>2</sub>O 3430 gm

2) Stop cell 4:30 PM

Wednesday April 12 1972

1) Start up CELL - low mode 10:00 AM

2) Stop 4:00 PM

Thursday April 13

1) Start cell - low mode 8:00 AM

2) Stop cell 4:30 PM



Friday April 14

- 1) Start Cell - low mode 8:30 AM
- 2) Stop Cell 4:30 PM

Monday April 17, 1972

- 1) Start Cell - Low mode 8:15 AM
- 2) Shut down 4:30 PM

Tuesday April 18 1972

- 1) Start Cell low mode 8:00 AM
- 2) Stop 4:15 PM

Wednesday April 19, 1972

- 1) Start Cell - low mode 8:00 AM
- 2) Molarity checked  $6.9 / 366.1 \text{ g/L} = 30\% \text{ KOH}$
- 3) Stop Cell 4:30 PM
- 4) Bubble separator - total run time 202 hrs

Thursday April 20, 1972

- 1) Start Cell - low mode - 8:00 AM
- 2) Shut down 4:30 PM

FRIDAY April 21, 1972

- 1) Start Cell - low mode 8:30 AM
- 2) changed KOH pump motor - bearings were beginning to go
- 3) Stop cell 3:30 PM

Monday April 24 1972

- 1) Replaced one manifold on H-X - leak around swagelok fitting - retapped hole 7/6-18
- 2) Started cell 1:30 PM
- 3) Polarity checked = 7.3<sup>md.</sup> = 409.0 g/L
- 4) Shut down 4:30 PM

Tuesday April 25, 1972

- 1) Started cell 75°C / 50 mA/cm<sup>2</sup> 8:00 AM  
11.2 mv
- 2) Calibrated new O<sub>2</sub> sensor
- 3) Added 150 cc N<sub>2</sub>H<sub>4</sub> 9:45 AM  
(mixed 2 times)
- 4) 17.2 2nd E.P. 15.3 (257) = 786  
15.7 1st End Point  
1.4 start 5 cc + 500 ml Polarity N<sub>2</sub>H<sub>4</sub>

for HCl mixture = 1000 cc HCl to 800 cc H<sub>2</sub>O  
for N<sub>2</sub>H<sub>4</sub> Titration

- 5) 12.6 2nd end point 3:52 PM  
11.3 1st end point 5 cc + 1.0 cc  
1.1 start  
 $\frac{10.2}{5} (257) = .464$  Polarity  
N<sub>2</sub>H<sub>4</sub>

- 6) Shut down 4:30 PM

Wednesday, April 26, 1972

1) started cell  
75°F / 150 mA / cm<sup>2</sup> 33.8 mV 8:30 AM

2) Added 150 cc N<sub>2</sub> H<sub>2</sub>  
(mixed 2 times) 9:05 AM

3) 21.0 2nd EP 9:45 AM  
16.6 1st EP 2 cc + 500 ml  
.1 start

$$\frac{16.5}{5} (257) = .845 \text{ molarity}$$

4) 25.2 2nd E.P. 11:00 AM  
22.2 1st End Point  
.4 start 5 cc + 1 cc  
 $\frac{21.8}{5} (257) = 1.02 \text{ molarity}$

5) Changed to low mode 1:00 PM

6) Shut down 4:30 PM

Note: N<sub>2</sub>H<sub>4</sub> was clear when added to system but turned pink when mixed with KOH in system during mixing cycle

Thursday April 27, 1972

- 1) changed Temp control bulb to 91°F
- 2) Started Cell
- 3) Added 152 cc  $N_2H_4$  - (mixed 2 times) 10:00 AM

$\begin{array}{r} 19.8 \\ 16.9 \\ \hline 1.5 \end{array}$ 
 $\begin{array}{l} \text{2nd E.P.} \\ \text{1st End point} \\ \text{start} \end{array}$ 
 2 cc + 500 ml 10:34 AM

$$\frac{16.4}{2} (257) = 2.1 \text{ molarity}$$

- 4) 11:20 AM

$\begin{array}{r} 24.7 \\ 24.3 \\ \hline 1.2 \end{array}$ 
 $\begin{array}{l} \text{2nd E.P.} \\ \text{1st End point} \\ \text{start} \end{array}$ 
 5 cc + 500 ml  
 $\frac{23.1}{5} (257) = 1.18 \text{ molarity}$

- 5) switched to low mode 1:05 PM

- 6) Shut down 4:30 PM

NOTE: Pink color still noted during mixing process

Friday April 28 1972

- 1) Removed extra reservoir from system - capped lines
- 2) started cell - low mode 9:15 AM  
 $91^\circ F$   $52 \text{ mA/cm}^2$  (11.2 mv)
- 3) Shut down 1:45 PM

Monday May 1, 1972

- 1) Started bubble separator and KOH pump - no power on cell - 9:00 AM
- leave on all night

Tuesday May 2, 1972

- 1) Bubble separator & pump operating OK 9:00 AM
- 2) on 24 hrs

Wednesday May 3 1972

- 1) Bubble separator & pump operating OK 9:00 AM
- 2) on 24 hrs

Thursday May 4, 1972

- 1) Bubble separator & pump operating OK 9:00 AM
- 2) on 24 hrs

Friday May 5 1972

- 1) Bubble separator & pump OK 9:00 AM

Monday May 8 1972

- 1) Bubble separator & pump OK 9:00 AM

Tuesday May 9 1972

- 1) Bubble separator & pump OK 9:00 AM

Wednesday May 10 1972

- 1) Bubble Sep. & pump OK 9:00 AM

---

Thursday May 11 1972  
1) Bubble Sep + pump OK 9:00 AM

---

Friday May 12 1972  
1) B/S + pump OK 9:00 AM

---

Monday May 15 1972  
1) B/S + pump OK 9:00 AM

---

Tues May 16 1972  
1) B/S + pump OK 9:00 AM

---

Wednesday - to Friday 5/26/72

1) B-S on 24 hrs / day  
performance OK.

---

#### PROTOTYPE HEAT EXCHANGER DEVELOPMENT

The following section presents the raw data taken during testing of the heat exchanger. A discussion of the results of this test appears in Section 2.3 of the text.

[illegible]